

Published in *Fundamentals of Cosmic Physics*, Vol. 16, pp. 111-220, 1996.

# COLLISIONAL RING GALAXIES

**P.N. Appleton and Curtis Struck-Marcell**

Erwin W. Fick Observatory and Department of Physics and Astronomy, Iowa State University, Ames, IA 50011

**Abstract.** We review the current state of knowledge of both the observational and theoretical nature of collisional ring galaxies. Ring galaxies represent a class of colliding galaxy in which nearly symmetrical density waves are driven into a disk as a result of an almost bulls-eye collision with another galaxy. Since the basic dynamics of the collision is now quite well understood, the ring galaxies can be used as a form of cosmic perturbation "experiment" to explore various properties of galactic disks. For example, as the density wave expands into the disk, it triggers the birth of large numbers of massive stars. This provides us with an opportunity to study the evolution of stars and star clusters in the wake of the ring. We review the now extensive observations of ring galaxies from the early photographic measurements to recent infrared, radio and optical studies. We also present a simple analytical treatment of the ring-making collisions and compare them to recent N-body and gas-dynamical models. The importance of ring galaxies lies in their relative simplicity compared with other colliding systems and the possibility that low-angular momentum collisions might have been more common in the past.

**Keywords:** Interacting galaxies, Colliding galaxies, Star formation in galaxies, Ring galaxies, Dynamics of interacting systems, Starburst activity in galaxies

## Table of Contents

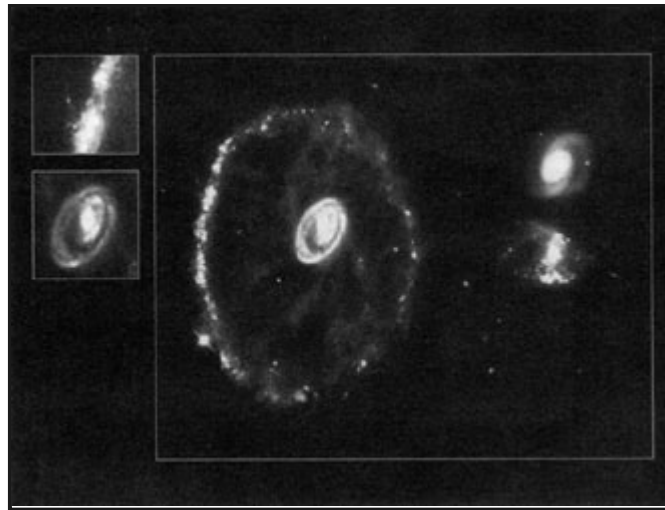
- INTRODUCTION
  - Why Study Rings?
- RINGS AS COLLISIONAL OBJECTS
  - The Collision Idea
  - Morphology of Ring Galaxies and Ring Galaxy Samples
  - Some Early Ideas about Ring Formation
- OBSERVATIONS OF RING GALAXIES
  - The Photometry and Colors of Ring Galaxies
  - Observation of the Diffuse and Molecular Gas Content of Ring Galaxies
  - Observations of Ring Kinematics
    - The Cartwheel Galaxy and its Companions
    - Model Velocity Fields
  - Star Formation Properties of Ring Galaxies
  - Radio Emission and AGN Activity in Ring Galaxies
  - Rings in Bulge-dominated Systems and Hoag-like Galaxies
- SIMPLE KINEMATIC MODELS OF RINGS AND RING-LIKE GALAXIES
  - Caustic Waves
    - Singularity Theory in Galaxy Formation and Ring Galaxies
    - Symmetric Ring Caustics in the Kinematic Orbit Approximation
  - Varieties of Symmetric Rings
  - Multiple Encounters?
  - Asymmetric Encounters
- SELF-CONSISTENT STELLAR DYNAMICAL MODELS OF RING GALAXIES
- THE GAS DYNAMICS OF RING GALAXIES
  - Lessons from Simple Models
  - Numerical Simulations of Ring Galaxy Hydrodynamics

- [The First Simulations: 1970s](#)
- [The Next Generation: 1980s](#)
- [The Current Generation of Models: 1990s](#)
- [Models of the Cartwheel](#)
- [What Are the Spokes?](#)
- [Explorations of Heating and Cooling Effects](#)
  
- [FUTURE DIRECTIONS](#)
  - [Observational Directions](#)
  - [The Next Steps in Modeling](#)
  
- [REFERENCES](#)
  
- [APPENDIX 1: Multiple Encounter Kinematics](#)
  
- [APPENDIX 2: Simple Models for Asymmetric Stellar Ring-Like Waves](#)

## 1. INTRODUCTION

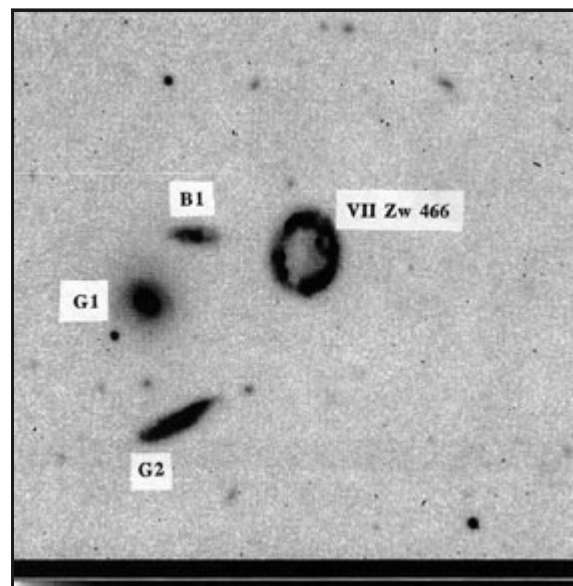
For over half a century astronomers have pondered the origin of a rare but beautiful class of galaxy, now called "ring galaxies". We believe that these peculiar galaxies, which take on the appearance of a "smoke ring" on photographic plates, are formed as a result of a cosmic accident of gargantuan proportions. An "intruder" galaxy plunges through the center of a larger rotating disk galaxy, triggering the birth of bright young stars in the wake of radially expanding ring waves. These driven oscillations, like vibrations on the surface of a pond or canal, can be thought of as perturbation experiments, but on a galactic scale. Once recognized as such, the waves can be used to probe both the shape and strength of the gravitational potential of the target galaxy, as well as the mechanisms which lead to star birth and star death in propagating density waves. The geometric simplicity of these near bulls-eye collisions, as attested by the success of even the simplest kinematic models of their evolution, make ring galaxies attractive tools for understanding galactic structure and evolution. In these "cosmic experiments", as the strength of the perturbation is increased, through successively more massive intruder galaxies, the system can be tested from the limit of small-order perturbation theory to the realm of highly non-linear behavior treated best by self-consistent numerical simulations. Although at one time thought to be rare, the collision between two galaxies is now believed to be an important mechanism in galaxy evolution. Ring galaxies in particular, may form the most tractable of a family of collisional scenario which end in merger and transmutation.

Interest in ring galaxies can be traced back to [Zwicky \(1941\)](#), where he presented the first photograph of the now famous "[Cartwheel](#)" ring in the constellation of Sculptor (see [Figure 1](#) for a Hubble Space Telescope view of the [Cartwheel](#)). His photograph, obtained with an 18-inch Schmidt camera on Palomar Mountain, showed an outer ring, a faint bar and spiral streamers (often referred to as "spokes") extending from the center to the ring. Modern observations also show an inner ring. Zwicky concluded that "this represents one of the most complicated structures awaiting explanation on the basis of stellar dynamics". Indeed over half a century later, a theory for the origin of the spokes is only just emerging by considering them as gravitational instabilities in a mainly *gaseous*, rather than a stellar disk.



**Figure 1.** The Cartwheel ring galaxy obtained with the WFPC-II camera on the Hubble Space Telescope. The image was created by combining a B-band and an I-band image of the galaxy and an attempt has been made to balance the colors to indicate red and blue regions in the galaxy. The spatial resolution of the observations is approximately 0.1 arcseconds which corresponds to approximately 50 pc at the distance of the Cartwheel. The Cartwheel is unusual in that it contains an inner and outer ring as well as the connecting "spokes" which so perplexed F. Zwicky when he first discovered the galaxy. (Image from Borne et al. 1995). (See Color Plate I at the back of this issue.)

In the years that followed, notably with the publication of major catalogs and atlases of peculiar galaxies by Vorontsov-Velyaminov (1959), Vorontsov-Velyaminov and Krasnogorskaya (1961; MCG Catalog) and Arp (1966), more of the peculiar ring galaxies were uncovered. Lindsey and Shapley (1960) discovered a large ring in the southern sky (see also Graham (1974)). Vorontsov-Velyaminov (1960) drew attention to the class of ring galaxies and presented numerous examples in Part II of the Atlas of Interacting Galaxies (Vorontsov-Velyaminov, 1977). In the north, Mayall's Object (see Smith 1941; Burbidge, 1964) was discovered as an example of a ring with a cigarshaped object extending from the ring (Arp 148 = VV32). Sersic (1968) drew attention to another classical ring in the constellation of Vela. We present in Figures 2a to 2d a sequence of recent views of some well known ring galaxies.



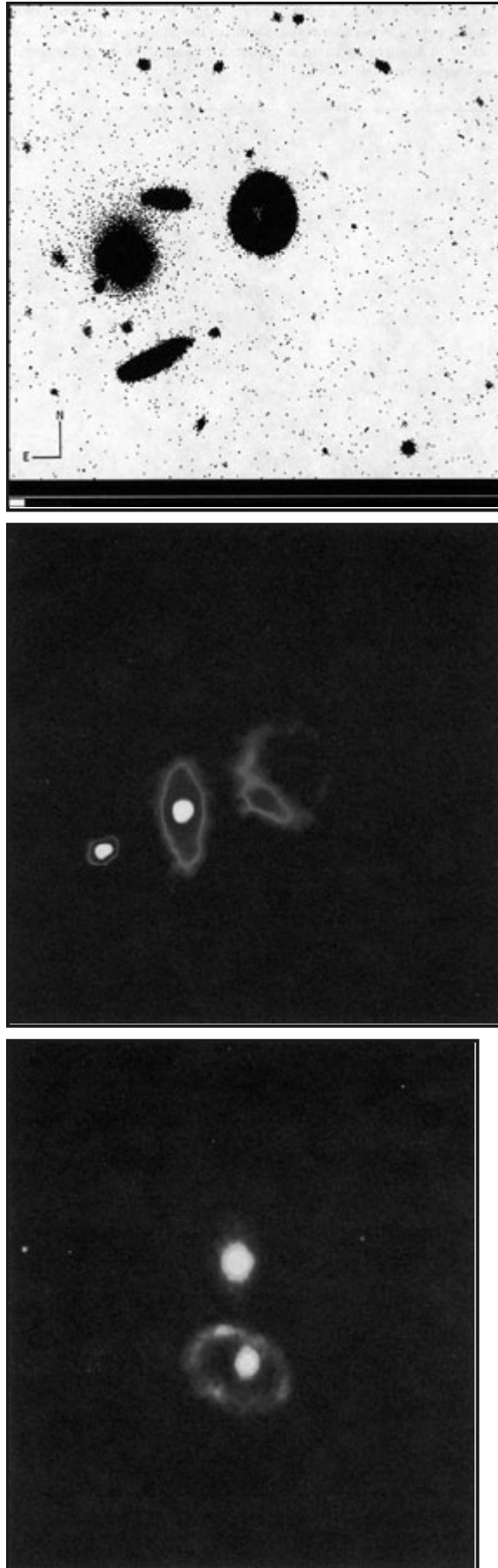


**Figure 2.** The "centrally smooth" ring galaxy VII

Zw466 does not have an obvious nucleus. This grey-scale B-band image emphasizes the brighter isophotes and shows the knots in the ring. b) VII Zw466 is not empty (despite its classification by Theys and Spiegel as RE type) but is filled with a red stellar population. In this grey scale stretch (of the same B image) the inner emission is clearly seen. Of the three galaxies seen nearby, the large elliptical galaxy seen to the left shows peculiar "boxy" isophotes and may be the intruder. On the other hand new HI observations (Appleton and Charmandaris, in preparation) link the southern (bottom) edge-on disk with the collision. (from Appleton and Marston 1995 B-band observations from the KPNO 2.1 m telescope). The small galaxy nearest the ring is a background galaxy. Cannon et al. (1970) discussed the class of ring galaxies appearing in the Arp atlas and the similarities between objects like Arp 146 and Arp 147 and some of the galaxies, particularly I Zw 45 (= NGC 4774; incorrectly named I Zw44 by Cannon) and VII Zw 466, found in the unpublished lists of Zwicky (see Sargent 1970). These authors were the first to note that ring galaxies are blue and that many of them appear to have close companions. Photographs of I Zw 45 showed a trail of material between the ring and the companion, strongly suggesting a causal connection. Their paper ends with a question which set the scene for the next ten years of work on ring galaxies: "Do ring-shaped equilibria exist and if so, are they stable, or are rings merely an ephemeral phenomenon?". Models strongly supporting the transient nature of the ring morphologies were quick to follow, although we shall see that the question of the stability of the ring wave, especially in the gas phase, is still of considerable interest today. A short review article on ring galaxies is presented by Dennerfeld and Materne (1980). c) One of the first near infrared images of a ring galaxy was this 2.2 micron image of Arp 147 shown here in false color. (From Bushouse and Stanford (1992), KPNO 2.1m telescope, IRIS Camera). (See Color Plate II at the back of this issue.) d) The beautiful RN galaxy LT41 has a redshift of  $z = 0.07$ . Unlike the Cartwheel, this galaxy does not show obvious "spokes". Its large companion is elongated, probably as a result of its slightly off-center collision with the target disk. ( Appleton and Marston 1995 . V-band image from the KPNO 2.1m telescope). (See Color Plate III at the back of this issue.)

### 1.1. Why Study Rings?

Ring galaxies are rare amongst samples of bright galaxies. Despite this, we believe that ring galaxies are important for the following reasons.

- Ring galaxies represent a class of colliding galaxies in which the disk of at least one of the participants of the collision remains sufficiently intact after the collision to allow its structure and star formation properties to be studied in detail. This is not often the case in colliding galaxy systems. In a sense, the ring galaxy serves as a galaxy-scale perturbation experiment that allows us to study the hydrodynamic and stellar evolutionary processes within the host disk. In many cases, the gravitational perturbation of the small companion galaxy is expected to be modest, driving low amplitude waves through its disk. In other cases the companion is more substantial, and large three-dimensional effects and strong

non-linear behavior is predicted. Models of rings have now been developed by a number of independent groups, and such tools can be used to make predictions which can be compared with observation.

- Ring galaxies are the sites of vigorous non-nuclear star formation. Typical knots in ring galaxies have optical luminosities similar to, or in excess of, the Large Magellanic Cloud. The colors and spectra and extreme luminosity of the HII regions in the rings suggest large numbers of OB stars are being born at high rates. Ring galaxies also have generally high global far-infrared (IR) luminosities and large far-IR color temperatures compared with "normal" galaxies. Recent observations also show that they contain substantial quantities of molecular gas. These properties are shared with nuclear starburst galaxies.
- Ring galaxies can provide a means of studying the time evolution of star formation across and inside the ring. The simplest models predict that stars form in the expanding ring. A star formation burst formed at the leading edge of the expanding density wave is expected to produce a monotonic color gradient in the wake of the ring, as evolving stars drift inwards from their birth sites. There is now mounting evidence for such color gradients and other indicators of stellar evolution behind the ring.
- Models indicate that off-center, moderate impact-parameter collisions often produce a strongly asymmetric ring initially, and many known ring galaxies appear to fall into this category. Interesting azimuthal and vertical variations are predicted from the models in these cases and these can provide interesting tests of the mechanisms of star formation which can be compared with observations.
- Because of its geometrical simplicity, as compared with more dynamically messy galaxy mergers, the collisional ring galaxy can be used to explore differences between the behavior of gas and stars in collisions. Dissipation can aid the development of local gravitational instabilities in the gas, causing the collapse and shearing of gas complexes, star formation and perhaps the formation of 'spokes' similar to those found in the [Cartwheel](#).

## 2. RINGS AS COLLISIONAL OBJECTS

### 2.1. The Collision Idea

The major breakthrough in our understanding of the curious ring galaxies came from two sources, namely the work of [Lynds and Toomre \(1976\)](#), and [Theys and Spiegel \(1977\)](#). In both cases ring galaxies were hypothesized to be the result of a head-on collision between a compact companion galaxy and a larger disk system. The resulting gravitational perturbation was shown to generate rings in the disk of the larger system. The backdrop to this rather startling idea was the earlier pioneering work on tidal interactions of [Toomre and Toomre \(1972\)](#) who had already begun to destroy the myth of the permanence of large scale galactic structure over a Hubble time. A common feature of the collisional ring formation picture is the generation of radially expanding density waves resulting from the crowding of stars in the disk. (A more complete description of the kinematics and dynamics is presented in [Section 4](#).) Although the most coherent effects are likely to be found in the dynamically cool disk stars and gas, the central perturbation will also have consequences for the halo stars and any dark matter present.

[Lynds and Toomre \(1976\)](#) first presented the elegant conceptual model that forms the basis of our understanding of the ring galaxy phenomenon. In the simplest form of this model, a small companion galaxy is assumed to pass down the symmetry axis of the larger primary galaxy, and move through the disk center. Prior to the collision the stars in the primary disk are assumed to be in circular orbits. At the time of impact the disk stars feel a strong pull toward the center as a result of the companion's gravity. (Note: the cross section of each star is so small that virtually all of the stars in the two galaxies will pass by each other in the "collision"). In the simplest case we also assume that the collision is so rapid that the disk stars do not have time to adjust to the sudden inward impulse. Specifically, in the so-called **impulse approximation (IA)**, the stellar positions are assumed to be the same immediately before and after the collision, but after the collision each star has acquired an inward radial velocity (see e.g., [Tremaine 1981](#)). As long as the perturbation is not too large, the resulting stellar orbits in the disk can be well approximated by radial epicyclic oscillations about a guiding center, i.e., the precollision orbit. Lynds and Toomre graphically illustrated this with the example of planetary orbits following a hypothetical near collision between the Sun and another star. This solar system example also reminds us of the ancient origin of epicycles as the simplest modification of "perfect" circular orbits.

Once we assume that the perturbing force only affects the disk stars for a short time, then subsequent motions are purely kinematic. Specifically, this **kinematic approximation** neglects the effects of the self-gravity of the perturbation. It is especially appropriate for collisions with large relative velocities (e.g., such as probably occur in galaxy clusters). The kinematic approximation assumes a decoupling of the perturbation from the resulting motions without specifying how the perturbation is derived.

After the companion passes through, the disk, individual stars begin their epicyclic oscillations. In general, the period of these

oscillations increases with radius throughout most of the disk. For example, in a flat rotation curve disk the epicyclic frequency scales as  $\kappa \propto v/r$ , so the period scales as  $P \propto r$ . Thus, while the stars at a given radius have rebounded and begun to move outwards, those at a slightly larger radius are still moving inwards. The consequence of this radial dispersion is that stellar orbits will bunch or crowd at some radii, yielding high densities there (see [Toomre 1978](#)). At other radii the orbits spread, giving rise to rarefied regions. These effects are well demonstrated by radius versus time diagrams. [Figure 3](#) shows the first such used for ring galaxies by [Toomre \(1978\)](#). The region of orbit crowding propagates outward as a density wave.

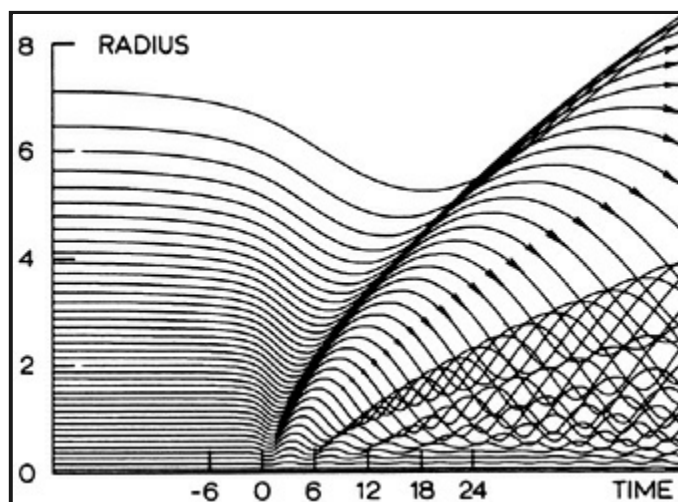


**Figure 3.** Radial trajectories of 40 particles from the symmetrical encounter model of [Toomre \(1978\)](#). The crowding of the particles into the "rings" is clearly demonstrated in this pioneering model.

[Figure 3](#) illustrates several other important points. In the first ring the orbit crowding occurs almost exclusively among particles rebounding outward. It also shows that a determination of the outflow velocity of an individual star or HII region in some part of the first ring probably gives a good indication of the outflow of all of the material in that region. In the second ring, infalling and outflowing stars cross each other in a sharply defined high-density region with sharp caustic edges. This is a qualitatively different behavior, and will be further examined in [Section 4](#). In this case, determining ring propagation speeds from individual stellar, HII region or gas cloud radial velocities is much more problematic.

The orbit crossing zones become wider in later rings, and they overlap each other. This radial phase mixing, together with the fact that the later rings include ever fewer stars, eventually renders the rings indistinguishable and ultimately invisible. There are a couple of caveats, however. First, even at very late times, the simple models indicate that individual rings can separate out at large radii. Secondly, even when the rings overlap, some memory of the collision is retained in the continuity of epicyclic phases with radius. Eventually collisional diffusion, through interactions between stars and massive molecular clouds, will erase this memory too.

Thus far, we have only considered perturbations to stellar orbits within the initial plane of the primary disk. This is justified because the perturbations *perpendicular to the disk plane* (i.e. in the "z" direction) are second order in the radial perturbation amplitude in the impulse approximation. The companion pulls the stars upward in the z direction when it approaches from above, and downward after it passes through. On the other hand, *in-plane radial impulses* are first order. This is because the companion pulls disk stars radially inward, towards the galaxy's center, when it is both above and below the plane. Yet in the z-direction, even second order effects can be important, especially when the companion is massive and moving slowly. Numerical simulations show several very interesting effects. One example is a vertical tidal effect that was well illustrated by [Lynds and Toomre's \(1976\)](#) [Figure 5](#), reproduced in [Figure 4](#). This figure shows that, as the companion approaches, stars in the central regions of the primary are pulled up towards it more than stars in the outer disk. Similarly, once the companion passes through the primary, stars near the center follow it downward while the outer disk stars are still moving upwards. Viewed edge-on the outer disk appears to flap like a bird's wings relative to the primary center. In conventional terms this leads us to expect a significant warping of the disk in any relatively young ring galaxy. Indeed, there is evidence from simulations ([Appleton and James, unpublished](#)) that the flapping can become so vigorous that stars in the outermost disk can be shaken off.

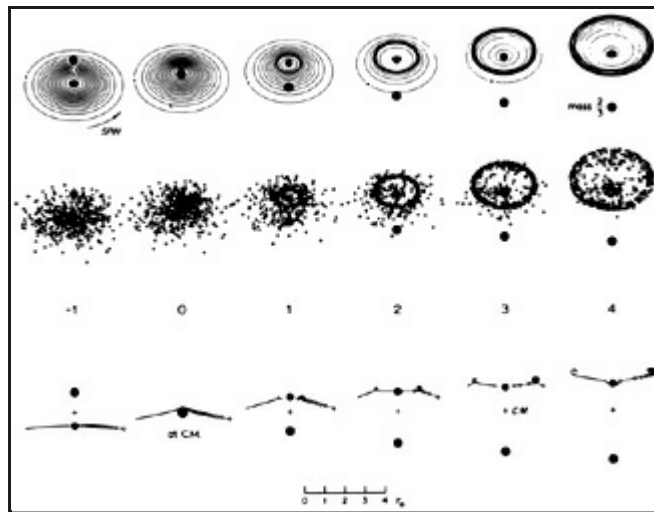


**Figure 4.** The first numerical simulations of collisional ring galaxies (Lynds and Toomre, 1976). The companion mass is  $2/3$  of the target mass, and "time is reckoned in units of  $(r_0^3 / GM)^{1/2}$ ", where  $M$  is the target mass, and the scale length  $r_0$  is shown.

## 2.2. Morphology of Ring Galaxies and Ring Galaxy Samples

The first paper that attempted to classify collisional ring galaxies was Theys and Spiegel's first, mainly observational, paper on ring galaxies (Theys and Spiegel 1976). They compiled a list of likely collisional rings based on miscellaneous early accounts of rings and developed a simple morphological classification scheme. Theys and Spiegel defined three basic ring types. The first, in some sense the "pure" ring, was the RE galaxy, defined as a galaxy which appears photographically as a well defined, approximately elliptical ring without a central nucleus. Although sometimes referred to as "Empty Rings", we now know, through modern CCD observations, that the rings are filled with redder light throughout the interior of the galaxy. Perhaps a better description of the empty rings would be to call them "centrally smooth" rings. Examples of this kind of ring are [Arp 146](#), [Arp 147](#), [VII Zw 466](#) and [AM 0051-271](#). However, in order to extend the study to objects that they considered to be close relatives of the RE galaxy, they also defined RN galaxies as galaxies containing an off-centered nucleus and the RK galaxies as ring-like galaxies with a prominent knot embedded within a markedly asymmetric light distribution. Perhaps the most famous of the RN galaxies is the [Cartwheel \(A0035-33\)](#) shown in visible light in [Figure 1](#). Although the [Cartwheel](#) is almost certainly a collisional ring system, Theys and Spiegel were aware of the sometimes difficult task of distinguishing between rings which may have been formed by collisions and the "resonance" ringed or pseudo-ringed galaxies first discussed by De Vaucouleurs and recently catalogued by Buta (1994, see also [Athanasoula and Bosma, 1985](#)). The RN class could potentially contain rings formed by processes other than that of galaxy collisions, although most of the resonance rings appear to contain symmetrical nested rings, whereas the RN rings are notable because the inner ring or nucleus is offset from the geometrical center of the ring. [Theys and Spiegel \(1976\)](#) also noted that the rings became increasingly elliptically shaped along the classification sequence RE, RN and RK. In addition, they also pointed out that very few rings were more flattened than  $b/a = 0.4$  ( $b/a$  is the ratio of the minor to major axis dimensions). This latter point is an indication of strong selection effects in many samples of ring galaxies, since ring galaxies seen nearly edge-on would be hard to recognize.

Very few ring galaxies have more than one ring. The [Cartwheel](#) has two rings, and the Vela ring galaxy has at least two rings, the inner of which emits strongly in  $H\alpha$  emission ([Dennefeld, Laustsen and Materne 1979](#); [Taylor and Atherton 1984](#)). Recently it was discovered that [Arp 10](#) has two  $H\alpha$  emitting rings and segments of a third outer ring ([Charmandaris Appleton and Marston 1993](#)). In these cases, the multiple ring systems are physically large. The development of multiple ring structure is not unexpected from the collisional models of [Lynds and Toomre \(1976\)](#) and their existence is a sign that the collision was not recent. Multiple rings and their relative spacing can be used to constrain the mass distribution of the target galaxy (see [Section 4](#)).

In the presentation of their small ring sample, [Theys and Spiegel \(1976\)](#) discussed a number of possible interpretations for ring galaxies. They noticed that, with the exception of [II Zw 28](#) (a small RK ring), all of the other ring galaxies had small companions within a few ring radii and that many of them lay within a few degrees of the projected minor axis of the ring. It was suggested that one very likely explanation for their structure was that the companion had passed through the center of the disk and was caught leaving the scene of the crime! In the simplest situation, that of a companion passing down the spin-axis of the target

disk, one would expect the companion to be seen close to the projected minor axis of the ring as observed. However, there was an apparent complication. It was not clear that the rings were intrinsically circular. For example, if the rings were truly elliptical but seen at some random viewing angle projected onto the sky, then the minor axis of the observed ring galaxy would not in general coincide with the rotation axis of the target disk projected onto the sky. [Theys and Spiegel \(1976\)](#) were concerned that the degree of flattening of the rings did not appear to be consistent with the position of the companion galaxy on the sky. Most of these problems have now been removed since it has been demonstrated that quite good rings can be created even with highly inclined collision trajectories and with moderately off-center collisions ([Huang and Stewart 1988](#); [Appleton and James 1990](#)). In slightly off-center collisions, the companion does not travel exactly down the spin-axis of the target and so, in general would not be expected to appear projected onto the center of the ring when viewed almost perpendicularly to the disk.

A less detailed classification scheme, but statistically more significant piece of work was performed by [Few and Madore \(1986\)](#) based on the extensive southern galaxy surveys of [Arp and Madore \(1977\)](#) and the *Catalogue of Southern Peculiar Galaxies and Associations* (CPGA) by [Arp and Madore \(1987\)](#). By a careful analysis of southern ESO and SERC J Schmidt plates, Few and Madore separated 69 ring galaxies into two main classes, the O-type and P-type galaxies. The O-type galaxies contained a central nucleus and smooth regular ring, whereas the P-type systems often contained an offset nucleus with a knotted ring. Both classes contained a fraction of barred galaxies. If the ring galaxies were caused by a collision, the authors argued, then companion galaxies should be found close to the ring at a higher frequency than that expected by chance. They therefore searched for companion galaxies in an area of up to 5 times the angular-diameter of the ring. In order to estimate the possibility of chance coincidences, control fields were also studied from each plate containing a ring galaxy, in order to estimate the local average surface density of galaxies in a similar direction to the ring on the sky. The results of the statistical tests were that P-type rings showed an excess of companions with small separations (separations of less than 2 ring galaxy diameters). For larger separations, the number of possible companions was found to be indistinguishable from that expected by chance. The O-type galaxies did not show any enhancement of possible companions over that expected by chance. They concluded that the P-type galaxies were good candidates for collisional galaxies and that the majority of the O-type galaxies were not. The O-type galaxies were found to be similar to the (R)S galaxies of [de Vaucouleurs, de Vaucouleurs and Corwin \(1976\)](#).

An important contribution made by Few and Madore was an estimate of the space density of ring galaxies. 214 ring galaxies are listed in the CPGA and the catalog is complete up to a declination of  $-21^\circ$ . They estimated that the volume space density of ring galaxies is  $5.4 \times 10^{-6} h^3 \text{ Mpc}^{-3}$  (here  $h = H_0/100$ ). This corresponds to an average of one ring galaxy in every spherical volume of radius  $35 h^{-1} \text{ Mpc}$ . This value is probably the most reliable measurement obtained so far for ring galaxies, and is in approximate agreement with two earlier, but less rigorous estimates made by [Freeman and de Vaucouleurs \(1974\)](#) and [Thompson \(1977\)](#).

The volume space density of rings derived above is about a factor of  $10^4$  less than the space density of average moderately luminous disk galaxies. Few and Madore were able to show that the scarcity of rings in nearby galaxy samples is consistent with the collisional formation picture. For example, the authors estimated that, because of the need to restrict the collisions to nearly bulls-eye impacts, only one in 5000 collisions would be expected to produce a ring (these restrictions may be a little conservative, see [Section 5](#)). Furthermore, the short lifetime of the ring phenomenon (typically a few  $\times 10^8$  yrs) further reduces the probability that a ring galaxy would be observed at any given instant. No comparable study has yet been made in the northern sky.

A question that is relevant to the statistics of nearby companions of rings is whether the companion always survives the encounter. In [Appleton et al. \(1987\)](#) we speculated that the long HI plume associated with [Arp 143](#) might be the remnant of a galaxy disrupted by the impulse it received after passing through the center of [NGC 2445](#). In cases such as [Arp 284](#) or [AM 1724-622](#), small companions are probably seen in the process of at least partial disruption. This process will become more significant if the intruder is both small and loosely bound. It is possible that, if the impulse the intruder receives becomes larger than its own binding energy, that is if  $(\Delta V)_{\text{impulse}}^2 \geq 2GM'/R'$ , the companion is unlikely to survive the encounter and would be severely disrupted. In such a case, the companion would likely be spread over a large area of sky, making its detection difficult, at least at optical wavelengths. Extremely deep optical and HI radio imaging around empty rings is long overdue to search for "relics" of such ill-fated companions.

### 2.3. Some Early Ideas about Ring Formation

Although now thought to be an unlikely interpretation of ring galaxy formation, it is of interest to review briefly the ideas of [Freeman and de Vaucouleurs \(1974\)](#). Their model was essentially a collisional one, involving the gas dynamical interaction of a cool intergalactic hydrogen cloud (IGC) with a pre-existing galaxy containing an external HI ring. This collision was expected to strip away the HI ring from the underlying galaxy, leaving behind the bulge which would lie on the minor axis of the HI ring. Subsequent star formation in the HI was believed to provide the characteristic ring galaxy appearance. [De Vaucouleurs and de Vaucouleurs \(1975\)](#) also suggested a similar mechanism for the formation of the ring in [NGC 985](#) (a Seyfert 1 galaxy). Although many ring galaxy candidates were mentioned by Freeman and De Vaucouleurs, two particular galaxies were discussed in detail.

They were [Arp 144](#) and [NGC 2444 / 5 = Arp 143](#). The case of [Arp 144](#) was particularly compelling, since the morphology of the ring seemed to suggest that the intruding cloud was caught in the act of peeling the ring away from the disk of the target galaxy. (The ring has a peculiar "folded" appearance on some optical photographs). The case for [Arp 143](#) was less secure, since [Burbidge and Burbidge \(1959\)](#) had already demonstrated that the "ring" in this case seemed to contain a nuclear "knot" in addition to the supposed displaced bulge. However, the overall morphology was approximately consistent with an IGC-galaxy collision. Burbidge and Burbidge suggested themselves that [NGC 2445](#) might have "formed in the wake" of the elliptical-like component, although no specific details were given.

Later searches for galactic-scale HI clouds have in almost all cases failed (Lo and Sargent 1976), although a few large HI complexes are known. Some of the known clouds are probably an extreme form of low-surface-brightness galaxy (see [Briggs 1990](#); [van Gorkom 1993](#)). It is now believed that the space density of truly isolated neutral hydrogen clouds is probably too low to account for the ring galaxies.

Secondly, the case for an interaction between a pure HI cloud and a galactic disk is almost certainly ruled out in two out of three of the above prototypical cases presented by Freeman and de Vaucouleurs. In the case of [Arp 144](#), [Joy et al. \(1989\)](#) have made near-IR observations of the system and conclude that it contains not one, but two nuclei: the second one heavily obscured by dust in the visible part of the spectrum. It would appear that [Arp 144](#) can now be explained in terms of an ongoing merger between two galaxies, without needing to invoke a separate HI cloud (see also [Higdon 1988](#)). The same is true for [NGC 985](#). There is now strong evidence that this system is also a double galaxy system (See [Section 3.5](#)).

The case of [Arp 143](#) is not quite so easy to dismiss as simply a two-galaxy interaction. At first glance, the huge HI streamer ([Appleton et al. 1987a, b](#)) extending away from it may be taken as evidence for the IGC model (see [Figure 5](#)). [Appleton et al. \(1987a, b\)](#) suggested that the ring-like morphology of [NGC 2445](#) (especially in HI) and the 150 kpc long HI streamer may be the result of a head-on collision between an HI rich low-surface-brightness galaxy and the disk of [NGC 2445](#). Evidently the plume is not a pure HI cloud, since faint traces of starlight are found associated with the plume, although it seems deficient in molecules ([Smith and Higdon 1994](#)). No completely convincing model has yet been put forward which explains all the known facts ([Appleton, Ghigo and van Gorkom, in preparation](#)).

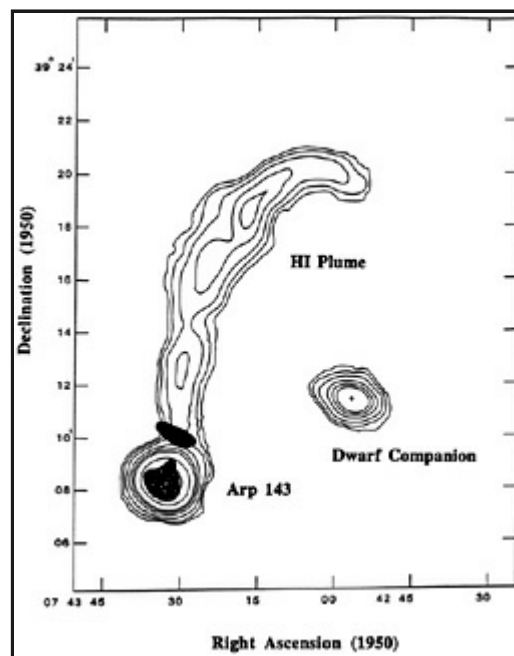


**Figure 5.** A contour map of the neutral hydrogen plume extending from the peculiar galaxy pair [Arp 143](#) (From Ghigo, Appleton and van Gorkom in preparation, using the *D* array of the VLA). The plume extends over an angular scale of more than 1/3 the diameter of the full moon. At the distance of [Arp 143](#), this corresponds to more than 200kpc in linear scale.

### 3. OBSERVATIONS OF RING GALAXIES

### 3.1. The Photometry and Colors of Ring Galaxies

The first quantitative indication that ring galaxies were blue came from global U-B and B-V photoelectric color measurements made by Theys and Spiegel (1976) for 4 ring galaxies (VIIZw466, I Zw45, IIZw28 and Arp 148). Colors were found to be in the range  $U - B = -0.24$  to  $-0.02$  and  $B - V = 0.3$  to  $0.7$ . Lynds and Toomre (1976) presented colors for IIH z4, also finding the ring to be blue.

The most detailed early study of the colors of an individual ring, VIIZw466, was the work of Thompson and Theys (1978). The work was based on the calibration of KPNO 4m prime focus photographic plates through  $U$ ,  $B$  and  $V$  filters. The main conclusion of the study was that all the knots in the ring have  $B - V$  colors  $< 0.4$ . The authors favored an explanation for the knots as being regions of young stars formed recently in a burst, although other constant star formation models were also considered as plausible. Figure 2b shows a peculiar loop or knot which extends inside this well defined ring. The knot appears much redder ( $B - V = 0.76$ ) than the other knots, leading these authors to speculate that the knot might be the remnant of a displaced nucleus of the precursor galaxy (a possibility also conjectured by A. Toomre). Recent observations by Appleton and Marston (1995) do not support this idea. Indeed, the reddest region of the ring lies between the knot and the geometrical center of the ring. It is very likely that the knot is a star forming region.

Although the main result of the Thompson and Theys study was the extreme blue colors of individual knots, another interesting result emerged from their study, one which is now known to be a common property of ring galaxies, namely the hint of radial color gradients. In addition to the knots, the colors of three extended regions inside the ring were also measured and found to be redder in both  $U - B$  and  $B - V$  color than the knots. This result is confirmed by recent CCD observations by Appleton and Marston (1995).

Another indication of color gradients in rings came from the discovery of the high redshift ring ( $z = 0.24$ ) from optical identifications of a deep radio survey (Majewski 1988). The ring's radio designation is 52W-036 (Windhorst et al. 1984) and it was recently observed as part of a driftscan CCD galaxy survey being carried out at Mt. Hopkins, and has the name KRN93-301 from that catalog (Kent, Ramella & Ninino 1994). Majewski observed the galaxy in UBVR and the infrared K-band. This was the first published near-IR image of a ring galaxy. After applying a substantial K-correction the ring was found to be quite blue ( $U - B = -0.79$ ,  $B - V = 0.44$ ) in line with other ring galaxies. Majewski noted that the morphology of the ring changed substantially from the blue, where it was crescent shaped, to the infrared, where it appears as a double source. The second source is probably the intruder galaxy. The change in morphology as a function of wavelength, appears more dramatic in 52W036 than that seen in the lower redshift rings (see below) and may indicate that it contains a substantial amount of dust.

Perhaps the most spectacular example of large radial color gradients is found in Zwicky's Cartwheel ring galaxy (Figure 1). Re-discovered by Lu (1971), the Cartwheel is perhaps the prototype ring galaxy. However, as we shall show later, it is far from representative of most ring galaxies in its global properties. In addition to the outer ring, there is a well defined inner ring (most easily seen in the near IR observations of Joy et al. (1988)). The Cartwheel was shown to contain extremely blue knots by the pioneering spectrophotometric study of Fosbury and Hawarden (1977). Strong optical and IR color gradients were found in the Cartwheel by Marcum, Appleton and Higdon (1992) and Higdon (1993). The change in color in the  $V - K$  color index was found to be over 2 magnitudes from the outer ring to the central nucleus (Figure 6). The colors are in approximate accord with a simple starburst model in which the stars are born in the ring with blue colors and evolve in the wake of the ring. These color changes are significantly larger than those found in normal spiral disks (typically no more than one magnitude in  $V - K$ , see de Jong 1995).

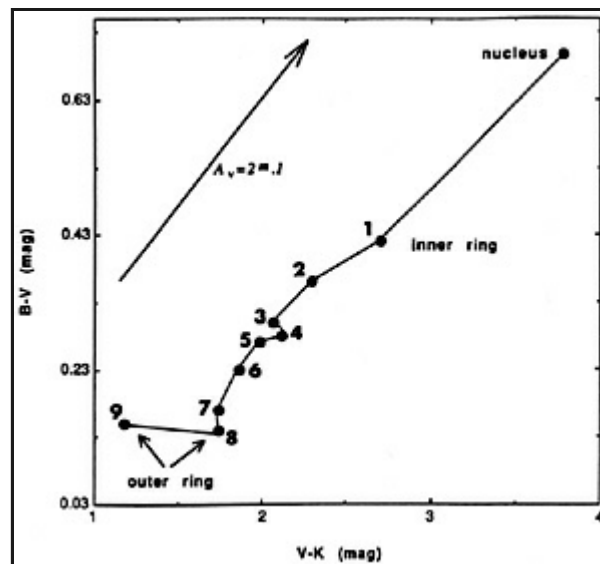


**Figure 6.** Figure 3 from Marcum, Appleton and Higdon (1992) showing the change in  $V - K$  color equally spaced annuli as a function of  $B - V$  color. The numbers refer to radius of the annulus, with 1 being the center and 8 and 9 being in the outer ring. Further results are also shown in Higdon (1993).

Recent observations of a sample of northern ring galaxies by Appleton and Marston (1995; see also Lysaght 1990) show that most of the larger ones observed exhibit radial color gradients similar to the Cartwheel. Figures 7a and 7b show two new examples, VII Zw 466, the RN ring LT41 (Thompson 1977). A similar result is found for Arp 10. These figures clearly show the radial change of color, from blue in the outer ring to red in the center, pixel by pixel across the face of the galaxy. The radial color gradients provide perhaps the clearest and most beautiful evidence that stars are born suddenly in the rings and are left behind as the ring wave expands further into the disk. (Note: The possibility that dust absorption is responsible for the color gradients will be tested with IR observations with ISO.)

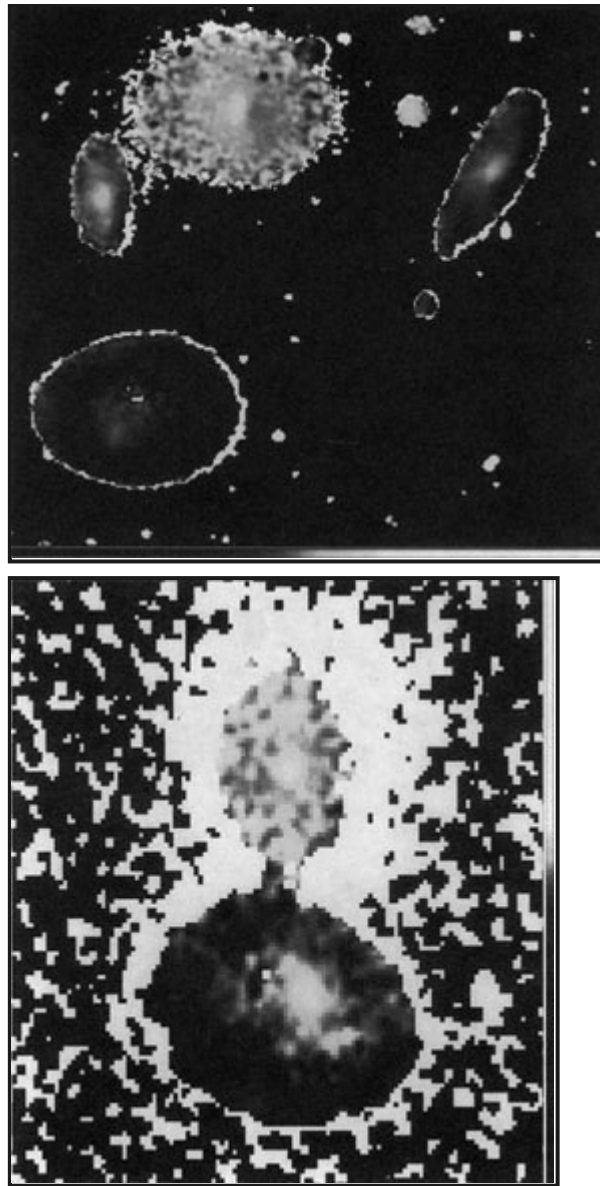


**Figure 7.** a) False color representation of the  $B - R$  color change in the VII Zw466 group. The colors represent changes in  $B - R$  color from the outer edge of the ring which are blue to the center which are significantly redder. In the picture (as in Figure 7b), the reddest regions in the galaxies are represented by yellow, the bluest by blue (see color bars). For comparison, notice the red featureless colors of the elliptical companion (Top). (See Color Plate IV at the back of this issue.)  
 b) A false color representation of the  $B - R$  colors of LT 41 (see caption for Figure 7a). (See Color Plate V at the back of this issue.)

Observations also provide additional confirmation that the basic expanding ring picture is correct. For example, the simple kinematic picture of an off-center collision (e.g. Toomre 1978; Appleton and Struck-Marcell 1987b) predict a strong rarefaction behind the densest part of the ring. Such a rarefaction would have two observational consequences. Firstly, the surface density of the original target disk would be significantly reduced just inside the segment of the ring with the highest surface density. Indeed, the  $2.2 \mu\text{m}$  IR emission is significantly reduced inside the bright southern segment of the Cartwheel (Marcum, Appleton and Higdon 1992). Secondly, the rarefaction should lead to a characteristic jump in velocity across the ring. In the leading edge of the ring, radial velocities are expected to be mainly directed outwards, whereas just inside the ring, the velocities should be

infalling. In principal, the measurement of this velocity jump would be another diagnostic of the ring models. This second diagnostic is far more difficult to measure because it requires the presence of gas on both sides of the ring. Most of the ionized gas in ring galaxies is concentrated in the rings (Fosbury and Hawarden 1977; Taylor and Atherton 1984; Marston and Appleton 1995) and so is not useful for this kind of measurement. Cooler interstellar gas (either HI or molecular emission) holds the best promise for this kind of measurement. A hint of such a change in velocity across the ring is seen in Higdon's HI observations of the *Cartwheel* (Higdon 1993).

Twelve, mainly northern ring galaxies have been imaged by Appleton and Marston (1995) and Marston and Appleton (1995) through *B*, *V*, *R* broad-band and narrow-band  $H\alpha$  filters. In addition,  $J(\lambda 1.25 \mu\text{m})$ ,  $H(\lambda 1.65 \mu\text{m})$  and  $K(\lambda 2.2 \mu\text{m})$  near-IR images were obtained of the same sample. The main aim of the study is to investigate the optical-IR colors of the ring galaxies and to test models of star formation. The results provide the first systematic study of the global properties of ring galaxies.

The median *B* - *V* and *V* - *K* color of the ring galaxies in the sample are 0.52 and 2.31 magnitudes respectively, confirming the earlier results that the majority of the ring galaxies are blue and contain a substantial young population. The results show that the global *B* - *V* colors are not dependent on the linear size of the rings. On the other hand, there is a suggestion that when the optical to infrared baseline is used, a trend emerges. Larger ring galaxies appear to have larger *V* - *K* colors than small ring galaxies (see Figure 8). This result, which is consistent with the discovery of large radial color gradients, supports the view that larger ring systems are more evolved objects from a stellar evolutionary point of view. In the smaller ring galaxies the dominant emission comes from young stars in the ring. However, as we proceed to larger systems, the overall color of the galaxy becomes more and more dominated by the redder material inside the bright blue rings leading to the trend seen in Figure 8. This result suggests that, at least in some cases, any pre-existing stellar disk contributes only in a minor way to the overall luminous output of ring galaxies. This is probably only true in the case of the gas-rich systems, which dominate in samples of northern ring systems.

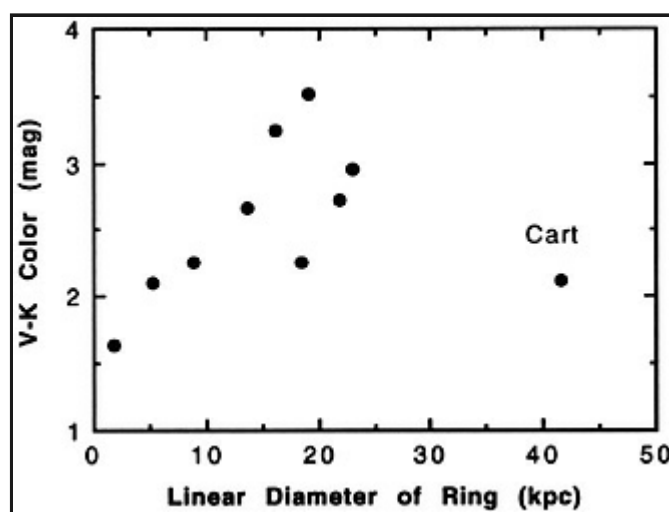


**Figure 8.** A plot of the optical to near-IR color (*V* - *K*) versus the linear diameter of the ring galaxy (from Appleton and Marston 1995).

### 3.2. Observation of the Diffuse and Molecular Gas Content of Ring Galaxies

Silverglade and Krumm (1978) made *Arecibo* observations of eleven ring galaxies and detected six of them. The authors concluded that the HI masses of ring systems were not significantly different from those of "normal" spiral galaxies. Observations at *Parkes* of the *Cartwheel* by Mebold, Goss and Fosbury (1977) showed that it contained significant amounts of neutral hydrogen. In the Ph.D Thesis of Jeske (1986), 16 out of 28 ring galaxies were detected using the *Arecibo* radio telescope.

Very few high-resolution aperture synthesis HI observations have been made of classical ring galaxies. In a VLA study of NGC 2793 by Ghigo, Hine and van der Hulst (in preparation), the HI was found to be clumpy and concentrated mainly in the bright knotty parts of the ring. Kinematically, this galaxy, identified as ring galaxy number 6 of Thompson's (1977) list, shows a rising rotation curve and the kinematics of the ring are consistent with a large expansion velocity (see section 3.3). (We note that new observations at the VLA have recently been made (J. Higdon, personal communication) and these higher sensitivity observations will soon be available.)

The Cartwheel ring galaxy has been the subject of a very detailed and elegant HI study by Higdon (1993) as part of his Ph.D thesis. Figure 9 shows that neutral hydrogen emission is seen associated with the ring, with some additional material found both outside and inside the ring. The HI surface density is lower in the region of the bright HII regions in the southern quadrant of the ring, but has a clumpy distribution that roughly follows the outer ring. Gas is concentrated in regions of the ring with less active star formation and some gas is found outside the ring. Although there is no obvious major concentration of gas associated with the spokes, a faint component of HI emission is found inside the ring. In general though, very little HI is found inside the ring. The kinematic results from these observations have been used by Struck-Marcell and Higdon (1993) to constrain models of the mass distribution in the Cartwheel and as the basis on numerical models of the collision (see Section 6.3). As in the case of NGC 2793, a rising rotation curve was found.

Figure 9 also shows another important fact. The extended HI emission found outside the Cartwheel is very asymmetrically distributed in the Cartwheel group: all of it being found in the general direction of the companions to the NE. A faint filament was discovered by Higdon (1993) extending from the Cartwheel all the way to the most distant companion G3. The asymmetric nature of the HI relative to the Cartwheel is strongly suggestive of an impact from the south-west which has scattered debris into the northeast quadrant. This is further evidence that the Cartwheel was formed by a collision.

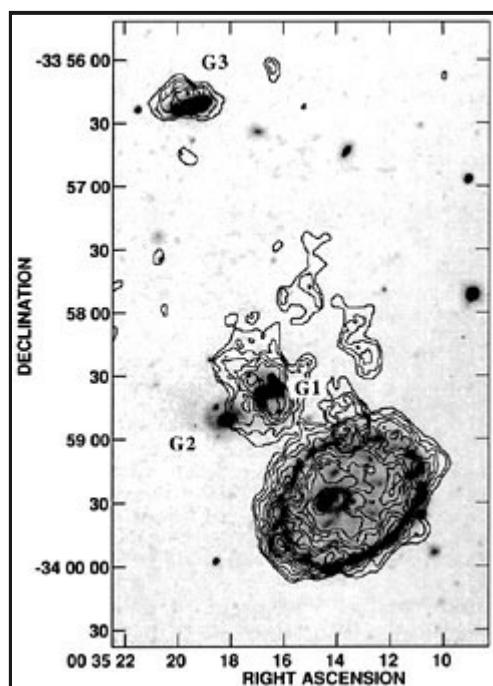


**Figure 9.** James Higdon's medium resolution ( $10.7 \times 9.1$  arcsecs<sup>2</sup> FWHM) HI observations of the Integrated HI emission from the Cartwheel obtained using the combined B, C and D arrays of the VLA superimposed on a CTIO 4-meter prime-focus plate of the galaxy (Higdon 1993; Figure 3a of Ph.D thesis). Strong emission is seen associated with the ring and is stronger away from the regions of intense star formation. Fingers of HI also point inwards towards the center of the Cartwheel which is generally deficient in HI. Gas is also seen to the north-east associated with the late-type companion and the far northern companion. Much scattered low-surface-brightness emission is also seen in this region.

At the time of writing, a number of new HI studies are underway in both the northern and southern hemispheres. Work is being performed by J. Wallin (G.M.U.) and J. Higdon (N.R.A.O.) to study a number of southern ring galaxies including Vela and AM064-741. In the north VLA observations of VII Zw 466 and Arp 10 have been made by V. Charmandaris and one of us (PNA). HI emission was detected and mapped in both cases and the observations are currently being analyzed. Both galaxies

appear to have extensive HI disks extending well beyond the optical rings. It is clear that the next few years will bring new and interesting dynamical information to add to the mainly photometric studies of ring galaxies performed so far.

Another area in which new ground is being broken is in the study of molecules in galaxies. Only in the last few years have searches been made for molecular gas in ring galaxies. The most systematic study made so far is by [Horellou et al. \(1994\)](#), using the 30m diameter IRAM telescope in the North and the 15m SEST telescope in the southern hemisphere. Horellou and collaborators have detected 14 out of 16 ring galaxies in the  $^{12}\text{CO}(1-0)115$  GHz (millimeter) line and six were also detected in the  $^{12}\text{CO}(2-1)230$  GHz transition. **The inferred total mass of  $\text{H}_2$  in the rings is, on average, twice the value of a control sample of normal galaxies.** A strong correlation was found between the implied  $\text{H}_2$  mass and the far IR luminosity of the galaxies, suggesting that the existence of copious molecular material encourages high star formation rates. In contrast, like Silverglade and Krumm before them, the authors conclude that the HI content of ring galaxies is similar to that of normal late-type galaxies.

Unlike nuclear starbursts, ring galaxies contain star formation regions exclusively in the ring. It is therefore of considerable interest to see how the molecular material is distributed. Unfortunately, very few of the rings detected by Horellou et al., were spatially resolved by the 30m IRAM telescope. Those that were, provide no obvious pattern. In [IIH4](#), emission was observed from the brightest star forming regions of the ring and very little from the center. On the other hand, the case of the Seyfert ring galaxy [NGC 985](#) is quite different. Here the emission is strongly centered on the "empty" region of the ring, although considerable emission is also seen associated with the peculiar star forming "bar" extending from the Seyfert nucleus. A clear understanding of the distribution of molecules in ring galaxies will have to wait mapping of the galaxies with millimeter aperture synthesis telescopes which will provide much higher spatial resolution.

The two ring galaxies not detected in the CO line by Horellou et al. are interesting. One of them is [II Zw 28](#), the small RK ring shown in [Figure 10](#). The upper limit to the total inferred  $\text{H}_2$  mass from [II Zw 28](#) is  $< 8.5 \times 10^8 M_{\odot}$ . Interestingly, this galaxy is only barely detected as a faint IRAS source, possibly indicating a lower level of star formation activity than other rings. On the other hand, [II Zw 28](#) has a high  $\text{H}\alpha$  luminosity similar to other ring galaxies observed by [Marston and Appleton \(1995\)](#). [II Zw 28](#) is one of the few galaxies to exhibit unusually strong Balmer absorption lines interior to the ring ([Sargent 1977](#); [Charmandaris and Appleton 1994](#)) and it is conceivable that a major burst of star formation has occurred in the recent past which has used up a large fraction of the molecular reservoir in this galaxy, as well as depleting its dust content. New HST observations ([Appleton et al.](#), in preparation) show two possible companion galaxies, one of which is of very low surface brightness.

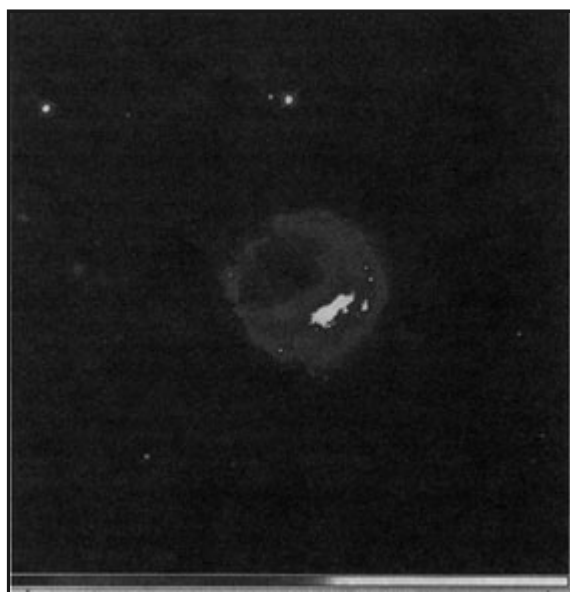


**Figure 10.** The RK ring galaxy [II Zw 28](#), like [Arp 147](#), was well known as an empty ring with no obvious companion. This I-band Hubble Space Telescope image shows both a possible companion seen just inside the ring. ([Appleton et al.](#) in preparation). (See Color Plate VI at the back of this issue.)

The other non-detection in the  $^{12}\text{CO}$  ( $J = 1-0$ ) line (made with SEST 43 arcsec beam) is the Cartwheel ring. Horellou et al place an upper limit on the  $\text{H}_2$  mass of  $M(\text{H}_2) < 1.5 \times 10^9 M_{\odot}$ . Because of the large angular size of the Cartwheel, a 5-point map was made and the total on-source integration time was 34 hours. Despite the non-detection of CO from the galaxy (the rms noise was 0.6mK in a  $30 \text{ km s}^{-1}$  channel after 34 hours of integration), the authors admit that the limit is not especially stringent. For example, they point out that the lower limit to the ratio of IRAS FIR flux to the molecular hydrogen mass,  $L(\text{FIR}) / M(\text{H}_2)$ , is  $> 17.7$ , which is not unusually high. Neither is the upper limit to the ratio of  $M(\text{H}_2) / L_{\text{B}} < 0.024$  unusually low, but lies within the range for normal galaxies. Other searches for CO from the Cartwheel have so far been inconclusive (Higdon, personal communication). As Horellou et al. point out, the Cartwheel may well contain significant quantities of molecular hydrogen, but may be deficient in carbon and therefore CO molecules. Oxygen atoms were also found to be deficient in the outer ring HII regions (Fosbury and Hawarden 1977).

### 3.3. Observations of Ring Kinematics

Some of the earliest studies of ring galaxies showed that the rings both expanded and rotated (e.g., Theys and Spiegel 1976; Fosbury and Hawarden 1977). Most optical spectroscopic studies of ring galaxies have involved obtaining long slit spectra at various position angles around the rings and assumed that the rings are true circles seen at some arbitrary angle (Jeske 1986; Few, Madore and Arp 1982; Charmandaris and Appleton 1994). If this simple assumption is made, the kinematics of the radial velocity field of ring galaxies can then be interpreted as both rotation and expansion of the ring. Typical ratios of radial expansion to rotation velocity in rings range from 5, in the case of NGC 985 ring to 0.1 in VII Zw 466 (from Jeske 1986). In Figure 11 we show this ratio plotted against the linear diameter of the ring. On naive grounds one might expect that the smaller rings may show larger radial expansion velocities than the larger rings, since the smaller rings presumably have responded to the perturbation most recently (1).

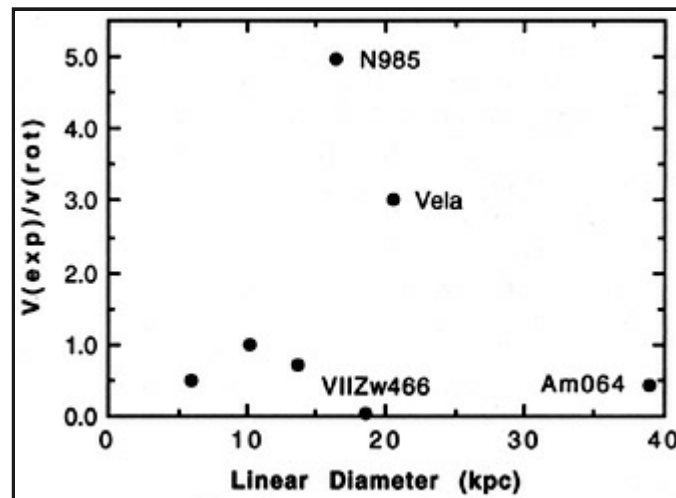


**Figure 11.** The ratio of  $V(\text{expansion})$  to  $V(\text{rotation})$  versus linear diameter from Appleton and Marston (1995) for a small northern sample of ring galaxies. On naive grounds it might be expected that the expansion velocity might dominate over rotation for small (young) rings as compared with larger more evolved systems. However no clear trend emerges (see text).

However, it seems that no clear trends emerge from this plot. NGC 985 and Vela (Taylor and Atherton 1984) show the largest expansion velocities relative to their small rotational velocities. However, it must be remarked that both these galaxies show marked deviations from simple ellipses and the assumption that their geometry is that of a deprojected circle may be incorrect. In Vela, the velocity field may be further complicated by the existence of a weak bar. Certainly for NGC 985 there is evidence that the ring is a tightly wrapped spiral probably resulting from a highly off-center collision (Appleton and Marcum 1993). In general, radial velocities tend to be comparable to or somewhat less than the local ring rotational velocity. Such values suggest that the perturbation is in most cases relatively strong.

Very few kinematic studies of ring galaxies have been published which provide full 2-dimensional information about the dynamics of ring galaxies. In cases where detailed  $\text{H}\alpha$  velocities are available around the entire ring (e.g., the TAURUS imaging of the Vela ring by Taylor and Atherton 1984) there are strong indications that a simple expanding and rotating circular

ring is only a first-order description of these data. Deviations are not altogether surprising. Firstly, if the companion makes a non-central collision, the ring will not be symmetrical, either in appearance or in the subsequent expansion of the ring into the disk. Secondly, if the companion is massive enough, it will induce large warping and other non-planar effects into the disk. The combination of these two effects is to lead to azimuthally dependent structure in the radial velocity field of the expanding ring.

In order to fully compare models to observation, it is necessary to detect the motion of the target disk both inside and outside the ring. Since the  $H\alpha$  emission is exclusively found in the ring component, observations have to rely on either detection of faint stellar absorption lines inside the rings (e.g., as in [IIZw28](#), Sargent 1977; Appleton and Charmandaris, in preparation) or from interstellar gas. As discussed above, very few galaxies have yet been mapped in the 21 cm HI line or in the CO millimeter line.

[Ghigo et al. \(1994\)](#) have performed VLA HI mapping of the ring galaxy [NGC 2793](#) with low spatial resolution. This galaxy has a companion which lies a few ring diameters away on the minor axis and appears to be a classical ring galaxy. The rotation curve is found to be rising from the inner regions to the outer edges of the ring, with evidence for significant non-planar motions in the gas. The best fit to a rotating and expanding ring was found in the regions of the optical ring, where the expansion velocity was found to be about one-half the rotation velocity at that radius. Asymmetries in the velocity field were observed and are to be expected in a collision in which the companion drives a 'banana' type wave of the kind discussed by [Appleton and Struck-Marcell \(1987b\)](#).

---

<sup>1</sup> The theory predicts that this depends sensitively on the structure of the gravitational potential of the ring galaxy (see [Section 4](#)). [Back](#).

### 3.3.1. The Cartwheel Galaxy and its Companions

An analysis of the velocity field of the [Cartwheel](#) is consistent with a slowly rising rotation curve ([Struck-Marcell and Higdon 1993](#); [Higdon 1993](#)) similar to that found in [NGC 2793](#). The ratio of ring expansion to ring rotation in the HI gas is significantly lower than that reported in the ionized component by [Fosbury and Hawarden \(1977\)](#), being around  $52 \text{ km s}^{-1}$  ([Higdon 1993](#)). Fosbury and Hawarden obtained a radial expansion velocity of  $89 \text{ km s}^{-1}$  based on optical spectroscopy of 5 HII regions. Unpublished work by Taylor and Atherton (1991) using Fabry-Perot imaging of the  $H\beta$  line emission provide a value of  $61 \text{ km s}^{-1}$ , in closer agreement with that of the HI observations. Based on Higdon's analysis, the time taken for the ring to reach its current radius (i.e., the time since the impact of the intruder) is approximately 300 million years. (assuming a value for  $H_0$  of  $100 \text{ km s}^{-1} \text{ Mpc}^{-2}$ .) Another interesting result of the [Cartwheel](#) HI observations is that neutral hydrogen surface density is significantly lower in the region of the bright star-forming knots in the southern quadrant of the ring. This may be due to the disruption of the HI clouds by the intense winds from the O-stars known to be present in the ring ([Fosbury and Hawarden 1977](#)).

Since the work of [Davies and Morton \(1982\)](#) there has been considerable debate not only about the identity of the intruder, but also whether the intruder candidates are massive enough to drive the observed expansion of the ring, and also create such a strong ring. The two galaxies nearest the [Cartwheel](#) (see [Figure 9](#)) were labeled G1, G2 by [Higdon \(1993\)](#) and a third more distant companion 3 arcminutes northeast of the [Cartwheel](#) G3. The question of the strength of the ring is addressed below. All three potential intruders have velocities close to the [Cartwheel](#) and are probable members of the group. G1 and G3 contain significant quantities of HI. The SO companion G2 was originally thought to be a high surface brightness elliptical by Davies and Morton (called Galaxy 3 by them). [Higdon \(1993\)](#) has analyzed the times needed for the three galaxies to reach their present projected separations if each was postulated to have passed through the center of the [Cartwheel](#), in the hope that this might rule out one or other of the companions. However, taking into account the projected distances and observed radial velocities, it appears that all three galaxies could have reached their current positions in the time needed to create the ring. There is no unambiguous "smoking gun".

[Davies and Morton \(1982\)](#) explored the idea that the early-type galaxy was the likely intruder. Based on a measurement of the central velocity dispersion, they calculated that the mass of G2 was approximately  $4 \times 10^{10} M_{\odot}$  (this would correspond to a mass of  $1.8 \times 10^{10} M_{\odot}$  for  $H_0 = 75 \text{ km s}^{-1} \text{ Mpc}^{-2}$ , a value we will use in the subsequent discussion here). Higdon's HI observations ([Higdon 1993](#)) provide a mass (similarly adjusted to common value for  $H_0$ ) for the [Cartwheel](#) based on the last measured point of the rising rotation curve of  $M(\text{total}) = 3.46 \times 10^{11} M_{\odot}$ , for an assumed inclination of 44 degrees. [Davies and Morton \(1982\)](#) pointed out that this very small implied mass ratio ( $\approx 1:20$ ) was a potential problem for the classical stellar model for ring formation (e.g., [Toomre 1978](#)). How could such a small mass intruder create such a dramatic ring? Indeed the ratio of the ring expansion to ring rotation velocity in the [Cartwheel](#) is approximately 20%, suggesting a larger perturbation than could be delivered by such a small companion. Do more recent observations shed further light on the problem? Davies and Morton speculated that the high contrast in the [Cartwheel](#) ring might result from the triggering of stellar birth in the ring, rather

than merely a classical bunching of old stars in the Lynds and Toomre picture. We believe that this is essentially correct. However, the question of relatively high ring expansion velocity is not so easily disregarded. We therefore reexamine the question of the mass ratio of the possible intruder galaxies.

The near-IR photometry of [Marcum, Appleton and Higdon \(1992\)](#) provided  $\lambda 2.2 \mu\text{m}$  magnitudes for all three potential companions as well as the [Cartwheel](#) itself. A surprising result of the *K*-band observations is that the early-type galaxy, G2 (in Higdon's terminology) and the more distant G3 are *only one magnitude fainter than the Cartwheel* at this wavelength. The third late-type companion (G1) is significantly less luminous at IR wavelengths although it exhibits evidence for new stars in its irregular disk ([Figure 1](#)). If we make the naive assumption that all the *K*-band light comes from old stars, we can use the relation of [Thronson and Greenhouse \(1988\)](#) to estimate the mass in old stars of the three companions and the [Cartwheel](#). The result of this approach is companions G1 through G3 have masses of 0.3, 2.5 and  $1.9 \times 10^{10} M_{\odot}$ , respectively, compared with the [Cartwheel](#) which, using the same argument, would have  $6 \times 10^{10} M_{\odot}$  of old stars. Notice that based on this simplistic argument, the mass ratio of old stars for G2 and G3 is 41% and 31% respectively of that found in the [Cartwheel](#). Hence we find that, in the absence of dark matter, the luminous mass of the companions is a substantial fraction of the luminous mass of the [Cartwheel](#). The assumption that all the *K*-band light originates from old stars is a dubious approximation, but seems in reasonable agreement with the dynamical mass derived for G2 by [Davies and Morton \(1982\)](#). In the [Cartwheel](#), supergiants may contribute a fraction of the light (see MAH) but this will serve to further increase the relative (old stellar) mass of the companion to the target galaxy.

We cannot, of course, ignore the dark matter. Based on the above argument, the [Cartwheel](#) contains significant quantities of dark matter, since  $M(\text{total}) / M(\text{old-star}) = 5.8$ . (Here  $M(\text{total})$  is taken from the HI work of [Higdon \(1993\)](#)). The crucial question, therefore, becomes one of the dark matter component of the companion galaxies. It is clear that if the companion galaxies (G2 or G3) contained dark matter fractions of the same order as the [Cartwheel](#), the perturbations needed to produce a substantial ring expansion velocity would be easily achieved. How likely is it that the companions have massive halos? [Higdon \(1993\)](#) has measured the masses of G1 and G3 using his VLA HI observations and finds total masses similar to those quoted above based on the old stellar population. However, it is not clear that the HI measures all the mass since the spatial resolution of the observations was insufficient to determine if the rotation curves were falling. Also, the fact that the mass derived for G2 based on the optical stellar velocity dispersion by Davies and Morton is comparable with the approximate mass derived from old starlight might suggest that this galaxy has little dark matter. However, it must be borne in mind that this was a mass derived for the central bulge of the galaxy. Recent observations with the HST confirm that G2 has two very extensive spiral arms and most likely has a larger mass than Davies and Morton inferred from what we now know to be the rather bar-like bulge of an SO. In conclusion, it seems likely that with the addition of modest dark halos, companion masses of the order of 20% of the [Cartwheel](#) are not out of the question for both G2 (the SO galaxy) and G3 (the more distant edge-on galaxy). [Davies and Morton \(1982\)](#) were probably correct to suspect that the contrast in the ring is a consequence of the triggering of star birth in the ring. Models suggest that such an effect could be produced in a companion with a mass as low as 15-20% of the mass of the [Cartwheel](#) ([Struck-Marcell and Higdon 1992](#); [Hernquist and Weil 1993](#)). More discussion of this interesting point can be found in [Section 6.3](#).

### 3.3.2. Model Velocity Fields

We conclude this section with some model velocity fields derived from hydrodynamic simulations by one of us (CSM). These provide a small glimpse of the rich velocity structure one might expect to see in future high resolution kinematic studies of ring galaxies. Model velocity fields are presented in [Figure 12 a-d](#) at four different times after the off-center collision of a 1/5 mass companion with a disk. They show the radial velocity field of the model as viewed along the original spin-axis of the target galaxy. The model is similar to that described by [Struck-Marcell](#) and [Higdon \(1993\)](#) and represents a model of the [Cartwheel](#) ring galaxy collision. A major effect in the velocity field is evident in [Figure 12a](#), namely that a large radial velocity gradient dominates at this early time. This gradient is primarily due to the differential motion of the gas clouds in the vertical direction in the inner disk relative to the outer disk, an effect which appears to dominate the appearance of the velocity field when viewed along this special direction, close to the axis of rotation. This vertical "flapping" of the disk is an interesting 3-dimensional effect and is likely to complicate the interpretation of the ring expansion velocities when the ring galaxy is viewed from a different orientation. This effect may, in part, explain the large apparent expansion velocities in the Vela ring galaxy. Later in the evolution of the model ([Figure 12b-d](#)), when the second ring and spokes begin to form, the disk exhibits significant warping which is reflected in the gradient in the velocity field, superimposed on the other motions. Also interesting is the fact that the lowest velocities tend to be found near the geometrical center of the outer ring, rather than centered on the inner off-center ring and spoke. Unfortunately, the [Cartwheel](#) ring contains very little HI in the central regions and so little is known about the actual velocity field of any faintly emitting gas in this region. Finally, it is clear that quite sharp velocity features are seen radially across the ring at late times. This is a result of 3-dimensional structure in the ring which becomes more pronounced as the ring develops. Similar effects have been observed in the simulations of [Gerber \(1993\)](#). We caution that if low spatial resolution observations of gas motions were obtained, this complex velocity structure might be interpreted as vertical outflow of gas in the ring. On the other hand, real outflows are quite likely because of the vigorous star formation present in most rings. In conclusion, none of the above effects have yet been unambiguously observed in ring galaxies because of the lack of available

high sensitivity, high resolution observations in neutral or molecular emission lines. It is clear that such studies, using either HI or CO emission as a probe, will ultimately provide one of the richest tests of the collisional model of ring galaxies. It is our hope that such comparisons will be made in the future.

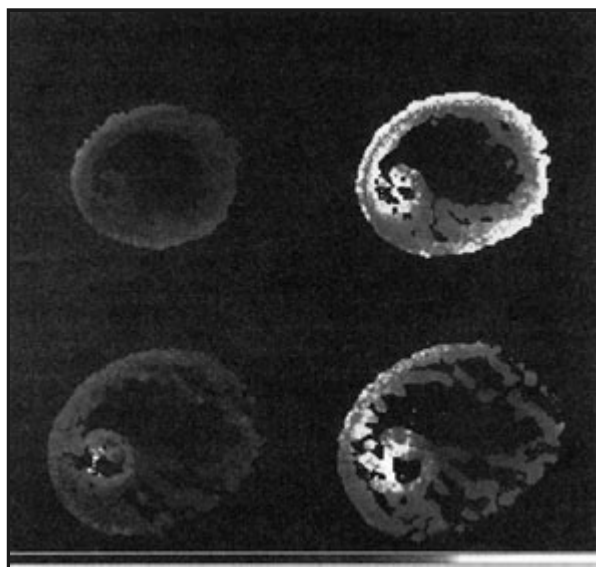


**Figure 12.** (a-d) False color pictures of the velocity field of a model ring galaxy at various times after an off-center collision (see text). (See Color Plate VII at the back of this issue.)

### 3.4. Star Formation Properties of Ring Galaxies

Shortly after the IRAS point source catalog became available it was realized that ring galaxies emit a substantial amount of luminosity in the far infrared ([Appleton and Struck-Marcell 1987a](#)). Many ring galaxies are IRAS sources at  $\lambda 100 \mu\text{m}$  and more have been detected at  $\lambda 60 \mu\text{m}$ , a result of the publication of the faint IRAS point source catalog. Ring galaxies, like other collisional galaxy systems, exhibit higher than normal 60/100 micron color temperatures and range in far IR luminosity from  $10^{10} L_{\odot}$  to a few  $\times 10^{11} L_{\odot}$ . It was argued by Appleton and Struck-Marcell that, in most cases, the bulk of the FIR emission was from extended regions of star formation. A similar conclusion was drawn independently by [Jeske \(1986\)](#) and [Wakamatsu and Nishida \(1987\)](#).

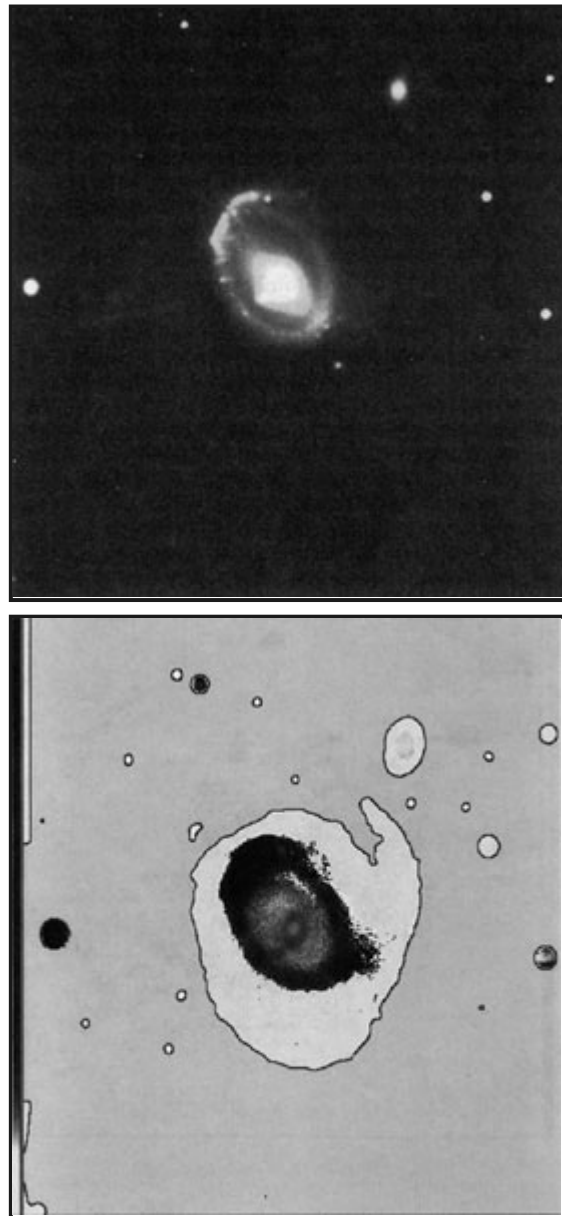
Until recently, very little systematic work has been done on the star formation properties of ring galaxies. The first detailed study of star formation in ring galaxies was made by [Fosbury and Hawarden \(1977\)](#), and they showed that the [Cartwheel](#) ring contains large numbers of O and B stars concentrated in bright knots around the ring. The recent study of the [Cartwheel](#) by [Higdon \(1993\)](#) confirms these results, considerably adding to our knowledge of the optical emission-line properties of this galaxy. These results will soon be published (Higdon, in preparation). Higdon found that the total energy output of the [Cartwheel](#) in the  $H\alpha$  line was a factor of 10 times larger than that of the most luminous normal late-type spiral studied by [Kennicutt \(1988\)](#). An interesting result of Higdon's study was the discovery that 80% of the  $H\alpha$  emission from the [Cartwheel](#) comes from just one quadrant of the outer ring, the rest coming almost exclusively from the other three quadrants of the outer ring. Like Fosbury and Hawarden before him, Higdon did not detect  $H\alpha$  emission from the inner ring, despite predictions from numerical models that the inner ring should contain highly compressed gas ([Appleton and Struck-Marcell 1987b](#); [Hernquist and Weil 1993](#)). In addition, 15% of the line emission was found to lie in a diffuse component associated with the ring, but not directly attributed to discrete star formation knots.

The brightest HII region complexes in the [Cartwheel](#) have  $H\alpha$  luminosities in excess of  $10^{41} \text{ ergs cm}^{-2} \text{ s}^{-1}$ , which is at the extreme end of the luminosity function for HII regions in late-type spirals. Higdon found that the total (instantaneous) star formation rate from the galaxy is currently  $67.5 M_{\odot} \text{ yr}^{-1}$  (assuming a Miller-Scalo IMF). This is 9.1 times the star formation rate estimated from the B-band luminosity which is sensitive to the integrated star formation rate over the last 15 Gyrs. Given the HI Mass ( $1.3 \times 10^{10} M_{\odot}$ ) distributed in the ring galaxy, Higdon found that the gas consumption timescale was 430 Myrs, a timescale similar to the ring propagation timescale.

[Marston and Appleton \(1995\)](#) have investigated the distribution and strength of star formation in a larger sample of northern ring galaxies via  $H\alpha$  imaging. Except for the case of [WN1 \(Wakamatsu and Nishida 1987\)](#), a Seyfert galaxy,  $H\alpha$  emission is found

exclusively in the rings and not interior to them, or within the nucleus. In all cases, a large fraction of the star formation appeared to originate in discrete knots. Like the Cartwheel, a large number of the galaxies studied showed significant azimuthal variation in the  $H\alpha$  distributions around the ring, often exhibiting major concentrations of star formation in certain regions of the ring. Also, like the Cartwheel, a faint but significant component of  $H\alpha$  emission was detected from a diffuse component upon which the brighter knots are superimposed. In all cases studied, the diffuse component formed a complete ring, whereas in many cases the bright knots of star formation are concentrated in one quadrant of the ring. Until higher spatial resolution is obtained (via upcoming Hubble Space Telescope observations) it is impossible to determine whether the diffuse  $H\alpha$  represents a different mode of star formation from the bright knots, or whether the bright knots represent stochastic regions of significantly enhanced star formation in the general background of lower-level star formation in the ring.

In an effort to understand the marked azimuthal asymmetries in the star formation regions in ring galaxies, Charmandaris, Appleton and Marston (1993), made a detailed study of Arp 10, (Figure 13a) which appeared to show a particularly striking example of a non-uniform ring. Figure 13b shows the  $H\alpha$  distribution in the galaxy. Like the Cartwheel, this galaxy shows a strong enhancement of  $H\alpha$  flux in one quadrant of the ring. Such global enhancements in star formation rates were predicted in the models of Appleton and Struck-Marcell (1987b) if the star formation rate had a threshold dependence on ring over-density. Charmandaris, Appleton and Marston (1993) were able to show that the star formation rate in the ring jumped suddenly from a low value to a high value in the relatively smooth underlying stellar ring, implying some form of "threshold" process was at work controlling the star formation rates. Observations of the cold gas phase in these galaxies will be needed to confirm these intriguing results.



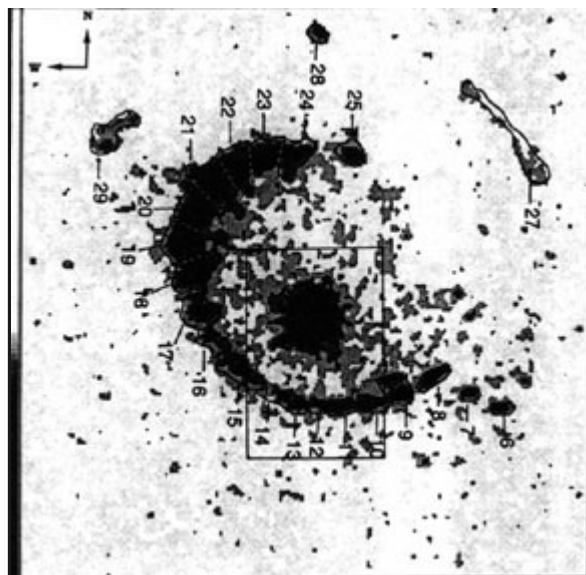


**Figure 13.** a) The RN ring galaxy Arp 10 (B-band from Appleton and Marston 1995 ; KPNO 2.1m telescope) exhibits extremely strong blue emission from one quadrant of the ring. b) B-R color map of Arp 10. Note the extremely blue quadrant of the ring and the color gradient inside the ring. Color coding is similar to that of Figures 7a and 7b. c) The  $H\alpha$  emission from the galaxy Arp 10 (from Charmandaris, Appleton and Marston 1993 ). The emission is concentrated in two rings and multiple ring arcs in the outer regions. (2.1m KPNO telescope). (See Color Plate VIII at the back of this issue.)

Whatever the detailed cause of the azimuthal variations in star formation rates, it is clear that something is regulating the global star formation rates in the rings. Only the most circular rings (e.g. VIIZw466) show a uniform smattering of bright knots around the ring. In most cases, the bright knots are concentrated in one or two major complexes. It is very likely that the appearance of enhancements in star formation relates to the underlying asymmetry of the off-center collision. The distribution of these "hot-spots" may also relate to the position of shocks in three dimensions (Gerber et al. 1994).

One of the remarkable recent numerical results which deserves some comment is that of the different behavior of gas and stars in the SPH models of Gerber (1994). This work has shown that depending on the strength of the perturbation, the gas ring will either lead or trail the stellar ring. In the case of strong perturbations (for example, massive intruders), the gas ring is so dissipative that it lags significantly behind the stellar density wave. In the case of a small perturbation, the gas tends to pile up on the front-edge of the wave, where gas clouds first cross one another (Gerber, personal communication). Such model predictions are of great importance since they illustrate the remarkable usefulness of the ring galaxy as a "cosmic experiment". For example, the fact that star formation is found exclusively on the leading edge of the underlying infrared wave in the recent study of ring galaxies by Marston and Appleton (1995) (see also Appleton, Schombert and Robson 1992) suggests that the ionized gas component leads any underlying density wave. If correct (we don't yet have information on the cool gas) this implies that either most ring-making collisions involve small perturbations, or that the K-band light does not represent a stellar density wave. If the former explanation is correct, then this must imply that many ring galaxy targets have extremely large massive halos, since many of the companions are quite luminous and would be expected to lead to a large rather than small perturbation of the target disk. Further work is clearly needed in this interesting area.

### 3.5. Radio Emission and AGN Activity in Ring Galaxies

Using the 3-element Greenbank interferometer, Ghigo (1980) made the first attempt to detect radio sources in ring galaxies. Only the brightest compact radio sources were detected, but these early pioneering measurements showed that compact non-thermal emission was present in the nuclei of some rings. Jeske (1986) made high resolution  $\lambda 20$  cm snapshot observations of 28 rings with the A array of the VLA and detected sources in 24 of them. This is a significantly higher detection rate than Ghigo's original Green Bank study, due mainly to the enhanced sensitivity of the VLA. Only in two cases (Arp 147 and the Cartwheel) was extended emission observed from the ring. In most cases the sources were compact low-power radio sources

with flux densities of typically 1 mJy at  $\lambda 20$  cm. Jeske's thesis observations showed that optical spectra taken of the nuclear regions of rings containing compact radio sources were in almost all cases indicative of a power-law ultraviolet continuum, such as an AGN.

Higdon (1993) made high resolution radio continuum observations of the Cartwheel ring galaxy at  $\lambda\lambda 6$  and 20 cm with the VLA. Radio emission was detected (at a level of approximately 11.5 mJy at 20 cm) most strongly from the southern quadrant of the outer ring in the region of the most intense star formation. An important result of this work is that large azimuthal variations are observed in the radio continuum observations which are mimicked in Higdon's  $H\alpha$  emission line observations. The fact that these azimuthal variations are seen at radio wavelengths strongly suggests that the  $H\alpha$  emission line strengths are not a result of selective extinction in the ring but are mapping real systematic variations in the star formation rate around the ring.

Recently, Ghigo and Appleton (1995) have made short (snapshot) VLA observations of 11 rings with the D-array at a wavelength of  $\lambda 2.3$  cm (8.4 GHz). In addition, 4 of the rings were also observed at  $\lambda\lambda 6$  and 20 cm. Out of their sample of 11 objects observed at  $\lambda 2.3$  cm, 9 were detected. As with Jeske's survey, the radio sources associated with the rings tend to be weak (typically 0.5-2 mJy at  $\lambda 2.3$  cm). At  $\lambda 20$  cm, Ghigo and Appleton detected twice as much flux as Jeske with the D-array. This implies that for those galaxies in common, a large fraction of the flux was missed in the higher resolution A-array observations because of incomplete coverage in the  $uv$  (fourier transform) plane. This flux is probably extended on the scale of 5-12 arcsecs, which is significantly larger than the scale of the star forming regions. A good example of this is the radio emission from Arp 10. The emission is seen from both a compact source centered on the galaxy, and extended emission associated with the ring and the inter-ring region. The existence of an extended component is interesting and perhaps not totally unexpected in the collisional picture. As the density wave propagates outwards, it is expected to leave evolving stars in its wake. The more massive stars will, after a few  $\times 10^6$  years, explode as supernovae, generating strong non-thermal radio emission. Given the commensurate timescale for the diffusion and aging of such a relativistic plasma and the propagation time of the expanding ring (both around  $10^8$  years), then not only is the radio emission likely to be quite extended behind the ring, but may also show spectral steepening. The steepening in the spectrum might be due to two effects, the change from a mainly thermal to a non-thermal spectrum as one proceeds inwards from the ring, and the aging of the highest energy relativistic electrons, which will also lead to a steeper synchrotron spectrum. In Arp 10 (the only galaxy in the sample near enough to be easily resolved even with the 10 arcsec resolution of the D-array observations) such a change in spectral index is observed. The results are tantalizing, since higher resolution VLA observations will be needed to see whether the effects seen in Arp 10 are universal in the ring galaxy population. On the other hand, the results strongly suggest that the concept of an expanding starburst wave driven outwards through the disk is correct.

The first ring galaxy found to contain an optically identified AGN was NGC 985 (de Vaucouleurs and de Vaucouleurs 1975). The galaxy is of the RK type of Theys and Spiegel (1976). The Seyfert I nucleus is found embedded in the bright knot seen on the SE edge of the ring. It is one of the few ring galaxies so far detected at X-ray wavelengths (Ghigo et al. 1983). A peculiar twisted "arm" extends roughly from the Seyfert nucleus (but see below). de Vaucouleurs and de Vaucouleurs suggested that the ring resulted in the collision between an IGC and a disk galaxy. The galaxy was not studied further until recently in a series of papers by Rodriguez-Espinosa and Stanga (1990) and Stanga and Rodriguez (1991). These authors showed that the peculiar twisted arm contains large numbers of blue massive O stars. Based on  $H\alpha$  imaging, Rodriguez-Espinosa and Stanga (1990) estimate that the total star formation rate in the entire galaxy is currently  $59 M_{\odot} \text{ yr}^{-1}$ . The star formation rate is the highest in the peculiar "arm", but large HII region complexes are found around the ring. The star formation rates are quite similar to those found in other ring galaxies (see Section 4.4).

The infrared observations made at  $\lambda 2.2 \mu\text{m}$ , by Appleton and Marcum (1993) show that a large fraction of the IR light comes from an  $r^{1/4}$  law bulge which is centered on the Seyfert nucleus, and not centered on the ring itself. It is now clear that NGC 985 has a double nucleus (Appleton and Marcum 1993; Garcia & Rodriguez-Espinosa 1995) first hinted at by Rodriguez-Espinosa and Stanga (1990). In addition to the Seyfert nucleus, a very red object is found approximately 3.8 arcsecs from it to the NW. The second nucleus is extended in both the IR and optical luminosity profile and appears like the brighter bulge, to follow an  $r^{1/4}$  law. However, the spectra of Stanga and Rodriguez (1991) show that the second object has an optically featureless continuum, leading Garcia and Rodriguez-Espinosa to suggest it is the bulge of a second galaxy. The extragalactic nature of the second nuclear source is now certain, since, like the merging systems Arp 220 (Norris 1988) and NGC 3256 (Norris and Forbes 1994), both nuclei have now been detected at radio wavelengths (Ghigo and Appleton, in preparation). Appleton and Marcum showed that when the smooth Seyfert bulge light was removed from their IR images, the second nucleus is attached to a straight bar-like structure. Another surprise from the IR observations is that the ring is not closed after bulge subtraction, but appears to take on the appearance of a tightly-wrapped spiral arm attached to the second nucleus by the bar. The evidence is now very strong that NGC 985 is a composite system of two colliding galaxies, one of which contains an active Seyfert nucleus, and both containing weak nuclear radio sources. It is likely that NGC 985 is an example of the kind of transition object first hinted at by Toomre (1978) in which the companion collides a significant distance from the center of the target disk, causing a breakdown of the ring into a spiral shape.

At the time of writing there are three Seyfert 1, ([NGC 985](#), [WN1](#) = Bootes ring, IR0302-5150) and one Seyfert 2 ([Arp 118](#)) ring galaxies known <sup>(2)</sup> ([de Vaucouleurs and de Vaucouleurs 1975](#); [Huchra et al. 1982](#); [Wakamatsu and Nishida 1987, 1991](#); [Lipari & Maccetto 1994](#)). It may not be a coincidence that in all these cases the companion appears embedded in the ring or is seen in close contact with it. WN1 ([Figure 14](#)) has a ragged companion, exhibiting a high star formation rate. The companion seems to be caught in the act of disintegrating, probably as a result of its recent passage through the target disk. As in the case of [NGC 985](#) above, both galaxies show 2.3 cm radio emission (Ghigo and Appleton, in preparation). The galaxy IR0302-5150 is an ambiguous case. [Lipari & Maccetto \(1994\)](#) favored the view that this was not a collisional system, but a resonant ring, in which the ring formed at the OLR. However, the similarity with WN1 is striking, and we believe that it may be a collisional system, despite the smoothness of the ring and the bar. The only Seyfert 2 system which might be classified as a ring ([Arp 118](#)) is a very messy object ([Joy and Ghigo 1988](#)), and we are inclined to think that it is not a simple case of a single two body collision. It appears to be a ring formed in a complex group environment. [Jeske \(1986\)](#) showed that radio continuum emission from [Arp 118](#) was of a markedly different morphology from the other rings, again suggesting that it is not a clear-cut case.

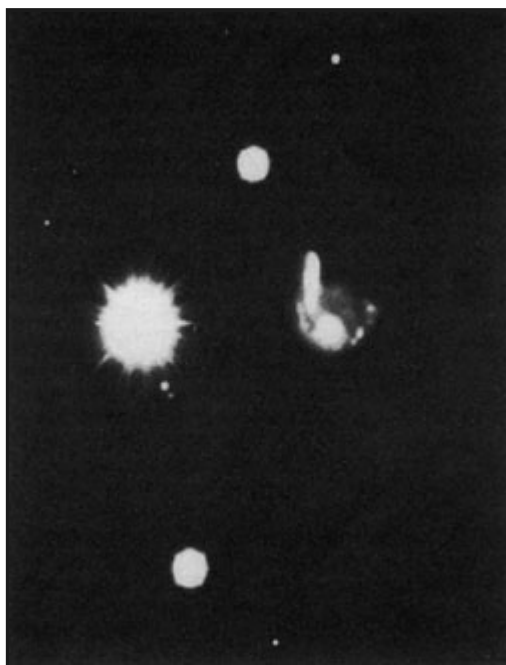


**Figure 14.** The Seyfert 1 ring galaxy WN1 discovered by [Wakamatsu and Nishida \(1987\)](#). Note the disrupted companion. This galaxy, like a number of other well known northern rings lies close to a bright star seen prominently in this CCD image (data from [Appleton and Marston \(1995\)](#) B-band- 2.1m KPNO telescope). (See Color Plate IX at the back of this issue.)

Obviously it is dangerous to draw conclusions from the small number of Seyferts and mini-AGN's found in the family of ring galaxies. However, it is tempting to speculate that the AGN activity is more prevalent in "contact" rings than those with well separated companions. This conjecture is supported by the data presented in [Figure 15a](#). [Ghigo and Appleton \(1995\)](#) showed that if the radio luminosity at 2.6 cm was plotted against the separation of the companion galaxy from the ring system, an interesting effect is observed. Those galaxies with companions which are seen in optical contact with the ring (or projected against it) show a larger dispersion in radio fluxes than those at larger separations. This effect is also seen (more weakly) in the  $H\alpha$  luminosities versus pair separation ([Appleton and Marston 1995](#)) as shown in [Figure 15b](#). The implication of [Figure 15a, b](#) taken together is that star formation activity is enhanced when the galaxies are in apparent contact. We note that [Figure 15](#) is also in accord with the work of [Hummel \(1981\)](#) and [Kennicutt et al. \(1987\)](#) who showed that large dispersions in radio continuum and optical emission lines are common in paired galaxies in close contact.

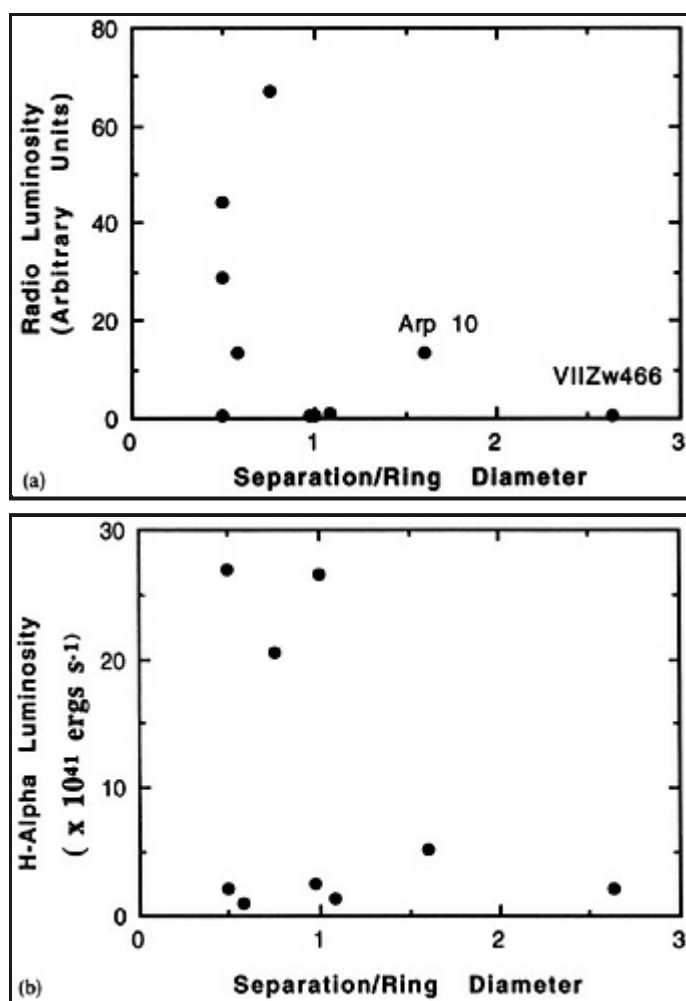


**Figure 15.** a) The 2.3 cm radio luminosity versus the separation of the companion from the ring. A large dispersion in radio luminosity is noted when the companion galaxy is in contact with the ring (when  $R_{\text{sep}} < D_{\text{ring}}/2$ ) perhaps suggesting that enhanced activity may be related to the collision event itself (from Ghigo and Appleton, in preparation). b) The H  $\alpha$  luminosity of the galaxy versus companion separation. As in a), there is a tendency for the galaxies to show higher luminosities when they are effectively in contact with the ring (from Appleton and Marston 1995).

<sup>2</sup> In another case (Davoust, Considere and Poulain (1991)) a large ring structure is found associated with a compact group of galaxies containing a Seyfert galaxy, although in this case it is not clear that the ring has formed by the Lynds and Toomre mechanism. [Back](#).

### 3.6. Rings in Bulge-dominated Systems and Hoag-like Galaxies

A recent study of an early-type system that is almost certainly a collisional ring system is the study of [AM 1724-622](#) by Wallin and Struck-Marcell (1994). This pair of galaxies was given the name "The Sacred Mushroom" by Arp and Madore (1987), since the ring forms the cap of the mushroom shape, and the bridge to the highly elongated companion appears as the mushroom's "stalk". In the AM catalog there are a number of such "mushroom-shape" ring galaxies, and northern examples may include [Arp 284](#). Perhaps [Arp 148](#) is also an early stage of the same phenomenon. [AM 1724](#) has a smooth morphology, which led Wallin and Struck-Marcell to speculate that it may be an example of an early-type ring system. This indeed proved to be the case, based on the photometry of the ring. Unfortunately only small parts of the ring could be measured to determine the color of the ring

material because of the large number of foreground stars contaminating the galaxy, which lies at a galactic latitude of  $-15$  degrees. Nevertheless, tentative colors for the ring confirmed that its colors are red ( $U - B = 0.67$ ,  $B - V = 0.87$ ) compared with the ring sample of [Appleton and Marston \(1995\)](#). Profiles of ring sections suggested sharp-edged caustics, predicted in a purely stellar ring. Ironically, this southern galaxy may be one of the few truly stellar ring systems studied so far which conforms to the models of [Lynds and Toomre \(1976\)](#), being free of the complicating effects of gas.

Of possible relevance to collisional ring galaxies in early type galaxies are galaxies like Hoag's object ([Hoag 1950](#); [Schweizer et al. 1987](#)). These galaxies are characterized by having a central nuclear bulge surrounded by a smooth, thick and extremely regular ring, often almost perfectly circular. Optical spectra of Hoag's object taken by [O'Connell et al. \(1974\)](#) showed the galaxy to be dominated by late-type stars in the core, and this is confirmed by the red colors of the galaxy ([Brosch 1985](#)). However, more recent observations by [Schweizer et al. \(1987\)](#) show emission lines of  $H\beta$  and  $[OIII] \lambda 5007$  in the ring and the detection of significant amounts of HI emission from the galaxy. These observations suggest that the ring contains a young population of stars, despite the overall red color of the system. Ever since its discovery, the origin of the almost perfect ring has been controversial. Hoag was unsure of its origin, but suggested that it might be a gravitational lens, although this would require an exceptionally large mass of the central bulge. [Brosch \(1985\)](#) suggested that the ring was produced at a resonance by a weak bar, similar to the ringed galaxies of [Buta \(1994\)](#). However, deep imaging by Schweizer et al. failed to show any evidence for a bar, apparently ruling out the formation of the ring by this mechanism. On the other hand, it is possible that any ring-making bar may have recently dissolved. The authors discuss the possibility that the galaxy is a collisional ring, but do not favor this interpretation because the central bulge has the same radial systemic velocity as the ring. If the central bulge was a small elliptical galaxy caught in the act of penetrating the disk and generating a ring, the authors argue that it should have a high radial velocity compared with the ring. The origin of these galaxies would still appear to be a mystery.

We believe that, although the case for a collisional origin for Hoag's object is not strong, it cannot yet be completely ruled out. For example, it is possible that the argument about the small velocity of the companion relative to the ring can be circumvented if the companion has been strongly decelerated by dynamical friction with a massive halo in the target galaxy and is about to fall back onto the target or has already merged (see [Section 3.4](#) for more discussion of this possibility). This would be consistent with the heavy halo around the galaxy postulated by Schweizer et al. based on the kinematics of the ring. We note that, if the ring in Hoag's object was formed collisionally, its relatively red colors and low ring star formation rates argue for an early-type target disk. Early-type galaxies may naturally contain a more dominant dark-matter component and bulge capable of significantly slowing and eventually absorbing a small intruder galaxy. However, such a scenario, whilst explaining some of the properties of Hoag's object, does require a combination of remarkable circumstances. For example, we would have to be viewing the collision from a special position (exactly along the symmetry-axis of the disk and target trajectory) and at a special time (either just at the moment when it has reached its furthest distance from the target and has zero relative velocity to the ring, or just after it has merged). Since such circumstances would be rare, we suggest that spectroscopic studies of the other Hoag-like galaxies would be worthwhile to increase the statistics on the velocity of the central objects relative to the ring.

## 4. SIMPLE KINEMATIC MODELS OF RINGS AND RING-LIKE GALAXIES

### 4.1. Caustic Waves

#### 4.1.1. Singularity Theory in Galaxy Formation and Ring Galaxies

In the field of galaxy and large-scale structure formation the Zeldovich approximation "has become a ubiquitous tool in analytical studies of clustering ..." ([Coles, Melott and Shandarin 1993](#)). The Zeldovich approximation is a kinematic approximation to the trajectories of particles within density perturbations in the expanding universe. In overdense regions it describes the initial collapse of (collisional) baryons and the collapse and non-linear clustering of collisionless dark matter ([Shandarin and Zeldovich 1984](#)). The kinematic Zeldovich equation has the same form as the equation for the epicyclic motions of stars in ring galaxies (see Eq. (4.1) below). The physical character of the solutions of the two equations is very different, since initially there is no significant angular momentum or centrifugal barrier in the Zeldovich problem, and no expanding background in ring galaxies. Nonetheless, the formal development of the two equations is almost exactly the same.

Solutions to the Zeldovich equation give the position of particles as a function of time, but we get a better idea of what the solution looks like from the density function. The initial cosmological collapse occurs primarily in one dimension, forming thin sheets, or "pancakes". At early times material near the plane collapses into it, with the Zeldovich approximation predicting a formally infinite density there. This is analogous to the stellar orbit crowding in the first ring discussed above. Later, in the case of collisionless dark matter, particles pass through the pancake plane, rise to a maximum distance (apoapse) on the other side, and fall back through the plane again. Between the particles at apoapse on either side of the central plane is a region of orbit crossing, much like that described above for second rings. In the cosmological case, particles falling from apoapse through the central plane move out to a second apoapse in their original half-plane. This second passage through the central plane leads to more orbit crossings in the pancake. This is analogous to a ring galaxy with the first, second, and subsequent rings all

superimposed. However, since the rings propagate out through the disk the analogy breaks down at this point.

In the collisionless pancakes, the particles at apoapse also have a formally infinite density. They lie on a fold in phase space, and so they are all crowded into the same positional volume with velocities near zero relative to the pancake center. This fold is the simplest caustic or singularity or catastrophe (see [Arnold, Shandarin and Zeldovich 1982](#)). Because of the finite number of particles, and the fact that each has a random velocity component, the density on the fold caustic is not really infinite. The same is true at stellar ring edges, which are also fold caustics. In the pancakes, successive crossings of the central plane lead to the formation of successive sets of fold caustics, like the formation of new rings from the successive radial epicycles.

Singularity theory is a well-developed subject (see e.g., [Poston and Stewart 1978](#); [Arnold 1986](#)). In two and three spatial dimensions it offers a complete classification of the generic, non-linear waveforms and their possible evolution. In the cylindrically symmetric case there are only two possibilities - either the compression wave is too weak to form caustics, or paired fold caustics marking the inner and outer ring edges form at some radius. A variety of ring widths and spacings are possible. In an off-center collision, several additional types of two dimensional waveform are possible within the disk. These include cusps, swallowtails, and pockets or purses (see [Arnold 1986](#)), and overlapping combinations.

The first attempt to understand waves in stellar disks as caustics was [Hunter's \(1974\)](#) modeling of spiral waves in non-interacting disks. [Kalnajs \(1973\)](#) also discussed the orbit crossing zones that developed in his kinematic spirals. Hunter pointed out the analogy between disk orbit crowding/crossing and the formation of optical caustics from ray crowding/crossing. This study showed that a spiral could consist of a crescent made up of fold and cusp caustics. Initially unaware of Hunter's work, [Struck-Marcell and Lotan \(1990\)](#) developed the caustics theory for cylindrically symmetric waves. [Struck-Marcell \(1990\)](#) presented some exploratory semi-analytic calculations showing that collisional disturbances could generate all of the two-dimensional caustics, and that the multiple streams of crossing orbits would provide distinct kinematic signatures. With limited spectral resolution these might not be recognizable, but would almost certainly appear as regions of high velocity dispersion. This is one important, observable difference between nonlinear caustic waves and linear density waves.

[Donner et al. \(1991\)](#) applied analytic caustics models to the study of more general tidal interactions. In addition to considering a broader class of interactions, this paper also presented some comparisons between the simple caustics models and self-consistent N-body simulations. The comparison was found to be good, which indicates the dominance of kinematic motions in the particular cases studied. Independently of [Donner et al. \(1991\)](#), [Gerber \(1993\)](#) carried out detailed comparisons of kinematic and tu-body (and hydrodynamical) calculations of disk waves created by asymmetric collisions. In these collisions the perturbation was also quite impulsive, and there was excellent agreement between the kinematic and self-gravitating models at the early stages of wave development and propagation through the disk. [Gerber and Lamb \(1994\)](#), [Gerber \(1993\)](#) also gave a very clear discussion of the dimensionless orbital and structural parameters in the kinematic equations, which determine the structure of the waves.

#### 4.1.2. Symmetric Ring Caustics in the Kinematic Orbit Approximation

In this subsection we will work through a simple example of the analytic theory of nonlinear disk waves. The goal is to derive a simple picture of how the structure and spacing of the rings depends on the structure of both primary and secondary galaxies and their mass ratio. Basic scaling equations will be derived in this section and limiting cases will be discussed. To begin, we adopt the following simplifications:

1. We consider only cylindrically symmetric collisions which generate circular waves in the (infinitely thin) disk. (The case of slightly asymmetric collisions is considered in Appendix 2).
2. We assume that the primary galaxy has a rigid potential, such that the disk rotation curve has the form,

$$v = v(\gamma) \left( \frac{r}{\gamma} \right)^{1/n}, \quad \text{with} \quad v(\gamma) = \sqrt{\frac{GM(\gamma)}{\gamma}}, \quad (4.1)$$

and where  $\gamma$  is a disk scale length,  $v(\gamma)$  is the rotation velocity at the radius  $r = \gamma$ , and  $M(\gamma)$  is the (spherically distributed halo) mass contained within the radius  $r = \gamma$ .

In this example we will generally follow the derivations of [Struck-Marcell and Lotan \(1990\)](#) and [Gerber and Lamb \(1994\)](#) see also [Struck-Marcell and Higdon \(1993\)](#). In [Struck-Marcell and Lotan \(1990\)](#) the primary galaxy was assumed to have a rigid softened point-mass (or related) potential, while Gerber and Lamb assumed a Plummer potential for the companion (and a flat rotation curve primary). These particular potentials were chosen to provide fairly realistic representations of the two galaxies, but they lead to algebraic expressions that are unnecessarily complicated for the present purposes. Here we will stick to tractable

power-law forms. Moreover, rings are generally contained within an annulus that only covers a fraction of the disk, and so it is likely that both the potential of the primary and the radial form of the perturbation can be well approximated by a power-law in that region.

The gravitational acceleration which gives the rotation curve of Equation (4.1) is

$$g(r) = \frac{-V^2}{r} = \frac{-V(\gamma)^2}{\gamma} \left(\frac{r}{\gamma}\right)^{(2/n)-1}. \quad (4.2)$$

The corresponding mass distribution is

$$GM(r) = \gamma V(\gamma)^2 \left(\frac{r}{\gamma}\right)^{(2/n)+1} \quad (4.3)$$

The radial epicyclic frequency is given by the equation (see [Binney and Tremaine 1987](#), Section 3.2.3)

$$\kappa^2(r) = \frac{d(-g)}{dr} + \frac{3(-g)}{r} = 2 \left(1 + \frac{1}{n}\right) \left(\frac{v(\gamma)^2}{\gamma^2}\right) \left(\frac{r}{\gamma}\right)^{(2/n)-2}. \quad (4.4)$$

These equations define the structure of the primary galaxy. The perturbed radial orbits are given by

$$r(t) = q - A(q)q \sin(\kappa(q)t), \quad (4.5)$$

where  $q$  is the initial unperturbed orbital radius, and the second term describes the epicyclic oscillations of amplitude  $A(q)$ . The sinusoidal form of the second term is appropriate for small amplitude oscillations.

3. We assume that  $A < 1$  throughout the disk. The radial velocity is obtained by differentiating Equation (4.5) with respect to time,

$$v_r = \frac{\partial r}{\partial t} = -Aq\kappa \cos(\kappa t). \quad (4.6)$$

For constant  $\kappa$  these equations describe simple bulk (solid-body) oscillations of the disk. For the more general radially dependent  $\kappa$  they describe propagating waves.

We should explicitly state another assumption -

4. that the amplitude  $A$  is time independent. Then we must consider the initial conditions. In the IA,  $t = 0$  at the moment of impact, and  $v_r(t = 0) = \Delta v_r(q)$ , where the latter is the radial velocity impulse calculated from the IA (see references above). Then Equation (4.6) can be solved for  $A$ ,

$$A = \frac{-\Delta v_r}{q\kappa(q)} \quad (\text{Impulse approximation}). \quad (4.7)$$

All that remains to complete the analytic model is an explicit expression for the oscillation amplitude. We will not discuss the specific forms of these functions that correspond to well-known analytic galaxy potentials. Instead we will simply assume:

5. a power-law form for the amplitude  $A$ ,

$$A = A_\gamma \left(\frac{r}{\gamma}\right)^{-m}, \quad (4.8)$$

We emphasize that all the structural information about the companion (e.g., mass and compactness), and the orbital parameters (e.g., the relative velocity) are contained in this expression.

Assuming conservation of mass in a thin annulus we find that the local density in the disturbed primary disk is given by

$$\rho = \frac{\rho_0(q)}{r \frac{\partial r}{\partial q}}, \quad (4.9)$$

where  $\rho_0(q)$  is the initial, unperturbed density profile. More generally, in regions with multiple star streams we have

$$\rho = \sum_i \frac{\rho_{0i}}{\left( \frac{r \frac{\partial r}{\partial q}}{q \frac{\partial q}{\partial q}} \right)_i}, \quad (4.10)$$

where the sum is over all of the streams. Caustics occur where  $\partial r / \partial q = 0$ , implying  $\rho \rightarrow \infty$ . With the orbit Equation (4.5) and our adopted forms for  $\kappa$  and  $A$ , we can now derive an explicit form for this caustic condition,

$$\frac{\partial r}{\partial q} = 0 = 1 - A \sin(\kappa t) A q t \cos(\kappa t) \frac{d\kappa}{dq} - \frac{\partial A}{\partial q} q \sin(\kappa t),$$

or,

$$\left( 1 + \frac{q \frac{\partial A}{\partial q}}{A} \right) \sin(\kappa t) + \left( \frac{q \frac{d\kappa}{dq}}{\kappa} \right) \kappa t \cos(\kappa t) = \frac{1}{A}. \quad (\text{caustic condition}) \quad (4.11)$$

Using Equations (4.4) and (4.8) both of the first two terms can be simplified,

$$\frac{q \frac{\partial \kappa}{\partial q}}{\kappa} = \left( \frac{1}{n} - 1 \right), \quad \frac{q \frac{\partial A}{\partial q}}{A} = -m, \quad (4.12)$$

Then the caustic condition becomes

$$(1 - m) \sin(\kappa t) + \left( \frac{1}{n} - 1 \right) \kappa t \cos(\kappa t) = \frac{1}{A_\gamma} \left( \frac{q}{\gamma} \right)^m. \quad (4.13)$$

This is the key equation for the caustics. The left-hand-side is in terms of a time-like quantity, the epicyclic phase  $\kappa t$ , and the right is a function of the dimensionless Lagrangian radius on the caustic edge. For any time  $t$ , equation (4.13) can be solved (numerically) for the values of  $q$  at the inner and outer edges. With those values of  $q$ , the radii of the ring edges at that time can be obtained from Equation (4.5).

Generally inner/outer caustic edges are born together at some non-zero radius and time after impact, at a cusp singularity in space-time. At the birthpoint we have both  $\partial r / \partial q = 0$  and  $\partial^2 r / \partial q^2 = 0$  (because it is a cusp singularity). An expression for the latter condition can be obtained by differentiating Equation (4.13), yielding

$$\left( \frac{1}{n} - m \right) \kappa t \cos(\kappa t) - \left( \frac{1}{n} - 1 \right) (\kappa t)^2 \sin(\kappa t) = \frac{m}{\left( \frac{1}{n} - 1 \right) A_\gamma} \left( \frac{q}{\gamma} \right)^m. \quad (4.14)$$

Combining Equations (4.13) and (4.14), we get the birthpoint Equation

$$\left[ \frac{m(1-m)}{\left(\frac{1}{n}-1\right)} + \left(\frac{1}{n}-1\right)(\kappa t)^2 \right] \frac{\tan(\kappa t)}{\kappa t} = \left(\frac{1}{n}-2m\right). \quad (4.15)$$

The separability of  $q$  and  $\kappa t$  in Equations (4.13) and (4.14) implies that the explicit dependence on  $q$  can be eliminated, as in Equation (4.15). Thus, the latter can be solved for  $\kappa t$  (in each phase interval of length  $2\pi$ ), and then  $q$ ,  $t$ , and  $r$  can be derived for the birth of the caustic ring. Equation (4.15) also shows that the birth phase  $\kappa t$  does not depend on the amplitude  $A_\gamma$ , though it does depend on the variation of amplitude with radius through the parameter  $m$ . The birth values of  $q(r)$  and  $t$  do depend on  $A_\gamma$ .

This completes the analytic caustics model for symmetric (power-law) rings. This model is very simple, involving no more than two derivatives of a sinusoidal function. However, the dependencies on the three parameters  $m$ ,  $n$  and  $A_\gamma$  allows for a wide variety of forms. Examples and limiting cases will be described in the following section. In comparing to observations, e.g., in looking at aging starburst populations behind a ring, the absolute length and time scales,  $\gamma$  and  $2\pi/\kappa$  are also important.

#### 4.2. Varieties of Symmetric Rings

To begin to appreciate the range of symmetric ring morphologies we show a number of different radius-time plots in [Figure 16](#). The first panel has a rising rotation curve and the amplitude  $A_\gamma$  is large, so both the first and second rings are orbit crossing waves. On the other hand, the perturbation amplitude falls with increasing radius, so both these caustic waves pinch off at finite radii. The second panel shows a case with a declining rotation curve and constant perturbation amplitude across the disk and is similar to [Figure 3](#). In this case both first and second waves are caustic rings that do not pinch off. The third panel shows a case whose rotation curve rises somewhat more rapidly than a solid body curve. This is not a physically very realistic case, but the inward propagating waves are an interesting result, perhaps relevant to galaxy formation.

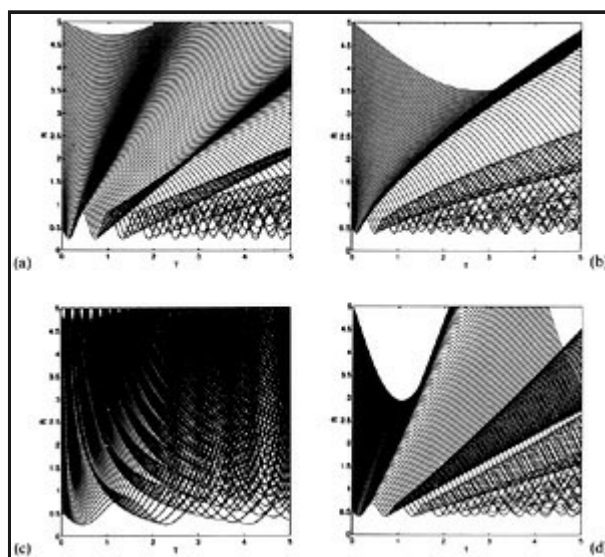


**Figure 16.** Examples of kinematic models of ring waves for different values of primary and companion structural parameters  $m$  and  $n$  defined in the text. Radius vs. time is plotted for a number of collisionless particles as in [figure 7](#). In all the cases shown the amplitude  $A$  (see equation (4.6) and discussion following) has a value of 0.3. For the effects of varying amplitudes see [Figure 3](#) of [Struck-Marcell and Lotan 1990](#). In plot a) (the upper left),  $n = 10$ ,  $m = 1$ , i.e., a quite flat primary rotation curve, with a perturbation amplitude that declines with radius. In plot b), (upper right),  $n = -2$ ,  $m = 0$ , a constant perturbation amplitude and a declining rotation curve. In c) (lower left)  $n = 0.5$ ,  $m = 1$ , a declining perturbation

amplitude and a primary rotation curve that rises more steeply than a solid body curve. In d) (lower right)  $n = 10$ ,  $m = -0.2$ , i.e. perturbation amplitude that rises with radius, corresponding to a very extended companion.

The success of the kinematic caustics theory is that the morphological variety of Figure 16 can be accounted for by the caustics Equation (4.13). This is demonstrated by Figure 17, which consists of a montage of the solutions of Equation (4.13) as a function of the parameters  $m$ , and  $n$ . In the low amplitude cases (e.g.,  $A(\gamma) \approx 0.1$ ) there are few caustic rings, although there will be significant orbit crowding, so these are not shown. Figure 17 shows the  $A(\gamma) = 0.3$  cases, i.e., relatively large amplitude cases. We will briefly consider some examples. First of all, in the  $m = 0$  case the right-hand-side of Equation (4.13) is constant, so the phases  $\kappa t$  must also be independent of radius. Thus, one only has to solve Equation (4.13) once for the phases of the inner and outer ring edges. At any given time the Lagrangian radius of the edges can be determined from the equations  $\kappa t = \text{constant}$ , and then the Eulerian radii  $r(t)$  are given by Equation (4.5). This case was considered in detail in Struck-Marcell and Lotan (1990).

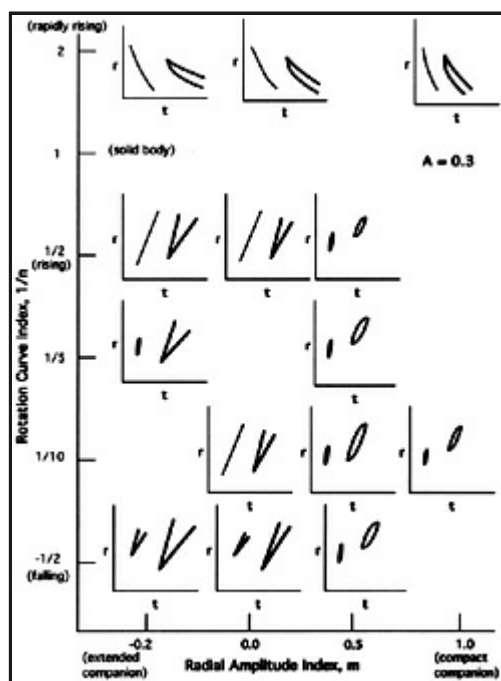


**Figure 17.** Schematic showing caustic borders of the first and second ring waves in radius-time plots as a function of the structural parameters  $m$ ,  $n$  defined in the text. Specifically, thick lines or curves showing an inner and outer edge at any time represent caustic edges. A thinner, single line or curve represents an orbit-crowding region, without the orbit crossings that define a caustic region. The amplitude  $A = 0.3$  is constant for all the figures in this assemblage. Individual cases are discussed in the text.

When  $n = 1$  the primary has a solid-body rotation curve, so that following the (impulsive) collision all stars in the disk should execute synchronous radial oscillations. Thus, there should be no rings, for rings are generally the result of orbital dispersion, which leads to orbit crowding. However, the caustic rings can result from an amplitude gradient in this case. Stars within two different annuli reach their minimum at the same time, but only if the amplitude of the stars in the outer annulus is greater than those in the inner annulus will there be orbit crossings.

Next consider rings at relatively large radii ( $q \gg \gamma$ ), when  $n > 1$  (i.e., the rotation curve rises less steeply with radius than for solid body rotation). In this case the second term on the left-hand-side of Equation (4.13) will usually dominate, since the first term is less than or of the order of unity. Then we also require that  $\cos(\kappa t) < 1$ , or  $(2p - 1)(\pi/2) < \kappa t < (2p + 1)(\pi/2)$ , for  $p = 1, 2, 3 \dots$ . In general, the first few rings will pinch off at radii that are not too large. In fact, Figure 17 shows that first ring caustics

are rare, the first rings are usually weak.

If  $n < 0$ , the primary disk has a declining rotation curve. In this case the absolute value of the  $(1/n - 1)$  term is greater than in the rising rotation curve case, and rings tend to be more robust and broader. Physically this is simply because this case is still farther from the solid body case, and the orbital dispersion is correspondingly greater. When  $0 < n < 1$ , the rotation curve rises more steeply than the solid body case and the rings propagate inward. To achieve this, the mass distribution would have to rise extremely rapidly with radius, for example if the galaxy contained a central deficiency of matter.

If  $m < 0$ , then the perturbation amplitude increases outward. Normally this is not physically realistic unless the "companion" is larger than the ring galaxy. In this case outward propagating rings become very broad with time.

[Figure 17](#) also provides information on ring propagation speeds through the disk. Rings in disks with flat rotation curves tend to have a nearly constant propagation velocity. This is often assumed in estimates of ring ages from measured expansion velocities.

To summarize, several generalizations can be derived from [Figure 17](#) and Equation (4.13).

1. **Broad stellar rings result from declining rotation curves, or large amplitude perturbations.** Thus, in cases with modest companions we suspect that the former is usually true. This seems to be the case in the "Sacred Mushroom", [AM 1724-622](#) (see [Wallin and Struck-Marcell 1994](#)).
2. **Widely spaced narrow rings occur in disks with flat or rising rotation curves.** This is confirmed in the case of the [Cartwheel](#) ([Higdon 1993](#); [Struck-Marcell and Higdon 1993](#)).
3. **The variation of the velocity perturbation with radius determines (in part) the annular zone where caustic rings can occur**, but this variation generally cannot be determined observationally.

#### 4.3. Multiple Encounters?

It is likely that most ring-making intruder galaxies are bound or almost bound to the target disk. Moreover, they will be more tightly bound after the collision as a result of dynamical friction. The amount of friction will depend on the mass and structure of the spheroidal components and halos of the two galaxies. Merger simulations of simple spheroidal galaxies indicate that friction can be very effective in many cases. In these cases the first collision will be followed by a second, and typically a prompt merger after that.

When the intruder galaxy initially strikes the target disk off-center on the first pass, the second collision is likely to be even more asymmetric. Nonetheless, it is useful to study the special case of two successive symmetric collisions as an introduction to the phenomena that can be produced in multiple interactions. This situation has been discussed in a manuscript of [Lotan and Struck-Marcell \(1991\)](#), and [Lotan-Luban \(1990\)](#), where models and numerical simulations were presented.

Equation (4.5) is based on the assumption that the disk stars were in simple circular orbits before the collision. This is clearly not the case at the time of the second collision, since the stars are executing radial epicyclic oscillations as a result of the first collision. The magnitude (and direction) of the radial velocities of the disk stars at the time of the second impact will be a smooth function of radius in the disk. That is, some stars will be moving inward, others outward, others will be near apoapse or periapse and will not have a significant radial velocity. If we assume that the second collision is also impulsive, the velocity impulse will be added to the star's current velocity. If the star already had a significant velocity inward, this will result in a considerable increase in that velocity. If the star was moving outward, the second collision may result in a net radial velocity of nearly zero. That is, in some range of radii within the disk the two perturbations will nearly cancel, while in others they will add, with intermediate values in between. The results can be dramatic, with very wide caustic rings in the large amplitude regions, and thin rings or only modest orbit crowding zones in the low amplitude regions. Moreover, simulations show that thick and thin rings tend to alternate (see [Figure 18](#), from [Lotan and Struck-Marcell 1991](#)). Further details are given in [Appendix 1](#).

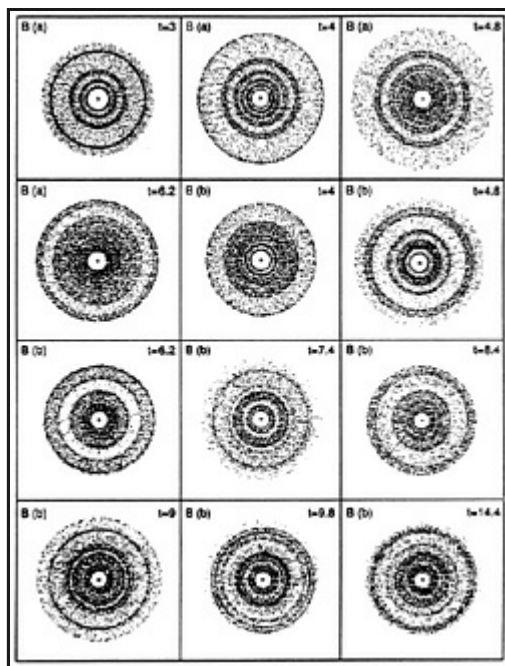


**Figure 18.** Pole-on view of a test particle disk from the multiple impact simulations of Lotan-Luban (1990, also Lotan and Struck-Marcell 1991). Upper case letter identifies the model, and it is followed by either an "a" for the (control) case of a single collision, or a "b" for the multiple collision case. Dimensionless time is also given (in units of the initial disk radius divided by the rotational velocity at that radius).

#### 4.4. Asymmetric Encounters

The perturbation caused by any collision in which the center of the companion passes through the primary disk at a large impact angle relative to the disk will have a strong radial component. Thus, a ring-like wave will result even if the impact point is well out from the disk center. The simple kinematic, impulse models above can be extended to model these asymmetric waves (see [Appendix 2](#)). A wealth of new caustic waveforms, i.e., combinations of the elementary caustics, are possible (see [Struck-Marcell 1990](#); [Donner et al. 1991](#); [Gerber and Lamb 1994](#); [Gerber 1993](#)). The type and structure of these waves as a function of the KIA parameters have not been completely analyzed. Gerber and Lamb's identification of several of the most important dimensionless parameters is an important step. However, as noted above, they assumed specific structural forms for both primary and companion galaxies, so additional parameters could be added.

Both the general theory and the work that has been carried out on modeling specific systems (see [Section 5](#), and [Appendix 2](#)) show that the wave morphology is very sensitive to how far off-center the impact is. The wave morphology is also sensitive to a number of other parameters. Thus, there are a myriad of morphologies possible within a limited range of parameter values. Yet the number of disk galaxies containing asymmetric waves with a strong radial component in the driving perturbation ("ring relatives") is probably only a few times greater than the number of nearly symmetrical rings. This means that many possible morphologies will not be found in any reasonably nearby sample of galaxies.

It is possible that each asymmetric wave morphology is unique, and is the result of a specific set of collision and structural parameters. If so, then a successful model of the morphology of an individual system would uniquely specify these parameter values. On the other hand, we have seen in the case of symmetrical collisions that there are several ways to generate broad rings. As a second example, the ripples produced in retrograde tidal interactions (e.g., [Hernquist and Quinn 1987](#)) can appear similar to the late-time ringing resulting from off-center collisions in early-type disk galaxies ([Wallin and Struck-Marcell 1988](#)). However, it is possible to tell the difference in these cases if sufficient morphological or kinematic detail can be observed.

## 5. SELF-CONSISTENT STELLAR DYNAMICAL MODELS OF RING GALAXIES

Although [Lynds and Toomre \(1976\)](#) were mainly concerned with a purely kinematic description of the ring formation, they did

include one model with massive selfgravitating coaxial rings and the results were qualitatively similar to the models involving massless particles. [Theys and Spiegel \(1977\)](#) performed the first N-body simulations of the ring formation using 7000 mass points. In their 2-dimensional models most of the stars were placed in a disk which quickly developed a bar instability since no massive halo was included in the calculation. Nevertheless, despite the unrealistic heating of the disk stars, rings were generated as a result of the collision. Theys and Spiegel also present the results of more realistic calculations involving massive selfgravitating coaxial rings. Some attempt was also made to include dissipation in the interaction of the rings. The edge-on views of these latter simulations are interesting in that they show the displacement of the second ring from the first in the direction perpendicular to the target disk plane. Also of interest is the structure of the intruder, which can be seen to undergo considerable distortion, especially along the direction of its trajectory.

More realistic N-body simulations were performed in the early 1980's with the advent of faster computers and the development of particle-mesh algorithms for solving the N-body problem. Two groups at the University of Manchester, UK, performed simulations of the ring problem. [Huang and Stewart \(1988\)](#) performed a small number of simulations of a rigid companion with a disk enclosed in a fully self-consistent (live) halo. R.A. James and P.N. Appleton, in a largely unpublished work (see for example, [Appleton and James 1990](#)) performed over 100 completely self-consistent simulations of the collision of a (live) companion with a disk and (live) spherical massive halo. The results of both groups was quite similar and can be summarized as follows: a) The formation of the first ring is relatively insensitive to the inclination of the companion's orbit. In fact, both [Huang and Stewart \(1988\)](#) and [Appleton and James \(1990\)](#) were able to produce respectable ring waves in disks with modest companions even when they approached the disk at a high angle of inclination (60-80 degrees). Huang and Stewart noted that the existence of the "live" halo accentuated the strength of the first ring and slowed its outward rate of propagation, as compared with a non-responsive "rigid" halo of the same mass and scale-size. b) Very rich and complicated structure was found to develop in the inner regions of the disk as second and multiple oscillations of the inner disk occurred. Here the structure was found to be very sensitive to the impact parameters. Amongst the complex structures found, Appleton and James report the formation of a single spiral structure inside the ring during slightly prograde collisions which might be termed "single-spoked". Such structures, which are likely resonances between the orbital motion of the intruder and the disk material are probably not a good explanation for the spokes in the [Cartwheel](#), although they may explain the faint structures seen in [HHz4](#). c) Even in the case of relatively low mass intruders, it was rare to see evidence for more than two stellar rings. The generic result from the simulations was either the formation of a bar-like structure or the formation of an inner lens which merged with the second ring after a few rotation periods. The lack of development of higher order rings is probably a result of the poor resolution of these particle-mesh algorithms, as well as strong phase-mixing of the higher-order rings, as expected in the simple kinematic model. d) Very few slightly retrograde models of ring collisions have been explored, although there were clear indications from the work of [Appleton and James \(1990\)](#) that rich structures are possible in these cases. e) [Toomre \(1978\)](#) had shown through restricted 3-body models that as the impact site of the intruder was shifted from the center to the outer disk, the structure underwent a transition from ring-like behavior to spiral-like forms. N-body simulations have confirmed this early work, showing that well defined rings can be produced when the impact is within 40-60% of the gravitational scale-length of the target galaxy.

More recently, supercomputers have allowed simulations with the much needed resolution required to investigate the possible effects of self-gravity in the rings. A careful comparison was made between analytical models of the ring kinematics, based on the impulse approximation, and the behavior of a fully self-consistent N-body and SPH gas disk ([Gerber 1993](#)). The results indicate that only during the late stages of the evolution of the expanding ring does the ring behavior differ significantly from that of the simple kinematic models. It is this fact, now seen in retrospect, that has led to the remarkable success of the original [Lynds and Toomre \(1976\)](#) models. In fact it is becoming clear that the most important component in the late evolution of the ring galaxy is the development of instabilities in the gas, not the stars. Indeed, as we have indicated in earlier sections, pure N-body simulations may be less relevant than we first believed because most definitive ring galaxies are defined primarily as a result of the morphology of the young stars which have formed from gas in the systems. Except for the possibility of interesting interactions between the perturbed massive halo and the disk (hinted at by Huang and Stewart), the emphasis has now shifted from studying purely N-body collisions to those models which also include the potentially important effects of the gas. In some cases, (see [Hernquist and Weil 1993](#)) the behavior of the gravitational effects of gas clouds on the underlying stellar dynamics can be significant. We therefore defer further discussion of the more recent N-body models to the next section.

## 6. THE GAS DYNAMICS OF RING GALAXIES

The strong star formation observed in many rings and discussed above is good evidence in itself that many ring galaxy disks are gas rich. In fact, there is probably a strong selection effect biasing us toward the discovery of bright, blue star-forming rings with late-type precursors. Red stellar rings in early-type disks will not announce themselves as loudly, and even when discovered are often accounted for as the result of non-collisional dynamical processes. Nonetheless, in many of the well-known systems, most notably the [Cartwheel](#), the rings are essentially a gas dynamical phenomenon.

This being the case, an important question is how the gas response to the dynamical disturbance differs from that of the stars? It is likely that the radial epicyclic motions are likely to be very supersonic in most systems, so collisional shock dynamics probably play an important role. However, even this conclusion is a bit simplistic, and must be qualified. The structure of any

shocks in the ring waves will depend on the nature and structure of the interstellar medium in the precursor galaxy. Although there is beginning to be some observational input in this area, it is still largely unknown territory. Indeed, the question might be turned around in that studies of rings may in some cases be used to determine conditions in the precursor disk.

However, the largest question in this area remains - how does the ring wave stimulate star formation? We will see below that simulations are beginning to provide some possible answers. We have long hoped that the relative simplicity of ring waves would allow us to understand them in enough detail to learn some generally applicable lessons about wave-induced star formation. Recent results from simulations appear to support this conjecture.

Finally, there are questions concerning nonlinear feedbacks, e.g., what effects do the wave and the induced star formation have on the interstellar gas downstream of the ring? Also, how do these effects interact with the strong rarefaction behind the compression wave? Answers to these questions require a realistic treatment of the effects of young star activity.

In the rest of this section we will review how the questions above have been addressed in models produced to date. We will focus on models specifically designed to simulate the ring galaxy phenomenon. However, there are clearly strong connections to gas dynamical modeling of general tidal interactions and collisions, especially as regards star formation activity and the resulting feedbacks. There are also connections to a very large literature of models of gas dynamics and wave-induced star formation in isolated galaxies. This includes the literature on the maintenance and the effects of spiral density waves, and of waves driven by stellar bars. An examination of these connections is beyond the scope of this review.

### 6.1. Lessons from Simple Models

The KIA (Kinematic Impulse Approximation) epicyclic models of Section 4 are strictly speaking applicable only to collisionless disk stars. Nonetheless, they can still provide some insight into the basic dynamics of the interstellar gas. The initial radial infall following the companion impact is essentially the same for both stars and gas elements. Different behaviors may begin in the compression of the first ring wave. Differences are inevitable if caustic edges are generated in the stellar wave, at least in the disk plane. The orbit crossing zone between these edges will collapse into a shock in the gas. However, [Gerber's \(1993\)](#) simulations showed that the disk may be sufficiently warped that the orbit crossing may not occur in a plane. The gas ring then looks surprisingly like the collisionless stellar ring. If the bulk of the gas is clumped in a relatively small number of giant molecular clouds of small cross section, they will also behave like stars in unwarped disks. Thus, the observation of shocks, or other dissipative effects, in rings would be an important discovery. Many first rings (see [Figure 17](#)) are too weak to form stellar caustics. Whether a (weak) shock forms in the gas or not depends on how closely the trajectories are squeezed compared with a typical cloud size, or how large are the cloud random motions within the ring.

In the case of caustic rings the approximations of [Section 4](#) (and [Appendix 2](#)) could be generalized to the gas. Equation (4.15) essentially describes the center of the stellar orbit-crossing zone. Thus, it provides a reasonable first approximation to the trajectory of the gas shock. We can assume that gas elements follow collisionless trajectories until they hit the ring shock. Then, knowing their velocities and the shock velocity, the jump conditions can be applied to determine the (e.g., isothermal) postshock velocities. Behind the ring shock we can assume that the gas elements resume collisionless motion, until the equations describing this motion predict a second orbit-crossing zone, at which point the approximation can be repeated. The postshock collisionless trajectories in the gas will have different phases than the stellar trajectories, so subsequent shocks may not lie within the stellar ring. More likely, the gas motions will be damped, and there may be no subsequent shocks.

Star formation may be greatly enhanced even in modest rings which do not form global shocks. For example, consider how this would occur within the context of the classical gravitational instability theory. [Kennicutt \(1989\)](#) (also [Struck-Marcell 1991](#); Taylor et al. 1994; and references therein) have argued that star formation in disks keeps the local gas surface density near a critical value,  $\Sigma_{cr}$ . If the surface density is pushed above this critical value, a range of wavelengths becomes unstable to gravitational collapse. We can estimate a critical volume density corresponding to this surface density as

$$\rho_{cr} = \frac{\Sigma_{cr}}{\Delta z} = \frac{\alpha c \kappa}{\pi G \Delta z}, \quad (6.1)$$

where  $c$  is the sound speed,  $\kappa$  is the local radial epicyclic frequency,  $\Delta z$  is the disk thickness, and  $\alpha$  is Kennicutt's empirical correction factor. The spherical free-fall time at this density is

$$\tau_{ff} = \left( \frac{3\pi}{64\alpha} \right)^{1/2} (P_z P_\tau)^{1/2}, \quad (6.2)$$

where  $P_r = 2\pi / \kappa$  is the radial epicyclic period, and  $P_z = \Delta z / c$  is the vertical acoustic period. With  $\alpha = 0.63$  as in [Kennicutt \(1989\)](#) the constant in Equation (6.2) is about 0.5. Throughout much of the disk  $P_r$  and  $P_z$  are comparable, and thus,  $\tau_{ff}$  is comparable to both. The time a typical gas element spends within a ring wave is also about  $P_r/2$  (see [Section 3](#)). Thus, for any density enhancement of order a few or greater, there will be two or more growth times while the gas element passes through the wave.

This classical analysis assumes an initially uniform gas. If instead the gas is clumped into giant molecular clouds that are in approximate virial equilibrium, then the addition of mass or an increase of ambient pressure will lead to collapse on a shorter timescale. On the other hand, if star formation is the result of direct cloud collisions, these may not be significantly enhanced in weak waves. Thus, we would not expect much increase in the star formation. This is especially true if the star formation enhancement depends on the relative velocity of the colliding clouds. In weak waves, where orbit crossing is not predicted by the simple models, the relative velocities will be low. Thus, weak ring waves can provide a key test of the role of different star formation mechanisms.

## 6.2. Numerical Simulations of Ring Galaxy Hydrodynamics

### 6.2.1. The First Simulations: 1970s

The first models of gas dynamics in ring galaxies were those of [Theys and Spiegel \(1977\)](#), using Prendergast's "beam scheme" ([Sanders and Prendergast 1974](#)). Theys and Spiegel presented simulations of both the gravitational breakup of isolated rotating rings, and galaxy-galaxy collisions with both gas and stellar components modeled by particles in the target disk. The ring breakup simulations were two-dimensional with self-gravity computed on a  $128 \times 128$  grid with particles representing individual clouds and obeying a polytropic equation of state with index  $\Gamma = 2$ . The ring was set up in centrifugal equilibrium, but evidently in a marginally gravitationally unstable state. The basic result was that the ring fragmented within a few free-fall times ( $\approx 10^8$  yr.) into dense clumps, and the number of clumps was about equal to the number of initial Jeans lengths along the circumference of the ring. The simulation also included the conversion of gas clouds to stars, but no significant differences developed between the stars and clouds over the duration of the simulation. Subsequently, this result for an idealized material ring has often been uncritically cited as proof of the existence of a bead instability in (propagating, not material) ring waves.

Theys and Spiegel carried out two types of collision simulation, one with complete cylindrical symmetry, and the other was apparently a fully self-consistent three-dimensional model. Unfortunately the primary galaxy did not include a massive halo, and by the authors' description it seems that the unperturbed disk was subject to the bar instability (see e.g., [Binney and Tremaine 1987](#), [Section 6.3](#)), and excessive disk heating in the stellar component. The number of particles was also quite small. Nonetheless, the development of the ring was evident in the gas. The ring formation and propagation are more obvious in the symmetric models, where the disk is made up of N rings.

### 6.2.2. The Next Generation: 1980s

The next generation of hydrodynamical models were based on a finite difference algorithm, Flux Corrected Transport or FCT ([Appleton, Struck-Marcell and Foster 1985](#); [Foster 1985](#); [Appleton and Struck-Marcell 1987b](#); [Struck-Marcell and Appleton 1987](#)). Although smoothed particle hydrodynamics (SPH) methods were beginning to show much promise at this time, finite difference algorithms were the method of choice for modeling shocks, which was one of the primary motivations of these models. Two results emerged from these models, which were at first somewhat surprising. The first was that, at least within the region of parameter space explored with these models, strong shocks did not occur within first rings. However, in second rings, the shocks were very strong. In the light of the KIA models of [Section 4](#) and the discussion of the above, this is understandable. The epicyclic motions of gas elements at adjacent radii do not generally get far out of phase until they have passed through the first ring.

The work of Appleton and Struck-Marcell also included a simple cloud fluid model for the effects of interstellar cloud coalescence, cloud collisional disruption, and young star activity on the local cloud mean mass, and the mean random velocities in the local cloud system (see the review of [Struck-Marcell, Scalo and Appleton 1987](#)). These models represented a first attempt to study the effects of ring waves on interstellar cloud structures, and to use the cloud fluid model to investigate the occurrence of wave-driven starbursts, and their nonlinear feedbacks. The primary success of the cloud fluid simulations was that they showed a very nonlinear star formation response in the ring wave in some cases, in accord with the suggestion of [Davies and Morton \(1982\)](#) for the [Cartwheel](#). Specifically, in the one-dimensional models of [Struck-Marcell and Appleton \(1987\)](#), if the ring pushed the gas density well above a critical value, where the model star formation function increased nonlinearly, a strong burst occurred in the wave. However, in collisions with 10% and 20% mass companions, the density enhancement in the first ring was generally not great enough to yield a burst. On the other hand, bursts occurred in the strong second wave in all cases. Moreover, there was a strong suppression of star formation in the rarefaction region between the two waves in all cases. Most ring galaxies have only one visible ring. This result implied that if these starburst rings are the first wave in the target disk, then

either the precollision gas density was quite close to the critical value, or the companions tend to be more massive. It now seems likely that the model threshold functions were unrealistically sharp. Since they were not intended to provide a highly realistic representation of the relevant physics, the results should not be over-interpreted. Nonetheless, several systems are known with a weak outer ring, but a much stronger inner ring (e.g., [AM 2159-330](#)). The result also highlights the possibility that some observed outer rings, especially in systems without nearby companions, might be second or higher order waves (see discussion on the [Cartwheel](#) in [Section 6.4](#)).

Another symptom of the nonlinearity of the cloud fluid terms was the generation of secondary bursts by a strong burst in the wave. That is, strong bursts generated pressures high enough to push the gas away to slightly larger and smaller radii, where new bursts occurred. [Struck-Marcell and Appleton \(1987\)](#) showed that subsequently, a rather chaotic pattern of star formation peaks were generated in the propagating wave (see [Figures 16, 22](#) in [Struck-Marcell and Appleton 1987](#)). This behavior is a specific instance of the general tendency of the cloud fluid to undergo a bifurcation cascade to chaos as the gas density is increased ([Scalo and Struck-Marcell 1986](#)). To date, there is little observational evidence for such pressure feedbacks in ring waves. Higher resolution observations (including Hubble Space Telescope observations) may yet discover multiple star formation peaks at adjacent radii, but it will be hard to determine whether they are the result of this effect, or of star formation occurring in different planes of a warped disk ring.

[Appleton and Struck-Marcell \(1987b\)](#) presented two-dimensional models of the primary disk following an off-center collision, with a limited version of the cloud fluid model. In these models the wave begins on the impact side of the disk (somewhat rotated) in a crescent or "banana" shape, extending over a limited range of azimuths (see [Figure 19](#)). The wave spreads in azimuth as it propagates outward, not because of shear, but because the perturbation appears more symmetric in the outer disk. Ultimately at large radii compared with the impact radius, the ends of the crescent join to form a complete if asymmetric ring. As discussed above, asymmetric rings are common, and "banana" waves are suggested by the observations (see for example, [Appleton, Schombert and Robson 1992](#)). Asymmetric waves are also apparent in earlier restricted three-body and N-body simulations, although they are much more dramatic in the hydrodynamic simulations because of the greater compression. The overall asymmetry is readily understandable as the result of the effect of the different distances between points on a circular annulus in the disk and the impact point on the perturbation amplitude. However, in the collisionless stars a stronger radial perturbation yields a thicker ring ([Section 4](#)), with overdensities that are less than those in the collisional gas.

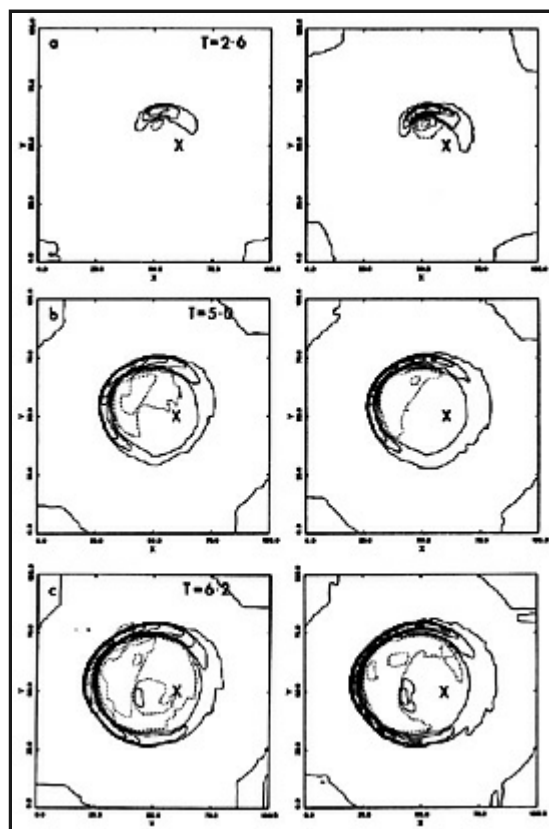


**Figure 19.** Figure 7 of [Appleton and Struck-Marcell \(1987b\)](#) showing contour maps of gas density (left hand panel) and star formation rate functions (right panel) for an off-center collision simulation. Solid contours indicate

COLLISION SIMULATION. SOLID CONTOURS INDICATE elevation above the initial unperturbed values and dotted contours show depressed levels.

The models of [Appleton and Struck-Marcell \(1987b\)](#) also yielded predictions about the variation of cloud collisional and star formation processes across a ring wave. Specifically, a region of cloud collisional buildup was predicted in the outer parts of a typical wave, followed by star formation and cloud disruption as the gas exits the inner parts of the wave (see [Figure 20](#), from [Appleton and Struck-Marcell 1987b](#)). High resolution multiwavelength studies of the spiral arms of [M51](#) (see review of [Rand and Tilanus 1990](#)) show evidence of the dissociation of the molecular gas in the vicinity of HII regions downstream of the gas and dust peak in the southern arm (but see also discussion by [Casoli \(1991\)](#) on the more complex situation in the northern wave). A similar phenomenon is observed in [M81](#) ([Kaufman et al. 1989](#)) and in the central regions of [M33](#) ([Wilson and Scoville 1991](#); [Regan and Wilson 1993](#)), though in both cases the dust or molecular gas doesn't seem to be concentrated in as sharp a front as in [M51](#). It will be more difficult to resolve comparable structures in the more distant ring galaxies. However, in many rings the star formation is more vigorous and violent, so the corresponding effects should be visible on larger scales. This is certainly the case in the [Cartwheel](#), as discussed below.

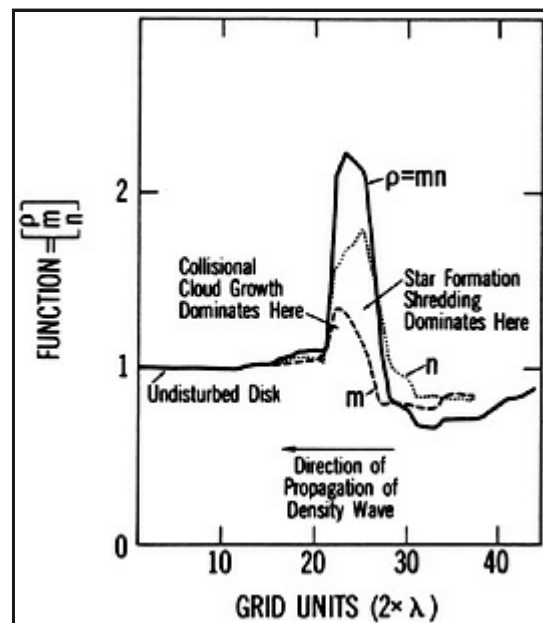


**Figure 20.** Figure 4 of [Appleton and Struck-Marcell \(1987b\)](#) showing an enlarged, sectional slice of the variation through a ring wave of the mean cloud mass  $m$ , and number density  $n$  in the cloud fluid model.

### 6.2.3. The Current Generation of Models: 1990s

Recently interest in ring galaxies has increased and there have been a number of new modeling studies published. These include: [Gerber, Lamb and Balsara \(1992\)](#), [Hernquist and Weil \(1993\)](#), [Gerber \(1993\)](#), [Struck-Marcell and Higdon \(1993\)](#), and [Horellou and Combes \(1994\)](#). [Gerber, Lamb and Balsara \(1994\)](#) also have made available to us a preprint of further simulations like those in [Gerber \(1993\)](#). All of these works use particle hydrodynamics algorithms, which are well-suited to modeling not only the target and companion galaxies, but also the empty space between them. This space and the galaxy edges are difficult to simulate with finite difference algorithms. All of these simulations are fully three-dimensional, which is one reflection of the increased computer power in recent years. Most of the models include a self-consistent computation of the gravity in either the stellar or gas components, or both. Up to this time, there had been no hydrodynamic modeling of individual ring systems, but such modeling is the goal of several of these papers. We will postpone consideration of [Hernquist and Weil \(1993\)](#) and [Struck-Marcell and Higdon \(1993\)](#) to the next section, since these papers focus on the [Cartwheel](#) and the question of the origin of "spokes" like those observed in the [Cartwheel](#).

[Gerber, Lamb, and Balsara \(1992\)](#) and [Gerber \(1993\)](#) modeled the [Arp 147](#) system, one of the original "empty" ring systems of [Theys and Spiegel](#). These simulations involved the collision of an elliptical (gas-free) companion, with an equal-mass primary consisting of a collisionless dark-matter halo, and a disk with both stellar and gas components. An SPH algorithm was used to compute the gas dynamics, and the gravitational interactions were computed with a particle-mesh algorithm. These simulations

confirmed the finding of earlier stellar dynamical calculations (e.g., [Appleton and James, 1990](#)), that an off-center target impact can displace the nucleus away from the disk center, and in fact out of the disk plane. (Note, however, that after the collision this plane becomes very warped.) They found that the "nucleus can appear buried in one edge of the ring depending on the orientation relative to the observer", as observed in [Arp 147](#) (see also photometry of [Schultz et al. 1990](#)).

The authors also described the formation of a "partial ring" in both gas and star components in the off-center impact models. This partial ring seems to be the same phenomenon as the banana or crescent wave discussed above and can be viewed as a confirmation of the basic theory, even though the three-dimensional structure of the numerical results was not considered in the earlier work. It appears that either the calculations were not run long enough, and the target disk was not large enough relative to the impact radius, to show the development of a complete ring as predicted by the theory.

A final interesting conclusion of this study was "that regions of high volume gas densities do not necessarily coincide with regions of high surface gas (and star) densities". This is an intrinsically three-dimensional result, not predicted by the planar theory. The theory does predict that the highest surface density regions will include material from the largest range of disk radii. If the disk is severely warped as in these simulations we can understand how this portion of the ring is the most three-dimensional, with gas clouds and stars executing their radial epicyclic oscillations in a range of vertically displaced planes. [Gerber, Lamb and Balsara \(1992\)](#) found that the strongest shocks and the highest gas volume densities were symmetrically located on both sides of the ring relative to the nucleus or surface density peak. This is in accord with the observations of [Arp 147](#) which show bright knots symmetrically placed in the ring (see [Gerber, Lamb and Balsara 1992](#)). This distribution of knots appears peculiar to [Arp 147](#).

Disk warping was also studied by [Horellou and Combes \(1994\)](#). Their work also consisted of three-dimensional N-body simulations, with a gas component in the disk. In this study, the gas dynamics was simulated by particles that were identified with individual molecular clouds, and which experienced inelastic collisions with other 'clouds'. Only head-on collisions between equal mass targets and companions were considered. The target galaxy had a bulge component of mass equal to the disk. However, in contrast to other recent studies, no dark halo component was included. The companion consisted of a rigid Plummer sphere.

Collisions in two velocity regimes were considered: fast collisions with relative velocities of  $2000 \text{ km s}^{-1}$ , and slow collisions with relative velocities of  $320 \text{ km s}^{-1}$ . In the former case disk particles received velocity increments that were in good agreement with the predictions of the impulse approximation. Ring density amplitudes were modest but significant in both stars and gas, and there was little disk warping. In the latter case, ring (surface density) amplitudes were much larger, warping was severe. In this case, a significant fraction of the gas was "removed" from the central regions of the target disk. In the last time slice shown in this paper the gas is distributed in a continuous bridge. A view at a later time, showing how much gas actually escaped, would have been useful. Nonetheless, these simulations provide extremely interesting results on previously unexplored regions of parameter space.

[Gerber \(1993\)](#) and [Gerber, Lamb and Balsara \(1994\)](#) present additional simulations like the one used to model [Arp 147](#). The [Gerber, Lamb and Balsara \(1992\)](#) results concerning disk warping and gas volume versus surface density in the ring as a function of azimuth are confirmed and generalized in these later works. Many more modeling details and a much more extensive analysis of the results are also given. Of particular interest for observational comparisons are star and gas density profiles as functions of time (see previous section). Many of the results presented in [Gerber \(1993\)](#) match the appearance of several well-known ring systems (in the tradition of [Toomre 1978](#) and [Appleton and James 1990](#)). The simulations should provide a good basis for detailed modeling efforts when kinematic data become available.

In sum, this generation of hydrodynamical models has provided considerable improvement over the earlier work, and promises a great deal more. This is especially true in the case of asymmetric collisions, and the three-dimensional dynamical evolution of the target disk after the collision. However, the exploration of the orbital parameter space is still at an early stage. For example, it would be very interesting to have an extensive sequence of N-body simulations, densely covering the range of impact parameters from zero to some value greater than the disk radius. Ideally, the target would have a simple disk-halo structure to facilitate a detailed comparison with kinematic models (and thus KIA theory), like that carried out on a coarse grid by [Gerber and Lamb \(1994\)](#) and [Gerber \(1993\)](#). This would provide a firm basis for interpreting a further simulation sequence with the gas component included. Such a project should yield fascinating new results on wave structures, including systematics of the development of different spiral modes, their importance relative to the ring mode, the appearance of bars, and the structure and evolution of large-scale shocks. With a dense model grid some systematic understanding of these waves and their evolution should be obtainable.

All of the simulation studies described above assumed an isothermal equation of state with the exception of [Struck-Marcell and Higdon \(1993\)](#), which contains a minimal description of simulations of an adiabatic gas, together with a simple approximation to radiative cooling. To date, thermal effects are almost completely unexplored. The work of [Appleton and Struck-Marcell \(1987b\)](#) and [Struck-Marcell and Appleton \(1987\)](#) can be viewed as an initial attempt to study some of these effects at the level of

interactions between typical clouds. However, there was no attempt in these studies to model a multiphase interstellar medium. Yet, the few available observational studies of the spatial distribution of HI (warm) gas and HII regions in rings, indicate interesting multiphase dynamics. This is also to be expected from detailed studies of nearby density wave galaxies cited in the previous subsection. This is clearly the frontier to be explored with the next generation of simulation codes.

### 6.3. Models of the Cartwheel

There has been much recent observational work on the Cartwheel which has long been the ring galaxy prototype (see especially Section 3). It is, thus far, the most studied of all the ring galaxies. A rotation curve and ring expansion rate derived from the 21 cm. data (Higdon 1993, Struck-Marcell and Higdon 1993) provides a basis for any modeling effort. The color and emission line data, discussed earlier, yielded the very exciting result that the material behind the ring appears to be well represented as a sequence of aging stellar populations (Marcum, Appleton and Higdon 1992). More surprising is the result that there is little evidence for an older stellar disk in most of the region contained within the large ring. The ring wave has evidently triggered the first SF in much of the gas disk. Of all the ring galaxies discussed in this article, the Cartwheel may well be the most appropriate for pure hydrodynamic modeling.

The wealth of new observations stimulated a new modeling effort by Struck-Marcell and Higdon (1993). Several techniques were used ranging from semi-analytic calculations of stellar orbits in the KIA model to restricted three-body numerical hydrodynamical simulations of the Cartwheel disk. These models were able to produce a reasonable fit to the morphology and kinematics of the Cartwheel by assuming a slightly off-center impact with a 20% mass companion. Specifically, the relative sizes of the two rings and the shape of the azimuthally averaged rotation curve were reproduced by an iterative process. This process consisted of estimating the form of the (initial) halo potential from the 21 cm. rotation curve, comparing the resulting post-collision rotation curve at the relevant time in the model disk to the data, and then updating the halo potential and repeating the process until a reasonable fit was achieved. Mean radial velocity profiles were found to be very sensitive to the way the averaging was performed, and to the time since impact. Improved fits were obtained in the later analysis of the 21 cm. data given in Higdon (1993).

Another basic result of the models of Struck-Marcell and Higdon (1993) is that the first ring wave is weak in galaxies with a slightly rising rotation curve like the Cartwheel. Many of the physical mechanisms suggested as star formation triggers in interacting galaxies cannot reconcile the vigorous starburst in the ring with the small density perturbation. Specifically, the wave is not strong enough to generate either shocks or a nonlinear increase in cloud collisions. Thus, neither direct triggering by cloud collisions, which is the basis of many popular models of star formation in interacting galaxies (e.g., Noguchi 1990; Olson and Kwan 1990a, b), nor density dependencies without a threshold (e.g., Mihos et al. 1992, 1993) can account for the starburst ring. Instead, the nonlinear response in the ring (first suggested by Davies and Morton 1982 and discussed recently by Charmandaris, Appleton and Marston 1993) argues strongly for a threshold (density) effect. The simulations of Struck-Marcell and Higdon show that when the precollision disk is not too far from the gravitational instability threshold the wave triggers strong cloud buildup in the ring, and spoke formation downstream. An alternate model in which the observed ring is actually the second wave is discussed below. Because the companion is slightly less massive, the second ring is similar to the wave described by Struck-Marcell and Higdon.

On the other hand, as noted above, Gerber, Lamb and Balsara (1992) describe evidence of the existence of strong shocks and shock-induced star formation in another ring, Arp 147. The physics of wave-induced star formation is complicated and the role of different processes probably varies from system to system, depending on, e.g., companion size and the perturbation amplitude. The main lesson of the Cartwheel example is that it demonstrates what kind of information can be obtained about modes of star formation from the rings.

Another aspect of the Cartwheel ring galaxy that has yet to be modeled in detail is the fact that most of the star formation occurs in the southern quadrant of the galaxy (see also discussion in Section 3.4). The early models of Appleton and Struck-Marcell (1987b) were able, with the threshold star formation models, to provide some explanation for why only parts of the ring are fully activated, yet neither these models, nor the recent SPH/Schmidt law algorithms of Mihos and Hernquist (1994a, b) can explain the absence of star formation in the second inner ring. Perhaps the explanation lies in the highly asymmetric distribution of the large-scale HI emission (Higdon 1992) which may indicate that a substantial amount of HI has been "punched" out of the center during the collision (see Foster 1986; Horellou and Combes 1994).

### 6.4. What Are the Spokes?

One topic of especial interest in the Cartwheel is the spokes which so perplexed Zwicky in 1941. Spokes in ring galaxies are rare. Indeed, the Cartwheel spokes are unique among the known collisional ring galaxies. AM0644-741 and II Hz 4 have spiral-like arms interior to the ring, but there are few of them and they are less flocculent in appearance. It is possible that these latter features are the direct result of a low order spiral mode driven by a slightly asymmetric collision. Similarly, the Cartwheel spokes might be the result of a higher order mode in the collisional perturbation, but their morphology makes it seem less likely.

We favor the alternative hypothesis that they are the result of internal gravitational instabilities following the impact, and if so, they may provide sensitive constraints on that process. Several of the simulation studies referenced above provide input on this question, including especially [Hernquist and Weil \(1993\)](#), [Struck-Marcell and Higdon \(1993\)](#), and [Gerber \(1993\)](#).

Let us consider the wave-triggered instability hypothesis in a little more detail. Before the collision, assume that the surface density in the disk is below, but near the threshold value for axisymmetric gravitational instability (e.g. [Binney and Tremaine 1987](#), Section 5.3). The disk already knows the approximate instability scale, because the wavelength of the fastest growing mode is determined only by parameters intrinsic to the target galaxy. Finite amplitude stochastic fluctuations can generate flocculent spirals on roughly this scale. After the collision, wave compression increases the surface density, pushing it over the critical value for instability. Unstable growth occurs in the rings, with the flocculent spirals or giant clouds serving as seeds. The simulations of Struck-Marcell and Higdon show that there need not be a one-to-one correspondence between seeds and spokes. Some seeds may merge in the ring, but the number of seeds and spokes (and star-forming knots in the ring) should be roughly the same since they are formed by the same instability. In the rarefaction behind the compression wave high density regions are stretched into spokes. Clearly these high density regions must not become so tightly bound in the wave compression that the shear and expansion are unable to stretch them apart. At the same time we assume that the wave compression is sufficient to lead to gravitational collapse and star formation on smaller scales within these proto-spokes. Some flocculent seeds may consist of such loose agglomerations that they do not grow significantly in the compression and are subsequently disrupted in the rarefaction.

This hypothesis has many interesting consequences. Firstly, no spokes are predicted if the perturbation is small and the pre-collision disk is well below the gravitational instability threshold, e.g., if the gas surface density is very low. However, the mass of the companion galaxy in most ring systems is usually fairly substantial compared with the target galaxy, if the optical or IR luminosity of the companion is any guide. Thus, even if the precollisional gas was quite stable, we might expect a substantial perturbation in most targets, which would be sufficient to push the gas density over the instability threshold. In this case a second factor enters, namely, the instability growth time relative to the compression time. The former is a local quantity, essentially the local free-fall time. The latter is one half of the local epicyclic period, which depends on the global gravitational potential, and so the compression time depends on global structure. Therefore, spoke formation depends on both local and global parameters.

One possible explanation for the apparent rarity of spokes is that most spokes may generally be hard to recognize. A reasonable estimate for the scale of spokes is given by  $\lambda_{\max}$ , the maximum unstable wavelength. According to the linear perturbation theory of the axisymmetric gravitational instability (see [Binney and Tremaine \(1987\)](#), Section 6.2),

$$\lambda_{\max} = \frac{2\pi^2 G \Sigma(r)}{\kappa^2(r)}, \quad (6.3)$$

where  $\Sigma$  is the gas surface density. The number of spokes can be estimated as the ring circumference divided by this scale,

$$N_{\text{spoke}} = \frac{2\pi r}{\lambda_{\max}}. \quad (6.4)$$

If this number is large, we might expect many small spoke segments, which would be poorly resolved on most ground-based CCD images presently available. Moreover, since each such "spokelet" only contains a small fraction of the gas in the disk, the enhancement of star formation within the spokelet may be modest. The brightness contrast between spokelet and inter-spoke regions should be small. **Thus, relatively bright spokes, stretching between two rings, or between an outer ring and the nuclear regions, may only form when  $N_{\text{spoke}} \approx 2\pi$ .** (Note: this criterion is closely related to the dependence of the swing amplification on the parameter  $X = \lambda / \lambda_{\text{crit}}$ , see [Toomre 1981](#)). Within the next few years it should be possible to obtain observations of sufficiently high resolution to test these ideas.

In the meantime, we can return to the published simulations, and ask what information they provide about spokes. At first sight, the fully self-gravitational N-body/SPH studies seem to give contradictory results. In the simulations of [Hernquist and Weil \(1993\)](#) strong spokes form, while spokes do not form in the simulations of [Gerber \(1993\)](#), and [Gerber, Lamb and Balsara \(1994\)](#). Spokes, if present, are not strong in the N-body/gas particle simulations of [Horellou and Combes \(1994\)](#). Spokes also formed in the models of [Struck-Marcell and Higdon \(1993\)](#), in which self-gravity was computed only on small scales.

Another mysterious fact is that in all these simulations the precollision target disks were evidently set up near the instability threshold. This statement can be quantified through the use of Toomre's  $Q$  parameter for axisymmetric stability (see e.g., [Kennicutt 1989](#)). Gerber's simulations were initialized such that  $Q = 1.5$  for the stars throughout the disk (where  $Q$  is defined as

$0.3\sigma_r \kappa / (G\Sigma)$ , and  $\sigma_r$  is the radial velocity dispersion). [Hernquist and Weil \(1993\)](#) quote a value of  $Q = 1.3$  (apparently also for the stars) in their model. In [Struck-Marcell and Higdon \(1993\)](#), the value of  $Q$  is similarly about 2.0-3.0 throughout the disk. Thus, it would appear that these simulations, starting from similar initial conditions, produce different results.

In fact, there are significant differences in the halo and disk density distributions between the various models. Gerber's target rotation curve increases roughly linearly out to about 1.5 disk scale lengths, and then is quite flat (though it does turn over). Hernquist and Weil describe the rotation curve of their target disk as nearly flat out to a cutoff radius,  $r_c$ . The rotation curve used by Struck-Marcell and Higdon was of the form  $v\theta \propto (r/\gamma)^{1/5}$ , which is slowly rising at radii greater than the scale radius  $\gamma$ . These differences and those in the initial conditions account for different radial distributions of  $\lambda_{\max}$  and  $N_{\text{spoke}}$ .

In [Hernquist and Weil \(1993\)](#), the value spoke ranges from a few in the inner regions to greater than 10 in the outer disk. According to our calculation, in Gerber's disk  $N_{\text{spoke}} \approx 11$  at  $r = 1.0$  (in computational units, or 0.8 disk scale lengths), and rises steadily at larger radii. Moreover, in Gerber's simulations the typical value of  $\lambda_{\max}$  is only of the order of a couple of mesh lengths used in the PM calculation. These results are in accord with the discussion above, i.e., spokes are seen in the models of Hernquist and Weil because of the low value of  $N_{\text{spoke}}$ . Only small spokelets are expected in Gerber's simulations, and these may be smoothed since their size is comparable to the finite difference algorithm scale. In the models of [Struck-Marcell and Higdon \(1993\)](#), self-gravity is only computed over a small range of wavelengths, but the target disk was initialized such that  $\lambda_{\max}$  falls within this range. Models with  $N_{\text{spoke}}$  of order of a few produced spokes much like those of Hernquist and Weil, though weaker. Models with larger values of  $N_{\text{spoke}}$  produced numerous spokelets (see Figure 8 of [Struck-Marcell and Higdon 1993](#)). Note also that heating and cooling effects have not been included in these "spoke simulations" (see [Section 6.5](#)).

In the figures of Hernquist and Weil, the spokes appear in the gas before the collision, and are then amplified by the ring passage. Their early appearance may be the result of a slightly lower effective  $Q$  than the other models, and greater intrinsic amplification because the most unstable mode is of relatively low order.

The story of the formation of the spokes is not yet a closed book. We have recently produced realistic looking spokes behind the second ring in a simulation which only produced rather weak small-scale spokelets (large  $N_{\text{spoke}}$ ) behind the first ring (Struck, in preparation). This [Cartwheel](#) model is based on the premise that the far companion (Galaxy G3 in Higdon's nomenclature; see [Section 3.3.1](#)) was the intruder, and that the *outer ring is the second*, not the first ring. The computational details are as in [Struck-Marcell and Higdon \(1993\)](#), except that the intruder model also contains a gas disk, and heating and cooling processes were included in the model ([Section 6.5](#)). The companion mass was also lower (about 15% of the [Cartwheel](#)). Such models open up the possibility that the disk need not be on the edge of instability for spoke formation initially, but that two cycles of ring compressional amplification could do the job. This would help to explain the rarity of spokes, since only well evolved ring galaxies would develop them.

We remind the reader that, thus far, no gas has been found unambiguously associated with the spokes as might be expected from the models above and they still remain enigmatic. The discovery of dust lanes crossing the inner ring in the vicinity of the spokes (based on the HST observations of [Figure 1](#)) does, however, suggest that the detection of molecules in the spokes may simply be a matter of time and the need for greater sensitivity than is currently possible (see [Section 3](#)).

## 6.5. Explorations of Heating and Cooling Effects

The interpretations of multiwavelength observations and a full understanding of nonlinear feedback effects in the interstellar gas require simulations that include heating and cooling processes, and the exchange between thermal phases. However, it is extremely difficult to see how some of these effects should be treated. For example, the short timescales of atomic and molecular cooling processes relative to galaxy dynamical times presents one problem, though, in fact, we need not time-resolve rapid cooling. Another problem is the wide range of heating processes and scales associated with energy input from stellar activity, including: *UV* photoheating, winds from many different types of star, multiple supernova explosions in young clusters, etc. Finally, adiabatic cooling in expanding flows is probably one of the most important processes. In the turbulent interstellar gas, expansion flows are likely to be found on many length and time scales. Fortunately, we will usually only need to resolve the effects of the scale on the interaction driven waves.

Very little work has been done in this area; there is almost no literature to review. CS has begun some exploratory simulations with very simple models for the thermal processes. In this subsection we will very briefly describe some simulations of off-center collisions. We expect it will be some time before there is any standard or consensus method of modeling these processes, but the example below provides an illustration of their importance. The following description of the model is derived from Struck (1995).

The simulation is based on a quite standard smooth particle hydrodynamics (SPH) algorithm, which is essentially the same as that used in [Struck-Marcell and Higdon \(1993\)](#). 19,000 particles were used to represent the gas disk of the target galaxy and 3000 particles were used to simulate the companion disk. The disk particles were initialized on circular orbits in centrifugal balance with a fixed, rigid gravitational potential (i.e., the halo) with a rotation curve of the form  $v_{\theta} \propto (r / \gamma)^{1/n}$  in the target disk, where  $v_{\theta}$  is the rotation velocity, and  $\gamma$  is the scale length of the potential. With the adopted value of  $n = 5$ , this rotation curve rises rapidly in the inner regions, but is nearly flat at large radii. A simple softened point-mass potential was used for the companion. These simulations did not explicitly include either a stellar disk or a separate stellar bulge component, and thus, represent late-type disk galaxies. The simulations do include a calculation of local self-gravity between gas particles on a scale comparable to the SPH smoothing length, as described in [Struck-Marcell and Higdon \(1993\)](#).

The simulation presented below used a simple step function cooling curve, with three steps. All gas elements are initialized to a single temperature  $T_0$ , assumed to lie in the range of about 5000-8000 K, corresponding to the warm interstellar gas. At temperatures between  $T_0$  and  $70 T_0$  the cooling timescale  $\tau_c$  is short relative to other timescales in this code, so it is assigned a value equal to a few times the typical numerical timestep. This high cooling rate represents the peak in the standard cooling curve due to hydrogen and helium line emission in an optically thin gas. At temperatures above  $70 T_0$  the cooling rate is decreased by a factor of 10. This decrease is meant to approximate the combined effects of heating and cooling, on the assumption that the hot gas is found near the sources of heating. On the other hand, the hot gas frequently cools rapidly by adiabatic expansion, so this part of the cooling function has a minor effect on the model results. At temperatures below  $T_0$  the cooling rate is decreased by a factor of 20 from the value immediately above  $T_0$ . Cooling is weaker at these temperatures in the interstellar medium. Moreover, another reason for using this decreased rate is to inhibit the gas particles from cooling to negative temperatures, but to do so without having to time-resolve the low temperature cooling.

When a gas particle is located in a dense or high pressure region (cloud), so that its internal density exceeds a fixed critical value, it is assumed that stars are formed. The particle is then heated by increasing its temperature by a fixed multiple of  $T_0$  at each timestep for a finite duration, or until it reaches a maximum  $T_{\max}$ . While it is being heated it is not allowed to cool except by adiabatic expansion. It is clear from the results that even these very simple approximations are capable of representing phenomena that do not occur in an isothermal gas.

Initially the gas is below the critical density for SF at all locations. The gas density in the initial isothermal disk is also below, but near, the threshold density for axisymmetric gravitational instabilities, i.e. the value of the well-known Toomre  $Q$  parameter indicates stability. Particles out of the plane of the disk are not quite in centrifugal balance, and therefore settle into the disk at the beginning of the simulation in the target disk. The companion is so far below the threshold that it remains cold.

[Figure 21a-c](#) shows three orthogonal views ( $x$ - $y$ ,  $x$ - $z$ ,  $y$ - $z$ ) of three timesteps from this simulation (dimensionless length units are as in [Struck-Marcell and Higdon 1993](#)). In this figure the gas elements are placed in three temperature bins, and are color-coded to indicate both this, and which galaxy the particle originally belonged to. The coolest elements, with temperatures less than 10 times the initial value (i.e.,  $< 50,000$  K). Hot elements with temperatures greater than 300 times the initial and intermediate temperatures ("warm") are also indicated by color.

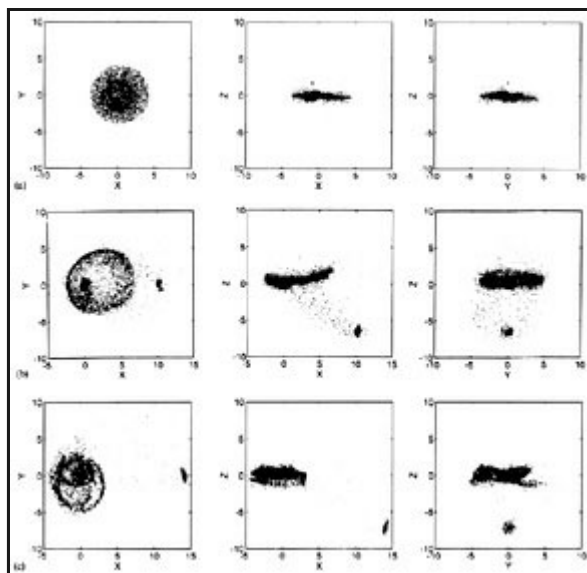


**Figure 21.** Particle snapshots of an SPH collisional simulation with heating and cooling as described in Section 6.6. Each row contains three orthogonal views -  $x$ - $y$ ,  $x$ - $z$ ,  $y$ - $z$  from left to right - at one time. The three rows show the model at: a) the time of impact, b) when the first ring has expanded significantly into the disk and c) when the second ring has almost reached the edge of the disk and a third ring has formed at the center. Note the formation of strong spokes inside the second ring in c). The color coding is as follows: For the target disk, red, green and cyan represent the "cool", "warm", and "hot" components. For the intruder galaxy, the same temperature sequence is represented by the color yellow, magenta and blue respectively. Only one in three SPH particles are shown in these low resolution plots. See Color Plate X at the back of this issue.

[Figure 21a](#) shows the disk at the time of impact. The companion disk is setup perpendicular to the primary disk in the  $y$  -  $z$  plane. The orbit of the companion center is in the  $x$  -  $z$  plane and it impacts at a significant angle. The strong shocks in the two disks are shown in the first frame as a thin zone of hot, blue and cyan particles. The effects of the shock are visible in the other two views, where it is evident that the (yellow) disk does not simply punch through the primary disk. The rotation directions of the two disks can also be deduced from the small stochastic spirals in the unperturbed regions.

A significant part of the primary disk, and all of the companion disk are disrupted by the impact, and much gas is splashed out in, a bridge-plume. Nonetheless, most of the primary disk remains intact, and the ring forms as in collisionless encounters. The second set of frames ([Figure 21b](#)) shows a time when the first ring has nearly propagated through the disk. The ring is complete, but with azimuthal density variations and significant warping. Green (warm) and blue (hot) dots mark the sites of recent heating (i.e., star formation). The preponderance of green relative to blue indicates that the density is falling below the heating threshold. There is little heating behind the ring, where strong cooling results from postshock rarefaction.

The hot central regions and the blue-green are primarily the result of infall from the bridge. It is also a result of azimuthal compression in the off-center collision, as in [Toomre's \(1978\)](#) ring-to-spiral models. The fact that the infall is concentrated in one narrow sector is surprising. However, it appears that most of this infalling material originated in the half-disk where the rotation velocity was opposite the orbital direction in the companion, or from gas in the primary that it collided with (yellow and red appear quite well mixed in the bridge).

Even more spectacular is the reformation of the companion disk, which was almost totally disrupted in the collision. At this time the disk is accreting from a stream of material that includes gas from the companion that was orbiting in the same sense as companions orbit at the time of impact. This material spirals into a smaller disk, so there is much heating. The heating algorithm may not be all that realistic here, but the accretion processes may in fact be responsible for the enhanced activity in rings with

attached companions.

The third set of frames ([Figure 21c](#)) is from a much later time when the companion has reached apoapse and begun to return. **The ring at the edge of the disk is now the second ring**, and, though the disk is warped, it is intrinsically noncircular. There are strong azimuthal variations in the heating (star formation) around the ring, a situation quite similar to that observed in the [Cartwheel](#). A third ring is forming in the central regions. The star formation in this third ring is a result of the relatively high gas densities due to infall there, and gas driven inwards by collisions with infalling elements. This is not entirely realistic, because gas consumption has not been included, and the heating algorithm only looks at the total gas density, not what fraction of this gas is truly in a state conducive to star formation.

This timestep also illustrates how the most distant companion (G3 of [Higdon 1993](#)) in the [Cartwheel](#) system might have managed to be the intruder without having a very large relative velocity (despite its size, the observed outer ring is the second ring in this model). The scenario is especially compelling in the light of Higdon's recent discovery (private communication) that the intergalactic HI plume extends all the way to G3.

In this simulation, the most unstable wavelength in the pre-collision primary disk, and the scale on which self-gravity is computed, is quite small (0.1 in the simulation units). Thus it is not surprising that there are no strong spokes in the wake of the first ring (except for the "accretion arm"). Several strong spokes are apparent behind the second ring (which becomes the outer ring in the [Cartwheel](#) analogy). Because of their significant width in the third dimension, the density in the spokes does not exceed the star formation threshold. As noted above, this provides an alternative explanation for the rarity of the spoke phenomenon - it may take two cycles of wave compression and rarefaction to create them. The simulation shows that there are other complications, such as infall and the long-term effects of the "swing" in the off-center collision.

This simulation has not yet been analyzed in detail, nor have parameter dependencies been studied with additional simulations. More particles and spatial resolution in the multiphase gas disk would certainly be desirable, as would the inclusion of gas consumption and full selfgravity. Nonetheless, it illustrates some of the possible effects of the thermal terms and is the first model we have seen of gas exchange in a direct collision.

## 7. FUTURE DIRECTIONS

The last few years have seen a revival of interest in colliding ring galaxies and these new studies are providing an important stimulus for future work. We therefore conclude our review with some general recommendations for future work in this area.

### 7.1. Observational Directions

The discovery of large radial color gradients in ring galaxies provides an important stimulus for obtaining observations of ring galaxies with high spatial resolution and high sensitivity. Clearly of great importance is the detailed examination of the cause of the radial color gradients. As we have discussed, the most likely explanation is in terms of an evolving starburst population in the wake of the expanding rings. However, as with most color diagnostics, the effects of both reddening by dust and variations in metallicity are always factors to be explored. High resolution observations with the Hubble Space Telescope and with ground based telescopes equipped with adaptive optics provide the best hope of understanding the details of this process. At the time of writing, HST images have been made of the [Cartwheel](#) and [IIZw28](#) by K. Borne and collaborators (including the authors of this review) and these data are currently being analyzed. These data have the potential of providing information about the time evolution and stellar content of the young star clusters formed in the rings and how they change with time downstream of the wave. In addition, new informations about the stellar make-up of the spokes will soon be forthcoming. Spectroscopic follow-up of these kinds of observation are vital. In particular, large ground-based telescopes will be required to obtain observations of stellar absorption lines of the faint material inside the "centrally-smooth" ring galaxies like [VIIZw466](#) and [Arp 147](#). Because these galaxies lack a complicating central bulge, the faint stellar material contained in their centers represents virgin territory in terms of following the evolution of the starburst from the outer ring to the center. These galaxies should be prime targets for future studies. Work on other less well studied centrally smooth southern rings (such as [AM2145-543](#) and [AM0417-391](#) in the south) should also be undertaken to build up a larger sample of "centrally-smooth" rings.

As the tantalizing work of [Charmandaris et al. \(1993\)](#) has shown, the HII regions in ring galaxies may hold some clues about different modes of star formation in galaxies. However, very little work has been done on the neutral and molecular gas content of these galaxies with the arcsecond resolution needed to begin to exploit the rings as star formation laboratories. Useful parallel studies on the distribution of dust (perhaps with ISO or focal plane arrays such as SCUBA on the JCMT) will help to answer questions about the importance of dust in the observed color gradients as well as its importance in density wave triggered star formation. Questions such as whether galaxies like [Arp 10](#) are showing evidence for "threshold" star formation behavior can only be properly tested if we can map the distribution of molecules with high spatial resolution. As the work of [Horellou et al. \(1994\)](#) has shown, very few of the ring galaxies are strong CO emitters, and so mapping the fainter ones will require more sensitivity than is available with current CO interferometers.

The recent models of ring galaxies using hydrodynamics with realistic heating and cooling terms incorporated into the dynamics shows that the ring will be the site of major vertical outflows which should be detectable with AXAF. Mapping of the soft X-ray emission from outflows associated with the rings should be possible with AXAF's HRC instrument, and such observations will provide the next important tests of the models. The models suggest that the degree of heating in the ring is crucial to both the formation of spokes (too much heating blows them apart) and the formation of a reasonably narrow dense ring. The combination of both high resolution optical and uv observations with 0.5 arcsec X-ray imaging from AXAF will strongly constrain the range of possible energetic behavior in the young stellar associations and this will ultimately lead to a better understanding of the importance of ISM heating from *O/B* association winds as compared with the selfgravity of the dense regions in the ring.

Additional information on the nature of the stellar evolution in and behind the ring waves will be obtained with high sensitivity radio continuum observations at a number of frequencies. These are well within the reach of the current capabilities of the VLA and some work is being done in this area by one of us (PNA). High resolution observations, particularly those sensitive to the polarization of the radio emission, will allow for a more detailed comparison to be made between the star formation regions and the structure of the magnetic field in the wake of the ring wave. It has been suggested (R. Allen, personal communication) that the outgoing density wave may lead to an ordering of the magnetic field lines behind the wave if most magnetic fields are generated locally within clouds on a scale smaller than the wave itself. Further interesting effects might be expected as the disk puffs up behind the ring, increasing the vertical scale-height for the cosmic-ray electrons. The spectral steepening in the radio continuum found in [Arp 10](#) behind the main ring (Ghigo and Appleton, in preparation) may also relate to an aging of the relativistic electron population as a function of time. Further observations are needed of a much larger sample of ring galaxies to determine how universal this effect may be.

Finally, observations of ring galaxies at high redshift would be of great interest. The majority of known ring galaxies have been found through inspection of photographic plate material. Observations with high angular resolution, such as those made with the Hubble Space Telescope, are yielding many background galaxies, often serendipitously. The large number of WFPC-2 images now being accumulated will be an important source of new high redshift ring galaxies and we urge efforts to be made to find new candidates.

High redshift ring galaxies are expected to be interesting for a number of reasons. Firstly, galactic collisions are likely to be more frequent in the past than at the present epoch and so HST images may yield a dramatic increase in the number of new ring galaxies known. Secondly, high redshift ring galaxies offer the possibility of exploring the evolution of the galactic potential as a function of redshift. We have discussed earlier how the existence of multiple rings is particularly useful in determining the form of the gravitational potential in the target galaxy. In particular, broad widely spaced rings suggest a rising rotation curve whereas more closely spaced double rings with narrow ring structure suggest a declining rotation curve. Relatively simple morphological studies of high redshift rings will provide an interesting test of models of galaxy evolution that lead to the growth of dark matter halos by mergers. As we have emphasized in this review, care has to be taken to find gas-poor ring galaxies if this approach is to yield meaningful results, since the ring morphology is heavily influenced by triggered star formation. High redshift galaxies that are similar to systems like [AM 1724-622](#) (which seem to be an example of a mainly stellar dynamical orbit crowding process - the classical Toomre process) would be the ideal candidates for tests of galactic structure.

On the other hand, if the recent models of Gerber are correct, then the relationship between the distribution of neutral gas and the underlying stellar disk may also provide information about the dominance of dark matter in high redshift ring galaxies (see [Section 4.4](#) for further discussion). Since HI and CO observations are unlikely to be able to compete for some time with the spatial resolution of HST, it would seem that measuring the gas distributions in high redshift ring galaxies is a project for future generations. On the other hand, as has been shown for nearby ring galaxies, the distribution of ionized gas in such galaxies can provide some information about the distribution of gas versus old stars.

If the large color gradients found in nearby ring galaxies turn out to be ubiquitous through the universe, and if they can be understood in terms of the evolution of stars in the wake of the ring, then one might be able to determine the distance to the ring galaxies, even at high redshift. The method would rely on our ability to determine the age of the ring based on the radial color gradient alone, assuming that (see [Section 4.4](#)) the gradient is the result of the evolution of starburst populations in the wake of the expanding ring. Then, having a measurement of the angular diameter of the ring and an independent measurement of the expansion velocity in the ring (through detailed modeling and spectroscopy), the distance to the ring could be estimated. Of course, the fundamental uncertainty would be the age of the stellar population and the corrections one might make for internal reddening within the galaxy. A crucial test of this method may soon come with the new HST observations of the [Cartwheel](#). Here it will soon be possible to determine how well models of the color evolution of a stellar population fit with the observed distribution of star clusters and their colors in the region between the first and second rings.

## 7.2. The Next Steps in Modeling

In the next few years computer power will undoubtedly continue to increase rapidly, but there are many challenges remaining in

ring galaxy simulation, and it is unlikely that the computers will be powerful enough to solve them all directly. Nonetheless, we can expect substantial progress in an evolutionary, and perhaps even revolutionary, sense. To begin with, there is still a good deal of work to be done with current simulation tools. This includes detailed modeling of specific systems, especially those that have been studied at many wavelengths. It also includes more complete explorations of the effects of varying target galaxy structural parameters, and orbital parameters. This is especially true for off-center collisions, where all indications are that the wave structure depends very sensitively on the parameters. Finally, the long-term evolution of ring galaxies, including companion capture and merger, has just begun to be investigated.

With regard to modeling specific systems, the first question that arises is - which ones? The simplest answer is to choose ones with the most observational data available, especially the larger ring galaxies which are probably the most dynamically evolved. In particular, the existence of kinematic data (especially HI observations) is of special value to the modeler. For example, there is still important work to be done on the [Cartwheel](#) ring. The models in [Struck-Marcell and Higdon \(1993\)](#) were based on low-resolution VLA 21 cm data. Since that time [Higdon \(1992\)](#) has produced higher resolution velocity maps. Models designed to fit the high resolution velocity data should also give us a better idea of how warped the [Cartwheel](#) disk is. New Hubble Space Telescope observations have also been obtained (by K. Borne, R. Lucas (STScI) and ourselves) and observations such as these will guide future models. Additional fully self-consistent combined N-body/gas simulations are needed. Overall, the [Cartwheel](#) is a good system to model with three-body simulations because the potential is probably halo dominated, and the companions are relatively small, so the halo perturbation is minimal. However, self-gravity is needed to study the growth of local gravitational instabilities in the disk, and some differences can be expected with "live" halos and disks. In addition, the behavior of the collisional effect of a gas-rich intruder galaxy will probably be best studied with a responsive self-gravitating disk.

As discussed above, a good deal of data is currently being acquired on many other systems. The [Lindsey-Shapley](#) ring, [Arp 10](#), [Arp 147](#), [VIIZw466](#) and a number of others will deserve detailed modeling efforts in the next few years. One specific hope we maintain is that new observations will provide further information on the mystery of spokes. Either they will be discovered in other systems with more sensitive, higher resolution data, or tighter constraints will be placed on their existence. This information, in conjunction with detailed modeling, would help enormously in determining whether the theoretical ideas discussed above are correct.

Even aside from models of specific systems, there is much general unfinished business in the realm of ring galaxy simulation - e.g., so much parameter space and so little time! Of course, the advantage of ring galaxies is that their symmetry eliminates or reduces the importance of some dimensions of parameter space. To begin with only relatively cursory explorations have been made of the effect of varying the disk/halo/bulge ratios ([Huang and Stewart 1988](#); [Wallin and Struck-Marcell 1988](#); [Horellou and Combes 1994](#)). As usual, kinematic models should provide a good guide to ring structure in purely symmetric collisions, but they should be tested, and the variations in phenomena like disk warping should be elucidated. Another factor that deserves further study is the effect of the gas to old star mass ratio in the target disk. Some idea of the effects of the gas on the disk stars can be gleaned from the work of [Gerber \(1993\)](#), and [Hernquist and Weil \(1993\)](#), but not enough models have been run to determine the systematics.

Similarly, we do not yet have a systematic guide to the morphological zoo of ring relatives formed in slightly off-center, slightly retrograde, prograde or direct collisions. As emphasized above and in [Appendix 2](#), kinematic (and restricted three-body) models could also be a useful guide in this area. However, because of the extreme parameter sensitivity, producing a thorough morphological map by any means will be laborious. It seems likely that this goal will continue to be accomplished piecemeal, e.g., by assembling the results of studies of individual (asymmetric) systems.

Another fundamental parameter is time. By and large published simulations are not run long enough to determine the long term fate of the ring galaxy. Since in most cases where there is kinematic data available for the companion the system appears bound, we can expect an eventual merger. Merger simulations lead us to expect that this will occur after no more than two or three encounters. Some of the possible effects through the second encounter in nearly symmetric cases are reviewed in [Section 4.3](#) and [Appendix 1](#). The studies of [Lotan and Struck-Marcell](#) described there are the only work we are aware of to date. If the initial collision is significantly off-center or the inclination differs significantly from 90°, we expect that the evolving system will become increasingly asymmetric, and have little relation to the ring galaxy phenomenon after the second collision. However, these preliminary results and reasonable conjectures await confirmation with more detailed and extensive modeling.

Moreover, the long term evolution of unbound or marginally bound systems is not without interest. An intriguing example was given in the thesis of [Lotan-Luban \(1990\)](#). She found that in direct, off-center collisions, and also in off-center, slightly inclined (retrograde) collisions, a one-armed leading spiral wave formed and persisted for a very long time. A similar phenomenon was found earlier in retrograde tidal interactions by [Thomasson et al. \(1989\)](#) and [Athanasoula \(1978\)](#). [Lotan-Luban](#) tested a variety of parameter values with her restricted three-body simulations, and discussed the parameter dependencies in some detail. Studies with kinematic models (CS unpublished) seem to indicate that the one-arm is the locus of overlap of very high order ring caustic edges. This is consistent with the fact that the one-arm has not been seen to form in simulations of gas disks, where the ringing tends to damp out after about the third ring. Coupled N-body plus gas simulations are needed to answer the question of whether

the one-arm appears in a self-consistent stellar disk in the presence of dissipative gas.

How dissipative is the gas, e.g., how does it respond to compression? This is not merely a question of the immediate (e.g., postshock) compressibility of the gas, but equally of the heating and cooling processes at work within it, the resulting (time and spatially varying) thermal phase structure. We will not repeat the discussion of [Section 6.5](#) where some preliminary explorations of cooling/heating were presented, but we want to reiterate that those models as well as the cloud fluid models of [Struck-Marcell and Appleton \(1987\)](#) highlight the importance of such processes in the wake of a starburst ring. The issues of the role of these processes and how best to treat them in numerical simulations extend far beyond the limited field of ring galaxies. However, in all cases it is clear that their inclusion will introduce at least several additional parameters, i.e., new dimensions of model phase space, much additional computational complexity, and inevitable disagreements between workers following different approaches. It seems likely that cooling/heating effects will be one of the main frontiers of numerical simulation of galaxies for at least another decade. Once again, we expect that the relative simplicity and symmetry of collisional ring galaxies will guarantee them an important role in this field. The propagating single burst nature of their disk star formation is very simple, and thus attractive to modelers, compared with the complexity of, e.g., merging gas disks. High resolution observations of large-scale cooling shocks or (heated) superbubbles in rings would be extremely useful and exciting to modelers, and such discoveries are probably imminent.

It is becoming clear that to model and understand individual interacting galaxies requires the inclusion of much relevant physics. We believe that this must include, at some level of approximation, stellar and gas dynamics of the multi-component galaxies with self-gravity, pressure and heating/cooling effects. In particular, to model most real ring galaxy systems, this will eventually require that the simulations include non-isothermal gas disks in both primary and companion galaxies. There are several reasons these simulations should include cooling and heating. The first is that the strong shocks resulting from direct collisions between gas elements in different galaxies may heat the gas to such high temperatures that radiative cooling is not essentially immediate. The second is that the adiabatic expansion cooling of gas pulled out of the disks may be so strong that the temperature of that gas falls below its original value, an effect which could be very important to the occurrence of star formation in extended tidal features. A third reason is that the thermal effects of gas falling back onto the primary disk may be very important.

The upshot is that as simulations get more realistic they will get much more complex, and because of computational limitations, it will not be possible to include all the relevant processes in a unique way, based on well-understood physical principles. Approximations and phenomenological treatments will still be necessary. Consequently, model predictions will have to be handled with care, and continually checked and constrained by observation. Nonetheless, in conjunction with future multiwavelength observations (especially in the X-ray and far-infrared) the next generations of models should substantially advance our understanding of star formation and the thermal physics of the interstellar gas in ring galaxies in particular and interacting galaxies in general.

### Acknowledgments

We thank the following people for supplying material, in some cases in advance of publication: K. Borne (STScI), R. Buta (U. of Alabama), F. Combes (Meudon), A. Garcia (IAC-Spain), R. Gerber (NASA-Ames), F. Ghigo (NRAO-GB), L. Hernquist (Lick Obs.), J. Higdon (NRAO-AOC), C. Horellou (OSO-Sweden), M. Joy (NASA-Marshall), S. Lamb (U. of Illinois), S. Majewski (Carnegie-Pasadena), A. Marston (Drake U.- Iowa), J. C. Mihos (Lick Obs.), R. Norris (ATNF-Australia), J. Rodriguez Espinosa (IAC-Spain), B. Smith (U. of Texas) and J. Wallin (GMU). For stimulating conversations on ring galaxies we also wish to thank F. Ghigo, K. Borne, J. Wallin, J. Higdon and C. Horrelou and R. Gerber. PNA wishes to thank the hospitality of Cathy Horrelou and Françoise Combes (Meudon) during a recent visit to Paris in which molecular observations were discussed. We are especially grateful for the insightful comments and extensive suggestions of A. Toomre and those of an anonymous referee. We also thank B. Elmegreen for additional suggestions. The latter part of this work was partially funded under NSF grant AST 9319596.

### APPENDIX 1: Multiple Encounter Kinematics

In this Appendix the epicyclic KIA model is used to further examine the effects of a second symmetric collision described in [Section 4.3](#). Specifically, immediately after the second collision, Equation (4.5) can be replaced with

$$r = q - A_2(q)q \sin(\omega(t - t_2) + \omega t_2 + \psi), \quad (\text{A1.1})$$

where  $t_2$  is the time of the second collision (with  $t = 0$  at the first collision). The amplitude  $A_2$  is defined through the velocity equation at time  $t_2$ ,

$$v(t_2) = -A_1 q \omega \cos(\omega t_2) + \Delta v_2 = -A_2 q \omega \cos(\omega t_2 + \psi), \quad (\text{A1.2})$$

where  $\Delta v_2$  is the velocity impulse in the second collision, and the second equality defines  $A_2$ . Equations (A1.1) and (A1.2) can be combined to eliminate the phase  $\psi$ ,

$$A_2^2 = \left( \frac{r_2 - q}{q} \right)^2 + \left[ -A_1 \cos(\omega t_2) + \frac{\Delta v_2}{q\omega} \right]^2, \quad (\text{A1.3})$$

with  $r_2 = r(t_2)$ , the radius of the given star at the time of the second impact. This can be simplified using the relations

$$\frac{r_2 - r}{q} = -A_1 \sin(\omega t_2), \quad \text{and} \quad A_1 = \frac{-\Delta v_1}{q\omega}. \quad (\text{A1.4})$$

Thus, we obtain

$$A_2 = A_1 \left[ \sin^2(\omega t_2) + \left( \cos(\omega t_2) + \frac{\Delta v_2}{\Delta v_1} \right)^2 \right]^{1/2}. \quad (\text{A1.5})$$

The orbit equation then becomes

$$\begin{aligned} r &= q - A_1 q \left\{ \sin^2(\omega t_2) + \left( \cos(\omega t_2) + \frac{\Delta v_2}{\Delta v_1} \right)^2 \right\}^{1/2} \\ &\times [\cos(\omega t_2 + \psi) \sin(\omega(t - t_2)) + \sin(\omega t_2 + \psi) \cos(\omega(t - t_2))]. \end{aligned} \quad (\text{A1.6})$$

In zones where the last term in the square brackets is small after the second impact, i.e.,  $\sin(\omega t_2 + \psi) \approx 0$ , Equation (A1.6) is **essentially the same as Equation (4.5), but with a position-dependent amplitude.**

In zones where the first term in the square brackets in Equation (A1.6) is small, i.e.,  $\cos(\omega t_2 + \psi) \approx 0$ , that equation is similar to Equation (4.5), but the perturbation term is off by a phase of  $\pi/2$ . As a result we expect a change in the morphology and rate of propagation at phases where there is a change of dominance from one term to the other. The models confirm that the rings do not propagate as rapidly outward following the second impact as they did during the first.

When  $\cos(\omega t_2) > 1$ , all of the terms in Equation (A1.5) add, and the wave amplitude will be relatively large (unless  $\cos(\omega t_2 + \psi)$  is small). When  $\cos(\omega t_2) < 1$  the last two terms on the right-hand-side of Equation (A1.5) will tend to cancel, resulting in weak waves in that region. Indeed if the phase  $\omega t_2$  is such that  $\sin(\omega t_2) \approx 0$ , then  $A_2 \approx 0$ , i.e., the second perturbation can essentially cancel the first. Such trajectories are seen in the models. If the amplitude of nearby trajectories is large enough they can cross the  $A_2 \approx 0$  trajectory. The result is a ring that does not propagate outward, but its width varies with time. Though it will be affected by stellar diffusion, such a stationary ring could be long-lived. Because their locations depend on the details of the collisions as well as the disk structure, they will in general have no relation to classical Lindblad resonances.

## APPENDIX 2: Simple Models for Asymmetric Stellar Ring-Like Waves

In this appendix we will briefly describe how the analytic kinematic, impulse approximation (KIA) model for caustic waves can be generalized to include waves that are not cylindrically symmetric. Because of the huge variety of such waves (see [Sections 4.4 and 6](#)) we cannot pursue this investigation very far in this review. However, nearly exactly symmetric collisions must be very rare, and in fact most known ring galaxies have some asymmetries. Thus, generalizing the theory is extremely important if it is to be tested against observations of real galaxies. Ring galaxy theory can serve as a prototype for studies of a wider set of interacting systems only to the degree that it can be readily generalized.

Analytic models for asymmetric caustic waves were explored in [Struck-Marcell \(1990\)](#), and a number of examples were presented for the case of a softened point-mass target and a Plummer potential companion galaxy. A more complete development of the SPM case, including an entirely analytic formula for the caustics as a function of time and the collision

parameters is given in [Wallin and Struck-Marcell \(1994\)](#). This formalism was used by [Donner et al. \(1991\)](#) to produce semi-analytic models of waves produced in tidal interactions, and for the first time numerically solved the asymmetric caustic condition to determine the caustic edges. (Wallin ([1989](#), [1990](#)) independently investigated caustics in tidal tails using restricted three-body simulations.) In their comparison study of analytic models vs. N-body simulations [Gerber and Lamb \(1994\)](#) included the perturbation of the potential center of the target galaxy in KIA models. Their analytic models assumed a target potential with a flat rotation curve, and a Plummer potential for the companion.

In the following we will assume that the gravitational potential and the collisional potential amplitude are simple power-law functions of radius in the target disk. Once again, this greatly simplifies the algebra, making it easier to follow the basic ideas. Otherwise the discussion parallels that of Section II of [Struck-Marcell \(1990\)](#), and [Wallin and Struck-Marcell \(1994\)](#), with some modest generalizations.

We begin by considering the geometry of the impulsive perturbation, with the help of [Figure A.1](#). Each panel shows a representative disk star at unperturbed radius  $q$ , and the companion impact point at radius  $r_*$ .  $R$  is the distance between the star and the impact point. The vector from the disk center to the impact point defines the  $x$ -direction, and  $\theta$  is the azimuthal angle of the disk star relative to that axis. The law of sines relates the angle  $\alpha$  to  $\theta$  by,

$$\sin(\alpha) = \frac{r_*}{R} \sin(\theta). \quad (\text{A2.1})$$

In the first panel of [Figure A.1](#) it is assumed that  $r_* \ll q, R$ , so  $|\alpha| \ll 1$ . This limit is valid through most of the disk for slightly off-center collisions, and can be viewed as a perturbation of the symmetric collision case. As pointed out in the discussion of Equation (16) of [Wallin and Struck-Marcell \(1994\)](#) the analytic theory is considerably simplified in this limit.

The second panel is relevant to the inner disk for a slightly off-center impact, or the bulk of the disk for an impact at the edge, or outside of the disk. In this case  $r_* > q$ , but  $R$  can range from  $r_* - q$  to  $r_* + q$ . The magnitude of the angle  $\theta$  is small in this case, but  $\alpha$  can range from  $-\pi$  to  $\pi$ . The former fact should simplify the analytic theory in this case, but this limit has not been much explored to date. This is unfortunate because that theory may be applicable not only to companions hitting at large angles to the disk, but also to all retrograde encounters. (In contrast to the prograde encounters which may not be sufficiently impulsive.)

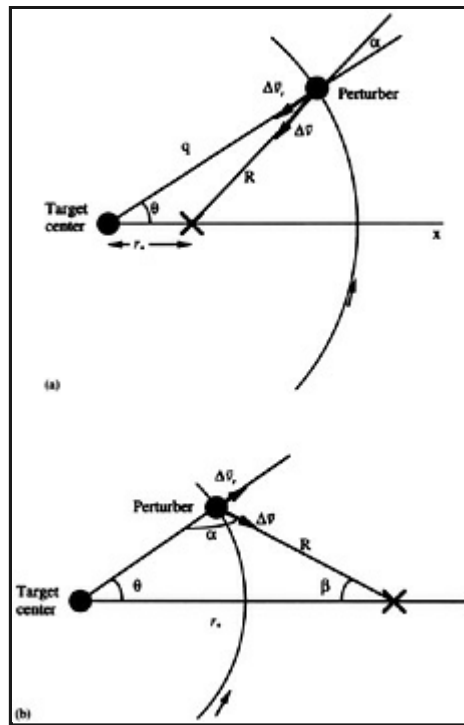


**Figure A1.** Schematic illustrating definitions of various collision variables and parameters (see text). a) shows a case when the point of closest approach is outside the orbit of a representative disk. Part b) shows a case where the impact is inside the stellar orbit.

Let  $\Delta v$  be the (positive) magnitude of the velocity impulse at a point. The radial velocity perturbation  $\Delta v_r$  is always inward and negative in the nearly symmetric case. In the case of a large collisional offset  $\Delta v_r$  is positive and outward directed in half of the disk where the impact occurred, and negative inward in the other half. In both cases these in-plane components of the velocity impulse can be written

$$\begin{aligned}\Delta v_r &= -\Delta v \cos(\alpha), \\ \Delta v_\theta &= -\Delta v \sin(\alpha), \quad \text{with } \Delta v > 0.\end{aligned}\tag{A2.2}$$

$\Delta v$  can be calculated as per the usual IA procedure (see e.g., [Binney and Tremaine \(1987\), Section 7.2](#)).

Generally, the disk plane will be tilted relative to the plane normal to the orbit at the moment of impact, and the angle of impact will not be perpendicular to the disk plane. Then the vertical impulse  $\Delta v_z$  will not be zero to first order as in symmetric collisions. Unfortunately,  $\Delta v_z$  will also not be easy to estimate accurately, nor will the modifications to  $\Delta v_r$  and  $\Delta v_\theta$  induced by this asymmetry. Although analytic estimates might be very helpful for interpreting simulations (in which such vertical effects are obvious), little work has been done in this area, and we will neglect these interesting effects here.

In the epicyclic approximation the post-collision orbit equations of a disk star are:

$$\begin{aligned}\tau &= q' - Aq' \sin(\kappa't + \psi'), \\ v_r &= -Aq'\kappa' \cos(\kappa't + \psi'), \\ \theta &= \theta_0 + \omega_{\text{cir}}(q')t, \\ v_\theta &= v_{\theta_0} + \Delta v_\theta.\end{aligned}\tag{A2.3}$$

The variables  $q, \theta_0$  are the precollision radius and azimuth of the star, and  $q', \theta'$  are the post-collision guiding center and azimuth. The epicyclic and orbital frequencies at the new guiding center radius are  $\kappa' = \kappa(q')$  and  $\omega_{\text{cir}}(q')$ , respectively. The epicyclic phase of the star immediately after the collision is  $\psi'$ .

The initial conditions at the moment of impact ( $t = 0$ ) in the IA are:

$$\begin{aligned} r &= q = q' - Aq' \sin(\psi'), \\ v_r &= \Delta v_r = -Aq'\kappa' \cos(\psi'). \end{aligned} \quad (\text{A2.4})$$

These equations can be solved for the perturbation amplitude  $A$  and the phase  $\psi'$  in terms of  $\Delta v_r, q'$  and the precollision quantities, i.e.,

$$\begin{aligned} \sin(\psi') &= \frac{q' - q}{Aq'} = \frac{\delta}{A}, \\ \cos(\psi') &= \frac{-\Delta v_r}{Aq'\kappa'}, \end{aligned} \quad (\text{A2.5})$$

where we have defined  $\delta = (q' - q) / q'$ , the fractional change of the guiding center radius. Squaring and adding these two equations, and using equation (A2.2), we obtain

$$A^2 = \delta^2 + \left( \frac{\Delta v \cos(\alpha)}{q'\kappa'} \right)^2. \quad (\text{A2.6})$$

The new guiding center radius  $q'$  can be obtained from the force balance equations for the guiding center orbit before and after the collision. Assuming a power-law rotation curve according to Equation (4.1) we have from Equation (4.2)

$$-g = \frac{v(\gamma)^2}{\gamma} \left( \frac{q}{\gamma} \right)^{2/n-1} = \frac{h^2}{q^3}, \quad (\text{A2.7})$$

where the specific angular momentum is  $h = qv\theta$ . After the collision we have

$$\frac{v(\gamma)^2}{\gamma} \left( \frac{q'}{\gamma} \right)^{2/n-1} = \frac{h'^2}{q'^3}, \quad (\text{A2.8})$$

with

$$h' = h + q\Delta v_\theta = q(v + \Delta v_\theta) \quad (\text{A2.9})$$

in the IA. Combining these and solving for  $q'$  yields,

$$\left( \frac{q'}{\gamma} \right) = \left( \frac{q}{\gamma} \right) \left[ 1 + \left( \frac{q}{\gamma} \right)^{-1/n} \frac{\Delta v_\theta}{v(\gamma)} \right]^{n/n+1}. \quad (\text{A2.10})$$

Thus, in the case of a power-law potential we can solve explicitly for  $q'$ . This is not the case for most potentials.

Once  $\Delta v(q, \theta)$  is determined it can be substituted into Equation (A2.10), and then with the aid of Equations (A2.1) and (A2.2) we have  $q'$  in terms of unperturbed variables. This result can be used with Equation (4.4) in Equation (A2.6) to solve for  $A$ , and the in Equations (A2.5) for  $\psi'$ . The expressions for  $q', \kappa', A$  and  $\psi'$  can be substituted into (A2.3), yielding the desire

expression for the post-collision stellar orbit in terms of the pre-collision values and the collisional parameters.

As a simple example, assume that the perturbation has a power-law dependence on the distance from impact, as in Equation (4.9), and write

$$\Delta v = \Delta v_\epsilon \left( \frac{R}{\epsilon} \right)^{-m}, \quad (\text{A2.11})$$

with

$$R = [q^2 + r_*^2 - 2qr_* \cos(\theta)]^{1/2}. \quad (\text{A2.12})$$

A particularly simple case which we will examine in some detail is when  $m = 0$ , and  $n \rightarrow \infty$  (i.e. a perfectly flat rotation curve in the primary). The perturbed guiding center is then

$$\frac{q'}{\gamma} \approx \frac{q}{\gamma} \left[ 1 - \frac{\Delta v_\epsilon}{v(\gamma)} \sin(\alpha) \right], \quad (\text{A2.13})$$

using Equations (A2.10), (A2.11), and (A2.2). Also,

$$q' \kappa' = \gamma \kappa_\gamma, \\ A^2 = \left( \frac{\Delta v_\epsilon}{v(\gamma)} \right)^2 \left[ \frac{\sin^2(\alpha)}{\left( 1 - \frac{\Delta v_\epsilon}{v(\gamma)} \sin(\alpha) \right)^2} + \left( \frac{v(\gamma) \cos(\alpha)}{\gamma \kappa_\gamma} \right)^2 \right]$$

and

$$\tan(\psi') = \frac{\gamma \kappa_\gamma \tan(\alpha)}{(v(\gamma) - \Delta v_\epsilon \sin(\alpha))}. \quad (\text{A2.14})$$

These formulae can then be substituted into the first Equation of (A2.3) to obtain an explicit expression for the perturbed radius  $r$ . The fractional radial deviation  $(r - q')/q'$  depends only on  $t$  and functions of the angle  $\alpha$ . This is because  $\Delta v$  is constant in this case, and there are no other  $q'$  dependencies in the functions of Equation (A2.14).

The azimuthal dependence is equally simple since  $\omega_{\text{cir}} = v_\gamma/q'$ , i.e.,

$$\delta\theta = \theta - \theta_0 = \frac{v(\gamma)t}{q'}, \quad (\text{A2.15})$$

This expression can be used to eliminate time from the radial equation,

$$\frac{\delta}{q'} = A \sin \left( \frac{q' \kappa'}{v_\gamma} \delta\theta + \psi' \right) = A \sin(\sqrt{2} \delta\theta + \psi') \quad (\text{A2.16})$$

which is the polar coordinate equation for the post-collision orbits. This  $r - \theta$  orbit equation is equivalent to that of the curve called the Limacon of Pascal, which looks rather like an off-center circle with an inward pointing pucker or cusp.

Having determined the orbit equations, the next step (following the example of [Section 4](#)) is to calculate the caustic conditions, i.e., the boundaries of orbit crossing zones. In this case, the caustics are given by the zeros of the Jacobean determinant, i.e., the

generalization of equation (4.12) is

$$\begin{vmatrix} \frac{\partial r}{\partial q} & \frac{\partial r}{\partial \theta_0} \\ \frac{\partial \theta}{\partial q} & \frac{\partial \theta}{\partial \theta_0} \end{vmatrix} = 0 \quad (\text{A2.17})$$

Because of the simplicity of the expressions (A2.13) for  $q'$  in the power-law model, we have not specialized to the limit of small  $\delta$  up to this point. A small radial amplitude approximation is implied when we adopt the epicyclic Equations (A2.13). However, this is not the same as assuming that the collisional perturbation is small. It is an approximation for the orbits in the primary galaxy which could, in principle, be replaced by a more exact form, e.g., in terms of elliptic functions. We could, in fact, proceed to work out the explicit analytic form for (A2.17) without further approximation. However, we will not pursue that here. At this point we will consider some limits.

The most important limit for present purposes is when the angle  $\alpha \ll 1$ , i.e., just slightly off-center collisions with  $r_* \ll q, R$ . It is also convenient (and reasonable) to assume  $A \ll 1$ , i.e., small amplitude perturbations. If instead of  $\theta$ , we adopt the corotating variable  $\Theta = \theta - \omega_{\text{crit}} t$ , then the cross terms in Equation (A2.17) are both proportional to  $A \sin(\alpha)$ . Thus, the product of these terms can be neglected to first order, and Equation A2.17 becomes

$$\begin{aligned} \left( \frac{\partial r}{\partial q} \right) \left( \frac{\partial \theta}{\partial \theta_0} \right) &\approx 1 - A(\sin(\kappa t) - \kappa t \cos(\kappa t)) \\ &+ A\kappa t \left( \frac{r_*}{q} \right) \cos(\theta_0) [1 - A(\sin(\kappa t) - \kappa t \cos(\kappa t))] \\ &- A\kappa t (\sqrt{2} \sin(\kappa t) + \cos(\kappa t)) \left( \frac{r_*}{q} \right) \sin(\theta_0) \\ &= 0. \end{aligned} \quad (\text{A2.18})$$

Given the simple potential adopted, and the approximations made, this is probably the simplest formula describing collisional asymmetric caustic waves in galaxy disks. The first two terms alone describe the (inner and outer) caustic edges of a symmetric ring, as can be seen by taking  $r_* = 0$ , or comparing to Equation (4.14).

If we assume that the radius  $q$  and the phase  $\kappa t$  are constant on a caustic, but with  $r_* > 0$ , then (A2.18) is recognized as the equation of a circle whose center is offset from the origin. More realistically, at a fixed time the value of  $q$  on the caustic must vary with azimuth  $\theta_0$  in order to solve (A2.18). If this variation is not too great then the caustic curves described by (A2.18) can be approximated by local circular arcs. Additionally it can be shown that Equation (A2.18) has banana or crescent-shaped solutions as well as complete circles. There are probably other, more complex waveform solutions as well. However, these have not yet been fully investigated.

We note again that it would also be interesting to study the analogous caustic equation in the retrograde encounter limit, i.e., where  $r_*, R \gg q$ , and  $\beta = \pi - \alpha - \theta \ll 1$ . This equation will be more complicated than (A2.18) because in this limit the cross terms of Equation (A2.17) are not negligible.

## REFERENCES

1. Appleton, P.N., Ghigo, F.D., van Gorkom, J.H., Schombert, J.M., and Struck-Marcell, C. (1987a), *Nature*, **330**, 140.
2. Appleton, P.N., Ghigo, F.D., van Gorkom, J.H., Schombert, J.M., and Struck-Marcell, C. (1987b). *Nature*, **330**, 500.
3. Appleton, P.N. and James, R.A. (1990). In *Dynamics and Interactions of Galaxies*, ed. R. Wielen, Springer Verlag, Berlin, p. 200.
4. Appleton, P.N. and Marcum, P.M. (1993). *Astrophys. J.*, **417**, 90.
5. Appleton, P.N. and Marston A.P. (1995). *Astr. J.*, (preprint).
6. Appleton, P.N., Marston, A.P. and Charmandaris, V. (1995). *Astrophys. J.*, (preprint).
7. Appleton, P.N. Schombert, J.M. and Robson, E.I. (1992). *Astrophys. J.*, **385**, 491.

8. Appleton, P.N., and Struck-Marcell, C. (1987a). *Astrophys. J.*, 312, 566.
9. Appleton, P.N., and Struck-Marcell, C. (1987b). *Astrophys. J.*, 318, 103.
10. Appleton, P.N., Struck-Marcell, C., and Foster, P.A. (1985). In *Cosmical Gas Dynamics*, ed. F.D. Kahn, VNU Science, Utrecht, p. 33.
11. Arnold, V.I. (1986). *Catastrophe Theory*, 2nd English edition, Springer, New York.
12. Arnold, V.I., Shandarin, S.F., and Zel'dovich, Ya. B. (1982). *Geophys. Ap. Fluid Dyn.*, 20, 111.
13. Arp, H.C. and Madore, B.F. (1985). *Q.J.R. Astr. Soc.*, 18, 234.
14. Arp, H.C. (1966). *Atlas of Peculiar Galaxies*. California Institute of Technology, Pasadena.
15. Arp, H.C., and Madore, B.F. (1987). *Catalog of Southern Peculiar Galaxies and Associations*, Vol. I and II, Cambridge University Press, Cambridge, UK.
16. Athanassoula, E. (1978). *Astr. Astrophys.*, 69, 395.
17. Athanassoula, E. and Bosma, A. (1985). *Ann. Rev. Astr. Ap.*, 23, 147.
18. Binney, J. and Tremaine, S. (1987). *Galactic Dynamics*, Princeton University Press, Princeton. New Jersey.
19. Borne, K.D., Lucas, R., Appleton, P.N., Struck, C., Schultz, A. and Spight, L. (1995). *Bull. A. Astr. Soc.*, 26, 1422.
20. Briggs, F.H. (1990). *Astron. J.*, 100, 999.
21. Brosch, N. (1985). *Astr. Astrophys.*, 153, 199.
22. Burbidge, E.M. (1964). *Astrophys. J.*, 140, 1617.
23. Burbidge, E.M. and Burbidge, G.R. (1959). *Astrophys. J.*, 130, 12.
24. Bushouse, H. and Stanford, S.A. (1992). *Astrophys. J.*, (Suppl.), 79, 213.
25. Buta, R.J. (1994). *Astrophys. J.*, (Suppl.), (In press).
26. Cassoli, F. (1991). In *Dynamics of Galaxies and their Molecular Cloud Distribuions*, IAU Symposium 146, eds. F. Combes and F. Casoli, Dordrecht, Reidel, p. 51.
27. Cannon, R.D., Lyoyd., C. and Penston, M.V. (1970). *Observatory*, 90, 153.
28. Charmandaris, V., Appleton, P.N. and Marston, A.P., (1993). *Astrophys. J.*, 414, 154.
29. Charmandaris, V. and Appleton, P.N. (1994). *Bull. A Astr. Soc.*, 26, 877.
30. Coles, P., Melott, A.L. and Shandarin, S.F (1993). *Mon. Not. R. Astr. Soc.*, 260, 765.
31. Davies, R.L. and Morton, D.C. (1982). *Mon. Not. R. Astr. Soc.*, 201, 69P.
32. Davoust, E., Considere, S. and Poulain, P. (1991). *Astr. Astrophys.*, 252, 69.
33. Dennefeld, M. and Materne, J. (1980). In the *ESO Messenger*, 21, 29.
34. Dennefeld, M., Lautsen, S. and Materne, J. (1979). *Astr. Astrophys.*, 74, 123.
35. de Jong, R.S. 1995, Ph. D. Thesis, University of Groningen, Groningen, Netherlands.
36. de Vaucouleurs, G. and de Vaucouleurs, A. (1975). *Astrophys. J. (Letts)*, 197, L1.
37. de Vaucouleurs, G., de Vaucouleurs, A., and Corwin, H.C. (1976). *Second Reference Catalogue of Bright Galaxies*, Austin, Texas.
38. Donner, K.J., Engstrom, S. and Sundelius, B. (1991). *Astr. Astrophys.*, 252, 571.
39. Few, J.M.A., and Madore, B.F. (1986). *Mon. Not. R. Astr. Soc.*, 222, 673.
40. Few, J.M.A., Madore, B.F. and Arp, H.C. (1982). *Mon. Not. R. Astr. Soc.*, 199, 633.
41. Fosbury, R.A.E., and Hawarden, T.G. (1977). *Mon. Not. R. Astr. Soc.*, 178, 473.
42. Foster, P.A., (1985). In *Cosmical Gas Dynamics*, ed. F.D. Kahn, VNU Science, Utrecht, p. 39.
43. Freeman, K. and de Vaucouleurs, G. (1974). *Astrophys. J.*, 194, 569.
44. Garcia, A. and Rodriguez Espinosa, J.M. (1995), (preprint)
45. Gerber, R.A. (1993). *Ph. D. Thesis*, Univ. of Illinois. Champaigne, Illinois.
46. Gerber, R.A. and Lamb, S.A. (1994). *Astrophys. J.*, 431, 604.
47. Gerber, R.A., Lamb, S.A. and Balsara, D.S. (1992). *Astrophys. J.*, (Letts), 399, L51.
48. Gerber, R.A., Lamb, S.A. and Balsara, D.S. (1994), preprint.
49. Gerber, R.A., Lamb, S.A. and Balsara, D.S. (1994). *Bull. A Astr. Soc.*, 26, 911.
50. Ghigo, F.D., (1980). *Astron. J.*, 85, 215.
51. Ghigo, F.D., and Appleton, P.N., (1995). (Preprint).
52. Ghigo, F.D., Hine, B.P. and van der Hulst, J.M. (1994). (Preprint).
53. Ghigo, F.D., Wardle, J.F.C., and Cohen, N.L. (1983). *Astron. J.*, 88, 1587.
54. Graham, J.A. (1974). *Observatory*, 94, 290.
55. Hernquist, L. and Quinn, P.J. (1987). *Astrophys. J.*, 312, 1.
56. Hernquist, L. and Weil, M.L. (1993). *Mon. Not. R. Astr. Soc.*, 261, 804.
57. Higdon, J.L. (1988). *Astrophys. J.*, 326, 146
58. Higdon, J.L. (1993). *Ph. D. Thesis*, University of Texas, Austin, Texas.
59. Hoag, A.A. (1950). *Astron. J.*, 55, 170.
60. Horellou, C., Casoli, F., Combes, F. and Dupraz, C. (1994). *Astr. Astrophys.*, (preprint).
61. Horellou, C. and Combes, F. (1994). In *N-body Problems and Gravitational Dynamics*, eds. F. Combes and E. Athanassoula, Observatoire de Paris, Paris, p 168.
62. Huchra, J.P., Wyatt, W.F. and Davis, M. (1982). *Astron. J.*, 87, 1628.
63. Hunter, C. (1974). *Astrophys. J.*, 181, 685.

64. Hummel, E. (1981). *Astr. Astrophys.*, 96, 111.
65. Huang, S. and Stewart, P. (1988). *Astr. Astrophys.*, 197, 14.
66. Jeske, N.A. (1986). *PhD Thesis*, University of California, Berkeley.
67. Joy, M. (1987). *Astrophys. J.*, 315, 480.
68. Joy, M., Ellis, H.B., Tollestrup, E.V., Brock, D., Higdon, J.L. and Harvey, P.M. (1989). *Astrophys. J., (Lett)*, 330, L29.
69. Joy, M. and Ghigo, F.D. (1988). *Astrophys. J.*, 332, 179.
70. Joy, M., Tollestrup, E.V., Harvey, P.M., McGregor, P and Hyland, A.R. (1988). *Bull. Am. Astr. Soc.*, 20, 1000.
71. Kalnajs, A. (1973). *Proc. A.S.A.*, 2, 174.
72. Kaufman, M., Bash, F.N., Hine, B., Rots, A.H., Elmegreen, D.M. and Hodge, P.W. (1989). *Astrophys. J.*, 345, 674.
73. Kennicutt, R.C., Jr. (1988). *Astrophys. J.*, 334, 144.
74. Kennicutt, R.C., Jr. (1989). *Astrophys. J.*, 344, 685.
75. Kennicutt, R.C., Keel, W.C., van der Hulst, J.M., Hummel, E., and Roettiger, K.A. (1987). *Astron. J.*, 93, 1001.
76. Kennicutt, R.C., Jr. (1990). In *The Interstellar Medium in Galaxies*, eds. H.A. Thronson and J.M. Shull, Kluwer Publications, Dordrecht, p. 405.
77. Kent, S.M., Ramella, M. and Nonino, M. (1994). *Astron. J.*, 105, 393.
78. Lindsey, E.M. and Shapley, H., (1960). *Observatory*, 80, 223.
79. Lipari, S. and Maccetto, F. (1994). *Astrophys. J.*, (preprint).
80. Lo, K.Y. and Sargent, W.L.W. (1979). *Astrophys. J.*, 227, 756.
81. Lotan-Luban, P. (1990), Ph. D. Thesis, Iowa State University, Ames, Iowa.
82. Lotan, P. and Struck-Marcell, C. (1991). unpublished.
83. Lu, P.K. (1971). *Astron. J.*, 76, 775.
84. Lynds, R., and Toomre, A. (1976). *Astrophys. J.*, 209, 382.
85. Lysaght, M. (1990). M.S Thesis, Iowa State University, Ames, Iowa.
86. Majewski, S.R. (1988). In *Towards Understanding Galaxies at Large Redshift*, eds. R.G. Kron and A. Renzini, Kluwer Publications, Dordrecht, p. 127.
87. Marcum, P.M., Appleton, P.N. and Higdon, J. (1992). *Astrophys. J.*, 399, 57.
88. Marston, A.P. and Appleton, P.N. (1995). *Astron. J.*, 109, 1002.
89. Mebold, U., Goss, W.M. and Fosbury, R.E. A., (1977). *Mon. Not. R. Astr. Soc.*, 180, 11p
90. Mihos, J.C., Bothun, G.D. and Richstone, D.O. (1993). *Astrophys. J.*, 418, 82.
91. Mihos, J.C. and Hernquist, L. (1994a). *Astrophys. J.*, 425, L13.
92. Mihos, J.C. and Hernquist, L. (1994b). *Astrophys. J.*, in press.
93. Mihos, J.C., Richstone, D.O. and Bothun, G.D., (1992). *Astrophys. J.*, 400, 153.
94. Noguchi, M. (1988). *Astr. Astrophys.*, 203, 259.
95. Noguchi, M. (1990) In *The Interstellar Medium in Galaxies*, eds. H.A. Thronson, Jr., and J.M. Shull, Kluwer Publications, Dordrecht, p. 323.
96. Norris, R.P. (1988). *Mon. Not. R. Astr. Soc.*, 230, 345.
97. Norris, R.P. and Forbes, D.A. (1994). *Astrophys. J.*, (preprint).
98. O'Connell, R.W., Scargle, J.D., and Sargent, W.L.W., (1974). *Astrophys. J.*, 191, 61.
99. Olson, K.M., and Kwan, J., (1990a). *Astrophys. J.*, 349, 480.
100. Olson, K.M., and Kwan, J., (1990b). *Astrophys. J.*, 361, 426.
101. Poston, T. and Stewart, I.N. (1978). *Catastrophe Theory and Its Applications*, Boston, Pitman.
102. Rand, R.J., and Tilanus, R.P.J. (1990), In *The Interstellar Medium in Galaxies*, eds. H.A. Thronson, Jr. and J.M. Shull, Kluwer Publications, Dordrecht, p. 525.
103. Regan, M.W., and Wilson, C.D. (1993). *Astron. J.*, 105, 499.
104. Roberts, W.W., Jr. and Stewart, G.R. (1987). *Astrophys. J.*, 314, 10.
105. Rodriguez Espinosa, J.M. and Stanga, R.M. (1990). *Astrophys. J.*, 365, 502.
106. Sanders, D.B., Soifer, B.T., Elias, J.H., Madore, B.F., Matthews, K., Neugebauer, G. and Scoville, N.Z. (1988). *Astrophys. J.*, 325, 74.
107. Sanders, R.H. and Prendergast, K.H. (1974). *Astrophys. J.*, 188, 489.
108. Sargent, W.L.W. (1970). *Astrophys. J.*, 160, 405.
109. Scalo, J.M. and Struck-Marcell, C. (1986). *Astrophys. J.*, 301, 77.
110. Schultz, A.B., Spight, L.D., Colegrove, P.T. and DiSanti, M.A. (1990), In *Massive Stars and Starbursts*, STScI workshop.
111. Schweizer, F., Ford, W.K., Jedrzejski, R. and Giovannelli, R. (1987). *Astrophys. J.*, 320, 454.
112. Sersic, J.L. (1968), *Atlas de Galaxias Australes* (Observatorio Astronomico, Universidad Nacional de Cordoba, Argentina).
113. Shandarin, S.F. and Zeldovich, Ya. B. (1984). *Phys. Rev. Letts.*, 52, 1488.
114. Silverglade, P.R. and Krumm, N. (1978). *Astrophys. J. (Letts)*, 224, L99.
115. Smith, B.J. and Higdon, J.L. (1994). *Astron. J.*, 108, 837.
116. Smith, R.T. (1941), *Pub. Astr. Soc. Pac.*, 53, 187.
117. Stanga, R.M. and Rodriguez Espinosa, J.M. and Mannucci, F. (1991). *Astrophys. J.*, 379, 592.

118. Struck-Marcell, C. (1990). *Astron. J.*, 99, 71.
119. Struck-Marcell, C. (1991). *Astrophys. J.*, 368, 348.
120. Struck-Marcell, C. (1994). *Mon. Not. R. Astr. Soc.*, submitted.
121. Struck-Marcell, C. and Appleton, P.N. (1987). *Astrophys. J.*, 323, 480.
122. Struck-Marcell, C. and Higdon, J. (1993). *Astrophys. J.*, 411, 108.
123. Struck-Marcell, C. and Lotan, P. (1990). *Astrophys. J.*, 358, 99.
124. Struck-Marcell, C. and Scalo, J.M. (1987). *Astrophys. J. (Suppl.)*, 64, 39.
125. Struck-Marcell, C., Scalo, J.M. and Appleton, P.N. (1987). In *Star Formation in Galaxies*, NASA Publ. No. 2466, ed. C.J. Lonsdale, NASA Publ. Washington D.C., p. 435.
126. Taylor, C.L., Brinks, E., Pogge, R.W. and Skillman, E.D. (1994). *Astron. J.*, 107, 971.
127. Taylor, K. and Atherton, P.D. (1981). *AAO Newsletter*, 17, 1.
128. Taylor, K. and Atherton, P.D. (1984). *Mon. Not. R. Astr. Soc.*, 208, 601.
129. Theys, J.C. and Spiegel, E.A. (1976). *Astrophys. J.*, 208, 650.
130. Theys, J.C. and Spiegel, E.A. (1977). *Astrophys. J.*, 212, 616.
131. Thomasson, M., Donner, K.J., Sundelius, B., Byrd, G.G., Haug, T.Y. and Valtonen, M.J. (1989). *Astron. Astrophys.*, 211, 25.
132. Thompson, L., (1977). *Astrophys. J.*, 211, 684.
133. Thompson, L.A. and Gregory, S.A., (1977). *Pub. Astr. Soc. Pac.*, 89, 113.
134. Thompson, L.A. and Theys, J.C. (1978). *Astrophys. J.*, 224, 796.
135. Thronson, H.A. and Greenhouse, M.A. (1988). *ApJ*, 327, 671.
136. Toomre, A. (1978). In *The Large-Scale Structure of the Universe*, IAU Symp. No. 79, ed. M.S. Longair and J. Einasto, D. Reidel Publications, Holland), p. 109.
137. Toomre, A., and Toomre, J. (1972). *Astrophys. J.*, 178, 623.
138. Tremaine, S. (1981). In *The Structure and Evolution of Galaxies*, eds. S.M. Fall and D. Lynden-Bell, Cambridge University Press, Cambridge, p. 67.
139. van Gorkom, J.M. (1993). In *The Environment and Evolution of Galaxies*, eds. J.M. Shull and H.A. Thronson, (Kluwer Academic Press, Dordrecht, Netherlands), p. 345.
140. Vorontsov-Velyaminov, B.A. (1959). *Atlas and Catalogue of Interacting Galaxies, Part I*, (Moscow, University, Moscow).
141. Voronov-Velyaminov, B.A. (1960). *Ann. Astrophys.*, 23, 384.
142. Vorontsov-Velyaminov, B.A. and Krasnogorskaya, A. (1961). *Morphological Catalogue of Galaxies*, Moscow.
143. Vorontsov-Velyaminov, B.A. (1977). *Astr. Astrophys. (Suppl.)*, *Atlas of Interacting Galaxies, Part II*, 28, 1.
144. Wakamatsu, K. and Nishida, M.T. (1987). *Astrophys. J. (Letts)*, 315, L23.
145. Wakamatsu, K.-I. and Nishida, M.T., *PASP*, 103, 392 (1991)
146. Wallin, J.F. (1989). *Ph. D. Thesis*, Iowa State.
147. Wallin, J.F. (1990). *Astron. J.*, 100, 1477.
148. Wallin, J.F. and Struck-Marcell, C. (1988). *Astron. J.*, 96, 1850.
149. Wallin, J.F. and Struck-Marcell, C. (1994). *Astron. J.*, (Pre-print).
150. Windhorst, R.A., van Heerde, G.M. and Katgert, P., (1994). *Astron. Astrophys.*, 58, 1.
151. Wilson, C.D., and Scoville, N. (1991). *Astrophys. J.*, 370, 184.
152. Zwicky, F. (1941). In *Theodore von Karman Anniversary Volume, Contribution to Applied Mechanics and Related Subjects*, California Institute of Technology, Pasadena, California, p. 137.